



Max-Planck-Forschungsstelle  
für Enzymologie der Proteinfaltung

**Conformation specific targeting of  $\beta$ -amyloid  
aggregates in a *Drosophila melanogaster* model of  
Alzheimer's disease**

D i s s e r t a t i o n

zur Erlangung des  
Doktorgrades der Naturwissenschaften (Dr. rer. nat.)

der

Naturwissenschaftlichen Fakultät I (Biowissenschaften)

der Martin-Luther-Universität

Halle-Wittenberg

vorgelegt

von Frau Dipl. Biol. Jessica Wacker  
geboren am 10.01.1983 in Schkeuditz

**Gutachter /in**

1. PD Marcus Fändrich
2. Prof. Hans-Ulrich Demuth
3. PD Damian C. Crowther

Promotionsgesuch eingereicht am: 20.11.2012

Tag der öffentlichen Verteidigung: 05.07.2013

*für meine Eltern*

---

## Content

---

<b>1. Introduction</b> .....	<b>1</b>
<b>1.1 Neurodegenerative diseases</b> .....	<b>1</b>
<b>1.2 Alzheimer's disease (AD)</b> .....	<b>1</b>
1.2.1 Tau pathology.....	2
1.2.2 Amyloid- $\beta$ pathology .....	4
<b>1.3 A<math>\beta</math> aggregates into amyloid fibrils</b> .....	<b>5</b>
<b>1.4 Animal models of Alzheimer's disease</b> .....	<b>6</b>
1.4.1 <i>Drosophila melanogaster</i> as a model organism for AD.....	7
1.4.2 Gal4-UAS-System.....	9
<b>1.5 Treatment of Alzheimer's disease using drugs and immunisation</b> .....	<b>10</b>
1.5.1 Conformation-sensitive antibodies against A $\beta$ .....	12
1.5.2 The camlid antibody domains B10 und KW1 .....	13
1.6 Aims of the thesis .....	15
<b>2. Material &amp; methods</b> .....	<b>17</b>
<b>2.1 Material:</b> .....	<b>17</b>
<b>2.1.1 Chemicals</b> .....	<b>17</b>
<b>2.1.2 Kits and readymade solutions</b> .....	<b>17</b>
<b>2.1.3 Equipment</b> .....	<b>18</b>
<b>2.1.5 <i>E. coli</i> strains</b> .....	<b>18</b>
<b>2.1.6 Plasmids</b> .....	<b>19</b>
<b>2.1.7 Proteins</b> .....	<b>19</b>
<b>2.1.9 Used cell lines</b> .....	<b>20</b>
<b>2.2 Methods</b> .....	<b>20</b>
<b>2.2.1 Drosophila work</b> .....	<b>20</b>
2.2.1.1 Husbandry of <i>Drosophila melanogaster</i> and generation of transgenic flies.....	20
2.2.1.2 Gal4-UAS expression of <i>Drosophila</i> transgenes.....	21
2.2.1.3 Survival and climbing assay .....	22
<b>2.2.2 Molecular biology methods</b> .....	<b>22</b>
2.2.2.1 Cloning : digestion, ligation, transformation.....	22
2.2.2.2 Site-specific mutagenesis .....	23
2.2.2.3 Isolation of genomic DNA.....	24
2.2.2.4 RNA extraction .....	24
2.2.2.5 Reverse transcription polymerase chain reaction (RT- PCR).....	24
2.2.2.6 Polymerase chain reaction (PCR) .....	24
2.2.2.7 Agarose gel electrophoresis .....	25
2.2.2.8 Protein synthesis in <i>E. coli</i> .....	26
<b>2.2.3 Biochemical methods</b> .....	<b>26</b>
2.2.3.1 Purification of B10-myc and B10A $P_i$ .....	26
2.2.3.2 Preparation of disaggregated A $\beta$ 1-40 .....	27
2.2.3.3 Preparation of soluble A $\beta$ oligomers.....	27
2.2.3.4 Preparation of A $\beta$ fibrils .....	27
2.2.3.5 <i>Drosophila melanogaster</i> protein extraction .....	27
2.2.3.6 Bradford Assay .....	28
2.2.3.7 Immunoprecipitation .....	28
2.2.3.8 Quantification of B10 and A $\beta$ .....	28
2.2.3.9 SDS-polyacrylamid gel electrophoresis (SDS-PAGE).....	29
2.2.3.10 Native Page.....	29

2.2.3.11	Coomassie staining.....	29
2.2.3.12	Western blot analysis.....	29
2.2.3.13	Enzyme linked immunosorbant assay (ELISA).....	30
2.2.3.14	Spot Blot.....	31
2.2.3.15	Dot Blot.....	32
<b>2.2.4</b>	<b>Biophysical methods.....</b>	<b>32</b>
2.2.4.1	Thioflavin T (ThT) fluorescence spectroscopy.....	32
2.2.4.2	8-Anilinonaphthalene-1-sulfonate (ANS) fluorescence spectroscopy.....	32
2.2.4.3	Congo red (CR) absorption spectroscopy.....	33
2.2.4.4	Aggregation kinetics.....	33
2.2.4.5	Transmission electron microscopy (TEM).....	33
2.2.4.6	Scanning electron microscopy (SEM).....	33
<b>2.2.5</b>	<b>Immunocytological methods.....</b>	<b>34</b>
2.2.5.1	Dissection and immunostaining of <i>Drosophila</i> brains (confocal microscopy).....	34
<b>2.2.6</b>	<b>Cytological methods.....</b>	<b>34</b>
2.2.6.1	Transfection and protein synthesis in insect cells.....	34
2.2.6.2	Cultivation of human neuroblastoma cells.....	35
2.2.6.3	Toxicity assays.....	35
<b>3.</b>	<b>Results.....</b>	<b>37</b>
<b>3.1</b>	<b>Selectivity of B10 and KW1-binding to A<math>\beta</math>(1-40), A<math>\beta</math>(1-42) and A<math>\beta</math>(1-42)arc peptides.....</b>	<b>37</b>
<b>3.2</b>	<b>B10 and KW1 can be functionally expressed in <i>Drosophila melanogaster</i> cells.....</b>	<b>39</b>
<b>3.3</b>	<b>Generating <i>Drosophila melanogaster</i> lines transgenic for B10 and KW1.....</b>	<b>41</b>
3.3.1	Characterisation of B10-transgenic flies.....	42
3.3.2	Characterisation of KW1-transgenic flies.....	43
3.3.3	B10 and KW1 do not affect the overall expression of A $\beta$ .....	44
<b>3.4</b>	<b>Quantification of B10 and KW1 expressed in <i>Drosophila melanogaster</i>.....</b>	<b>45</b>
<b>3.5</b>	<b>Quantification of A<math>\beta</math> peptides expressed in <i>Drosophila melanogaster</i>.....</b>	<b>47</b>
<b>3.6</b>	<b><i>In vivo</i> interactions of B10 and KW1 with A<math>\beta</math>.....</b>	<b>50</b>
3.6.1	Immunofluorescence studies on adult fly brains suggest co-localisation.....	50
3.6.2	Spot blot assay demonstrate the presence of the B10 epitope in <i>Drosophila</i> .....	51
3.6.3	B10AP and KW1AP do not cross-react with <i>Drosophila melanogaster</i> proteins.....	53
3.6.4	Immunoprecipitation analysis of A $\beta$ and B10 expressing flies.....	53
<b>3.7</b>	<b>Phenotypic characterisation of A<math>\beta</math> dependent neurodegeneration.....</b>	<b>55</b>
<b>3.8</b>	<b>B10 does not alter the A<math>\beta</math> dependent neurodegeneration.....</b>	<b>57</b>
<b>3.9</b>	<b>KW1 potently effects the lifespan of A<math>\beta</math>-transgenic flies.....</b>	<b>59</b>
<b>3.10</b>	<b>B10 and KW1 demonstrate no <i>in vivotoxicity</i>.....</b>	<b>62</b>
<b>3.11</b>	<b>KW1 positive A<math>\beta</math>40 aggregates accumulate in the fly brain while ageing.....</b>	<b>63</b>
<b>3.12</b>	<b>KW1 induces neurotoxicity on two A<math>\beta</math>(1-40) expressing fly lines.....</b>	<b>66</b>
<b>3.13</b>	<b>Mechanism of A<math>\beta</math>(1-40) mediated toxicity.....</b>	<b>68</b>
<b>3.14</b>	<b>KW1 stabilised A<math>\beta</math>(1-40) aggregates are structurally different from A<math>\beta</math>(1-40) aggregates.....</b>	<b>71</b>
<b>3.15</b>	<b>KW1 forms toxic aggregates <i>in vitro</i>.....</b>	<b>72</b>
<b>4.</b>	<b>Discussion.....</b>	<b>75</b>

<b>4.1 <i>Drosophila melanogaster</i> are appropriate for targeting A<math>\beta</math> aggregates .....</b>	<b>75</b>
<b>4.2 Antibody mediated A<math>\beta</math> clearance of AD .....</b>	<b>76</b>
4.2.1 Therapeutic benefits emerging from conformation- and sequence-sensitive antibodies .....	78
<b>4.3 Antibody domains B10 and KW1 are functionally expressed in <i>Drosophila melanogaster</i> .....</b>	<b>80</b>
4.3.1 A $\beta$ peptide variants are successfully expressed in <i>Drosophila melanogaster</i> .....	81
<b>4.4 The pathogenic role of A<math>\beta</math> fibrils characterised <i>in vivo</i> using the fibril binder B10. ....</b>	<b>82</b>
<b>4.5 The pathogenicity of A<math>\beta</math> oligomers is analysed <i>in vivo</i> using the oligomer-specific antibody domain KW1. ....</b>	<b>83</b>
4.5.1 A $\beta$ (1-40) is able to form neurotoxic aggregates <i>in vivo</i> .....	84
4.5.2 Oligomer targeting <i>in vivo</i> leads to increased neurotoxicity.....	86
4.5.3 A $\beta$ (1-40) oligomers mediate toxicity via neuronal cell surface receptors.....	87
4.5.4 KW1 induces the formation of neurotoxic off-pathway aggregates .....	89
<b>4.6 Conformational targeting <i>in vivo</i> is essential for understanding AD pathogenesis .....</b>	<b>90</b>
<b>5. Summary.....</b>	<b>92</b>
<b>6. Zusammenfassung .....</b>	<b>93</b>
<b>7. Literature .....</b>	<b>94</b>
<b>8. Appendix.....</b>	<b>110</b>
Appendix A Amino acid sequences.....	110
Appendix B Establishment of <i>Drosophila melanogaster</i> transgenic for bivalent antibody domains.....	111
<b>Curriculum vitae.....</b>	<b>117</b>
<b>Publication.....</b>	<b>118</b>
<b>Acknowledgements .....</b>	<b>119</b>
<b>Eidesstattliche Erklärung .....</b>	<b>120</b>

---

## Abbreviations

---

A $\beta$	amyloid- $\beta$ peptide
AD	Alzheimer's disease
ANS	8-Anilinoanthralene-1-sulfonate
APP	amyloid precursor protein
APPL	amyloid precursor protein-like
BSA	bovine serum albumin
cDNA	complementary DNA
<i>C. elegans</i>	<i>Caenorhabditis elegans</i>
CR	Congo red
<i>D. mel</i>	<i>Drosophila melanogaster</i>
DEPC	Diethylpyrocarbonat
DMSO	Dimethyl sulfoxide
DNA	Deoxyribonucleic acid
DNase	Deoxyribonuclease
dNTP	Deoxynucleotide triphosphate
<i>E. coli</i>	<i>Escherichia coli</i>
EDTA	Ethylenediaminetetraacetic acid
ELISA	enzyme linked immunosorbent assay
<i>et al.</i>	and others
FAD	familial AD
FDA	U.S. Food and Drug Administration
<i>g</i>	gravitational acceleration
GnHCl	Guanidine hydrochloride
hAPP	human APP
HFIP	1,1,1,3,3,3-Hexafluoro-2-propanol
LiCl	Lithium chloride
kDa	kilo Dalton
KOAc	Potassium acetate
LTP	long term potentiation
min	minute
MSD	meso scale discovery
NFT	neurofibrillar tangle
NGF	nerve growth factor
NMDA	<i>N</i> -methyl-D-aspartate
NSAIDs	nonsteroidal anti-inflammatory drugs
PAGE	polyacrylamid gel electrophoresis
PBS	Phosphate buffered saline
PBST	Phosphate buffered saline + 0,05 % TritonX-100
PBT	Phosphate buffered saline + 0,5 % TritonX-100
PCR	polymerase chain reaction
PFA	paraformaldehyde
pGlu	pyroglutamate
RAGE	Receptor for Advanced Glycation Endproducts
RNA	ribonucleic acid
rpm	rotations per minute
RT-PCR	reverse transcription PCR
SDS	sodium dodecyl sulfate
sec	second

SEM	scanning electron microscopy
TAE	Tris-acetate-EDTA
TBS	Tris buffered saline
TBST	Tris buffered saline + 0,1% Tween20
TEM	transmission electron microscopy
TEV	Tobacco Etch Virus
TFA	Trifluoroacetic acid
ThT	Thioflavin T
Tris	Tris(hydroxymethyl)aminomethane
UAS	upstream activating sequence
WT	wildtype

---

## 1. Introduction

---

### 1.1 Neurodegenerative diseases

Neurodegenerative disease is the umbrella term for a group of diseases which are linked to neuronal degeneration and subsequent neurological symptoms like dementia and cognitive dysfunctions. These diseases are frequently caused by aggregation prone proteins <sup>[1]</sup> (table 1.1). For example, abnormally folded proteins can lead to neurodegeneration as seen with the prion protein in Creutzfeldt-Jakob disease or amyloid- $\beta$  peptide ( $A\beta$ ) and Tau protein in Alzheimer's disease (AD).

Table 1.1 Polypeptides involved in neurodegenerative diseases <sup>[1-4]</sup>.

disease	deposited polypeptide	pathologic characteristics
Alzheimer's disease	$A\beta$ peptide Tau	neuritic plaques neurofibrillar tangles
Fronto-temporal dementia with Parkinsonism	Tau	Pick bodies
Parkinson's disease	$\alpha$ -Synuclein	Lewy bodies, Lewy neurites
Huntington's disease	Huntingtin	nuclear inclusion cytoplasmatic aggregates
Amyotrophic lateral sclerosis	Superoxid dismutase 1	nuclear and axonal inclusions
Spinocerebellar ataxis	Ataxins	nuclear inclusions
Creutzfeldt-Jakob disease	prion protein ( $PrP^{Sc}$ )	florid $PrP^{Sc}$ deposits

Many of the sporadic forms of neurodegenerative diseases are late-onset, suggesting that they are linked to factors which change due to ageing. Cells, for example, lose their ability to degrade misfolded proteins, leading to accumulation of such proteins <sup>[5-7]</sup>. There is also evidence that mutations can cause an early onset of such illnesses and lead to familiarly-inherited diseases. In Parkinson's disease, a gain of function mutation in the  *$\alpha$ -synuclein* gene causes autosomal dominant Parkinson's disease <sup>[8]</sup>. In case of the inherited Huntington's disease, the disorder is caused by repeated sections in the *Huntingtin* gene resulting in polyglutamine extension of the Huntingtin protein and subsequent aggregation <sup>[9]</sup>.

### 1.2 Alzheimer's disease (AD)

AD is characterised by memory deficits and cognitive impairment due to neuronal degeneration. In addition, AD is the most common form of dementia <sup>[10]</sup>. 1,2 million people in Germany are estimated to currently suffer from AD and the number is predicted to increase up to 2,3 million in 2030 <sup>[11]</sup>. Every year 200 000 people in Germany are diagnosed with AD and the chance of developing AD increases with age <sup>[11]</sup>. The disease was first described by Alois Alzheimer who discovered that his patient, Auguste Deter, suffered from presenile dementia including a rapid memory loss <sup>[12]</sup>. Later it was found in post-mortem brain studies that neuronal cells and synapses

are lost in specific brain regions<sup>[13]</sup> along with histological changes. Two major lesions are predominant in the brain of AD patients: extracellular A $\beta$  plaques and intracellular neurofibrillary tangles (NFTs) consisting of hyperphosphorylated tau protein (figure 1.1)<sup>[14]</sup>.

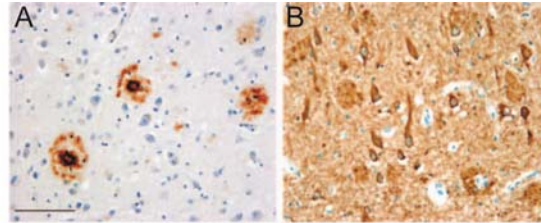


Figure 1.1 Histopathology of AD in post-mortem brain sections. (A): A $\beta$ -positive senile plaques. (B): Tau-positive neurofibrillary tangles (adapted by Haass & Selkoe, 2007<sup>[14]</sup>). Scale bar represents 100 $\mu$ m.

The toxic role of both proteins has been investigated individually but there is increasing believe that tau and A $\beta$  need to functionally interact to mediate neurotoxicity<sup>[15]</sup>. Primary neurons derived from *tau* knockout mice were resistant to the toxic effects of A $\beta$ <sup>[16]</sup> and immunisation of mutant *tau* mice with A $\beta$  exacerbated the NFT pathology<sup>[17]</sup>. Additionally, reducing Tau prevented behavioural deficits in mice<sup>[18]</sup>.

It is thought that A $\beta$  induces the phosphorylation of Tau and exerts Tau toxicity in neurons (figure 1.2A). Alternatively the presence of Tau is critically required to mediate A $\beta$  toxicity towards neurons (figure 1.2B). A third option is that both proteins act synergistically, thereby enhancing their toxicity and for example attacking cell membranes organelles (figure 1.2C).

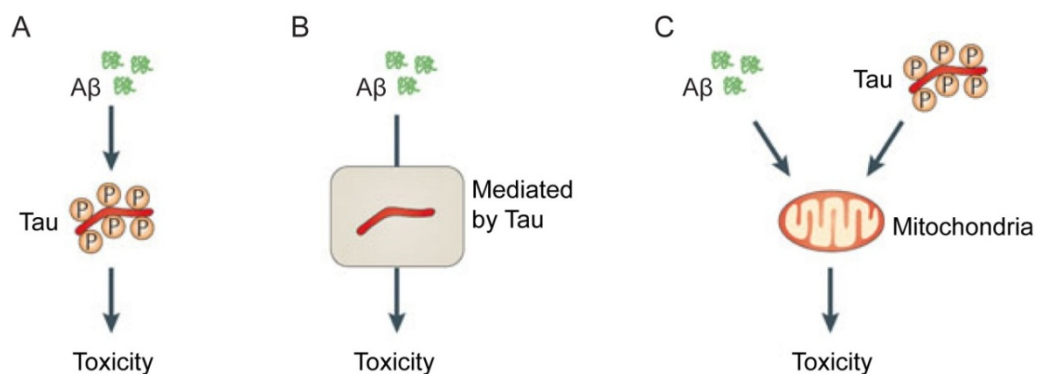


Figure 1.2 Potential interaction between A $\beta$  and Tau (adapted from Ittner & Götz, 2011<sup>[15]</sup>). (A) A $\beta$  could exert Tau toxicity. (B) A $\beta$  toxicity could be mediated by Tau or (C) A $\beta$  and Tau act synergistically leading to increased toxicity.

### 1.2.1 Tau pathology

The neuronal microtubule-associated protein Tau is known to cause neurodegenerative disorders, collectively called tauopathies such as Alzheimer's disease and fronto-temporal dementia

with Parkinsonism linked to chromosome 17 (FTDP-17) (table 1.1). Normally, Tau is required in neurons to maintain microtubule assembly and stability. In addition, it has been demonstrated that over-expression of *tau* disrupts the axonal transport<sup>[19-21]</sup>. In the human brain six Tau isoforms exist. As a result of alternative splicing, these isoforms have either 3 or 4 C-terminal microtubule-binding domains (MTBD). Tau has around 80 possible phosphorylation sites; most of them are on Ser-Pro or Thr-Pro motifs, but some were identified on other motifs<sup>[22]</sup> and the number of phosphorylation events in the MTBDs correlates negatively with the binding ability to the microtubules. In general the phosphoprotein Tau contains 2-3 moles of phosphate per mol of Tau and several serine and threonine residues are known to be phosphorylated in humans<sup>[23, 24]</sup>. Nevertheless, in brains of individuals suffering from a tauopathy the phosphorylation levels of Tau are 3-4 fold higher than in healthy brains<sup>[23]</sup>. Abnormally phosphorylated Tau forms paired helical filaments, lowering the levels of microtubule binding Tau, thus disrupting axonal transport and leading to degeneration of axons<sup>[25-27]</sup>. Additionally, it has been shown that Tau-dependent neuronal dysfunction can occur without neurodegeneration<sup>[21, 28, 29]</sup> and that Tau-dependent neuronal loss has occurred in *in vivo* models<sup>[30, 31]</sup> implying that there may be different mechanisms by which Tau mediates its toxicity.

Characteristic of tauopathies is the presence of intracellular neurofibrillar structures and soluble non-fibrillar forms of abnormal or hyperphosphorylated Tau protein<sup>[32, 33]</sup>. Fibrillar Tau accumulates in dystrophic neurites forming NFTs which appear extracellular subsequent to neuronal death<sup>[34, 35]</sup>. In Alzheimer's disease, the presence of intracellular NFTs correlates strongly with neuronal loss and progress of the disease, however the pathologic mechanism remains unclear<sup>[35, 36]</sup>. Mutations causing FTDP-17 in humans established that dysfunctional Tau leads to neurodegeneration<sup>[37]</sup>. Nevertheless mutations in *tau* have not yet been linked to AD. Studies suggested that Tau might act downstream of A $\beta$  as demonstrated using *tau* transgenic *Drosophila melanogaster*<sup>[38]</sup>. Co-expression of A $\beta$ 42 and Tau resulted in higher Ser262 phosphorylation levels and enhanced Tau-dependent neurodegeneration<sup>[38]</sup>.

### **1.2.2 Amyloid- $\beta$ pathology**

The term amyloid is derived from the greek “amylon” (starch) and was used first in a medical context by Rudolf Virchow to describe pathogenic deposits in human tissue and organs which displayed starch-like iodine and sulphuric acid staining <sup>[39-41]</sup>. This first assumption led to the opinion that these deposits contained of carbohydrates, but eventually these amyloid deposits were found to consist mainly of proteinaceous material <sup>[42]</sup>. Nowadays, the pathological term amyloid is defined by *in vivo* deposited material with characteristic fibrillar structures when analysed using transmission electron microscopy (TEM) and a typical X-ray diffraction pattern displaying a cross- $\beta$ -sheet structure. Furthermore, amyloid fibrils can be identified under polarising light when stained with the amyloid-specific dye Congo Red by the resulting apple-green birefringence <sup>[43, 44]</sup>.

The A $\beta$  peptide is a hydrophobic peptide with a critical tendency to assemble into stable amyloid fibrils. It is derived from cleavage of the amyloid precursor protein (APP). There are two principle ways to cleave APP (figure 1.3) <sup>[45-47]</sup>. The non-amyloidogenic pathway consists of the cleavage of APP by  $\alpha$ -secretase, which occurs within the A $\beta$  sequence, followed by cleavage with  $\gamma$ -secretase. These processes release the neuroprotective, soluble APPs $\alpha$  and an APP intracellular domain (AICD) <sup>[48]</sup>. The amyloidogenic pathway of APP cleavage is the origin of the aggregation prone A $\beta$  peptides including A $\beta$ (1-40) and A $\beta$ (1-42). These peptides are produced by APP cleavage with  $\beta$ - and  $\gamma$ -secretase and both are found in A $\beta$  plaques as fibrillar structures. The amyloid cascade hypothesis states that mutations in APP or other genes (e.g. secretases) lead to an increase of A $\beta$  production which then leads to the disease. As an example, mutations occurring in presenilin increase the amount of A $\beta$ (1-42) and have been linked to familial forms of AD <sup>[49, 50]</sup>. Additionally, mutations within the A $\beta$  sequence are known to change its aggregation propensity and toxicity <sup>[51, 52]</sup>, for example the arctic mutation A $\beta$ (1-42)E22G (APP: E693E) aggregates faster than A $\beta$ (1-42) and is highly toxic <sup>[53]</sup> whereas mutations around the  $\beta$ -secretase cleavage site enhance the overall A $\beta$  production <sup>[54]</sup>. An extra copy of the APP gene, as occurs in trisomy 21, causes a duplication of APP and accelerates the aggregation of A $\beta$ , thus leading to early-onset AD <sup>[55, 56]</sup>.

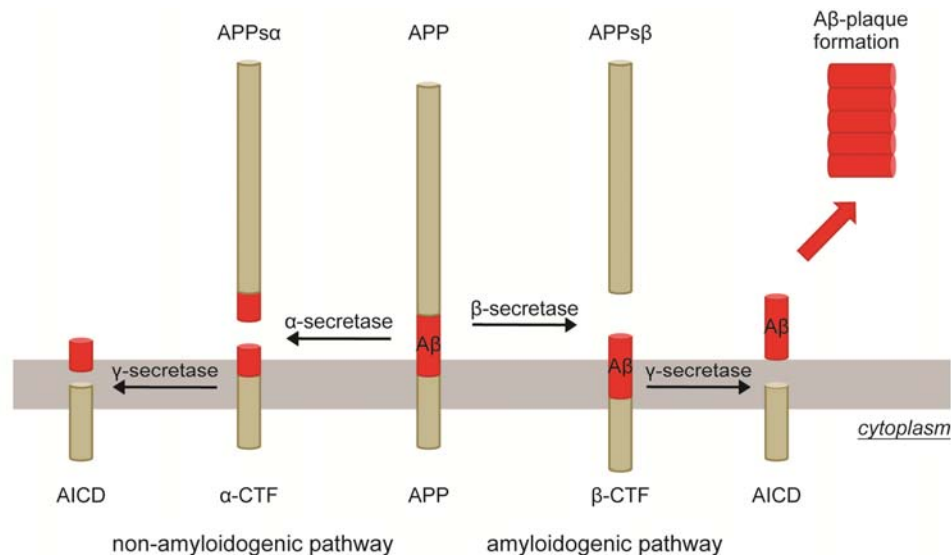


Figure 1.3 Proteolytic cleavage of APP by  $\alpha$ -,  $\beta$ - and  $\gamma$ -secretases (modified from Zhang & Saunders, 2007<sup>[57]</sup>). In the amyloid hypothesis two different proteolytic pathways are suggested for APP: the non-amyloidogenic (left) and the amyloidogenic (right) pathway. Abbreviations: APP = amyloid precursor protein, A $\beta$  = amyloid  $\beta$  peptide, AICD = APP intracellular domain, APP<sub>s</sub> = secreted APP fragment, CTF = C-terminal fragment.

Postmortem analysis of AD patients revealed that the extracellular amyloid plaques consist primarily of fibrillar A $\beta$  peptides<sup>[14]</sup>, but there is evidence that the number of plaques does not correlate with the loss of cognitive function<sup>[46, 58]</sup>. Indeed, transgenic mice expressing APP have demonstrated that soluble levels of A $\beta$  correlate better with the cognitive decline than amyloid plaque load<sup>[59, 60]</sup>. However, analysis of the soluble and insoluble A $\beta$  fractions from human brains demonstrated that a shift occurs from soluble to insoluble A $\beta$  during AD progression, whereas most A $\beta$  remains soluble in normal ageing brains<sup>[61]</sup>.

### **1.3 A $\beta$ aggregates into amyloid fibrils**

*In vitro* studies revealed that mature A $\beta$  fibrils are formed *via* several aggregation intermediates (figure 1.4)<sup>[62, 63]</sup>. This process is a molecular self-assembly that depends on the formation of aggregate nuclei. In the beginning, monomeric peptides start to aggregate into soluble non-fibrillar structures known as oligomers which occur as spherical structures. These oligomers are transient and convert into short, curvilinear shaped, fibrillar intermediates, termed protofibrils. The metastable protofibrils mature into long, straight fibrils with highly regular morphology, as can be seen with techniques such as atomic force microscopy.

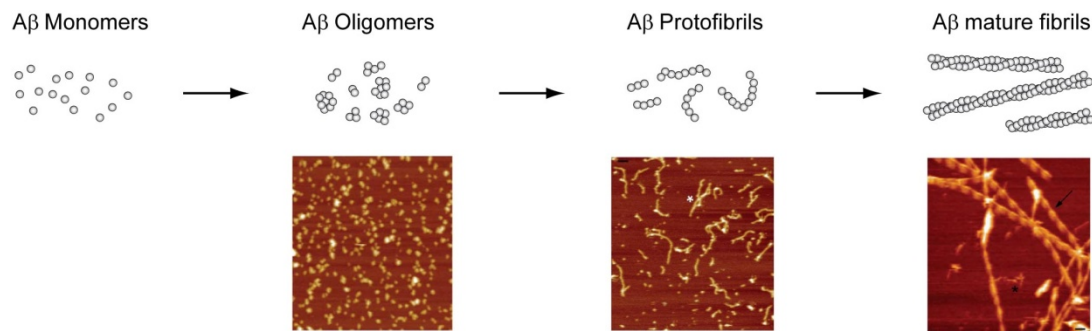


Figure 1.4 Schematic representation of fibrillation of A $\beta$  peptide. The unstructured A $\beta$  peptide aggregates into mature fibrils *via* transient existing intermediate structures (modified from Goldsbury *et al.*, 2005<sup>[62]</sup> and Scheidt *et al.*, 2011<sup>[63]</sup>).

There is evidence that each A $\beta$  aggregate species has toxic effects, as has been shown by Deshpande *et al.* who applied high molecular weight oligomers, A $\beta$ -derived diffusible ligands (ADDLs) and mature A $\beta$  fibrils to primary human neurons<sup>[64]</sup>. All three species were toxic to the cells, although with different effects and to different extents. These results were also seen in analyses of the toxicity of A $\beta$  fibrils towards rat cells and mice brains<sup>[65, 66]</sup>. Overall, it remains unclear if a single intermediate is responsible for causing AD or if it is a combination of the varied species.

#### **1.4 Animal models of Alzheimer's disease**

Although there are *in vivo* data from post mortem human brains available, the mechanism by which A $\beta$  accumulation leads to neurotoxicity and degeneration of neuronal tissue is still unexplored. To gain new insights into the pathogenicity of AD, researchers use animal model systems to reflect the complexity of living organisms. The usage of model organisms provides many advantages, e.g. allowing transgenic manipulation and observation of strong changes in behaviour and cognitive function, while being cost effective and easy to handle. But these models must also fulfil some criteria, such as the possibility of genetic manipulations, usage for drug and immune therapy and reproducibility of the experiments<sup>[67]</sup>. Animal models for AD have been established in both vertebrate (mouse, rat, dog, non-human primates) and invertebrate organisms (worm and fruit fly) depending on the scientific aim of the model<sup>[67]</sup>. Human and non-human primates are closest to humans since both share a high gene homology<sup>[68]</sup>. They are known to develop amyloid plaques and Tau inclusions spontaneously, which can be, but generally are not accompanied by the full neuropathological phenotypes such as cognitive impairment<sup>[69-72]</sup>.

Rodents do not spontaneously develop amyloid plaques, but the advantages of using mice to study AD include the variety of genetic tools available to create transgenic mice and the easy way of handling the animals. In the mid-1990s the development of AD mouse models started with the

PDAPP mouse model, expressing the Indiana familial AD (FAD) mutation hAPP (V717F) <sup>[73]</sup>. The Tg2576 and APP23 mouse models, expressing the Swedish FAD mutation hAPP (K670N M671L) <sup>[74, 75]</sup>, followed and together these three models became the most widely used mouse models in AD research. Nevertheless, other models exist such as TgCRND8 or TgAPParc, modelling different FAD mutations of hAPP <sup>[76, 77]</sup>. The 5x transgenic mouse model (5xFAD) combines 5 mutations linked to FAD, resulting in rapid accumulation of A $\beta$  deposits, memory decline and neuronal loss <sup>[78]</sup>. Additionally, there is a 3xTg-AD model <sup>[79]</sup> available that expresses hAPP (K670N M671L), tau (P301L) and the  $\gamma$ -secretase PSEN1(M146V). These animals develop extracellular A $\beta$  deposits and intracellular NFT's as well as deficits in the long-term potentiation (LTP). Consequently, this mouse model closely recapitulates the human AD pathology. However, a drawback of such models are that large gene or compound screenings are time consuming.

The zebrafish *Danio rerio* is the model of choice for primary toxicity studies in living animals because its high sensitivity to toxins is combined with low costs and easy handling. Gene homologues for APP and the  $\gamma$ -secretases PSEN1 and PSEN2 exist in zebrafish. The inhibition of the  $\gamma$ -secretase is an approach currently undertaken in this model investigating possible compounds that are able to specifically inhibit the activity of the  $\gamma$ -secretase on APP cleavage without affecting its other substrate processing activity <sup>[80]</sup>.

The nematode *Caenorhabditis elegans* is another well established animal model to study A $\beta$  development and gene expression. The advantages of the transparent worm are its short lifespan and the ability to easily monitor the deposition of A $\beta$  and analyse its toxicity. The APP homologue API-1 as well as two presenilin homologues are present in the nematode. The expression of A $\beta$  in the muscle cells led to deposit formation and the animals became progressively paralytic <sup>[81]</sup>. Expression of A $\beta$  in the neurons also resulted in A $\beta$  deposition, however the phenotype involving movement was much weaker <sup>[82]</sup>. Another study demonstrated that A $\beta$  expression caused oxidative stress in the worm, and that this occurred before fibril deposition <sup>[83]</sup>.

#### **1.4.1 *Drosophila melanogaster* as a model organism for AD**

Several advantages exist that make the fruit fly a more useful model organism than other animals. Its genome was sequenced in 2000 <sup>[84]</sup> and homology was found in 77 % from approximately 1000 known genes related with human hereditary diseases <sup>[85]</sup>. The central nervous system (CNS) of *Drosophila melanogaster* works roughly like the one of higher organisms, but is simplified because it has a lesser number of neurons and glia cells. *Drosophila melanogaster* also has a blood-brain barrier, that permits the selective passage of molecules <sup>[86]</sup>. As the efficacy of many neurological

drugs depend on their ability to cross the blood-brain barrier, the fruit fly is an ideal model organism for compound testing.

A high number of genes and signal transduction pathways are conserved from fly to humans. *Drosophila melanogaster* has an amyloid precursor protein-like gene (*appl*), whose amino acid sequence has a high homology to the sequence of the human APP<sup>[87]</sup>. Its analysis provided insights that APPL plays an important role in axonal transport and is essential for optimal nervous system function<sup>[88, 89]</sup>. Nearly a decade later the human APP gene was expressed in *Drosophila melanogaster* and its processing was analysed<sup>[90]</sup>. No A $\beta$  was produced when expressing full length APP, but A $\beta$  could be produced by using a short form which included the A $\beta$  sequence, transmembrane domain and cytoplasmic tail. Thus, the researchers claimed that  $\alpha$ - and  $\gamma$ - secretase activity is conserved, while the  $\beta$ -secretase seems to be altered in insects<sup>[90]</sup>. As a result, in AD fruit fly models A $\beta$  has to be expressed either directly or as APP together with a  $\beta$ - secretase. However, recently a fly  $\beta$ -secretase was identified in *Drosophila melanogaster* that was able to produce A $\beta$  from APPL, leading to A $\beta$  deposition and neurodegeneration<sup>[91]</sup>. But the predominant APPL cleavage appears to be carried out by the  $\alpha$ -secretase. Another approach was carried out in a *Drosophila melanogaster* model created by Greeve *et al.* expressing human APP, the  $\beta$ -secretase BACE1 and the  $\gamma$ -secretase presenilin together<sup>[92]</sup>. Correctly processed A $\beta$  occurred and led to amyloid plaques, neurodegeneration and even a reduced lifespan. This model demonstrated the basic principle of APP processing, including A $\beta$  peptide production, and allowed genetic manipulation of the pathway. However, it had the disadvantage that it was not possible to study single A $\beta$  variants, such as A $\beta$ (1-40) or A $\beta$ (1-42).

In three other fly models, the peptides A $\beta$ (1-40) and A $\beta$ (1-42) were expressed in the fly brain and revealed that the expression of A $\beta$ (1-42) caused amyloid deposition and massive neurodegeneration that was absent when A $\beta$ (1-40) alone was expressed<sup>[93-95]</sup>. Crowther and colleagues additionally expressed the arctic A $\beta$  mutant E22G (A $\beta$ (1-42)<sub>arc</sub>) and showed a dose and age-dependent toxicity of the wildtype (WT) and mutant A $\beta$ (1-42) peptides, resulting in profound phenotypes such as impaired locomotor function, reduced lifespan and damage of the eye structure (rough eye phenotype)<sup>[95]</sup>. In 2007, Luheshi *et al.* compared the aggregation propensity of several A $\beta$  mutant peptides with their neurotoxicity in live fly models, showing a good correlation between the propensity of A $\beta$  to form fibrils and *in vivo* toxicity<sup>[51]</sup>. This correlation was even stronger for A $\beta$  variants with a high propensity to form protofibrillar aggregates. The *Drosophila melanogaster* models were also successfully used to study the subsequent mechanisms of A $\beta$  expression, as well as the efficacy of drugs and the influence of genetic manipulation. Firstly, treating the flies with MK-801 or Congo Red reduced the A $\beta$  dependent phenotypes<sup>[95]</sup>. Secondly, a genetic screen revealed the

occurrence of A $\beta$  dependent oxidative stress and the importance of the iron-binding protein ferritin [96, 97]. Additionally, the influence of neprilysin on A $\beta$  toxicity was discovered [93, 98]. Thirdly, Iijima-Ando and co-workers showed that A $\beta$  expression causes mitochondrial mislocation followed by neuronal dysfunction [99]. These data demonstrated the eligibility of *Drosophila melanogaster* models for testing the effects of drugs and antibodies, as well as to study the mechanism of A $\beta$  induced toxicity in rapid and large scale experiments.

### 1.4.2 Gal4-UAS-System

To create a simple fly model, single A $\beta$  variants are expressed using the Gal4-UAS system, which is commonly used for controlled expression of genes. In particular, the Gal4-UAS system is used in *Drosophila melanogaster* AD models since permanent expression of toxic A $\beta$  peptides leads to unwanted death of fly stocks. In Gal4-UAS models the transgenes to be expressed are fused with an Upstream Activating Sequence (UAS) and use Gal4 binding as a trigger to allow transcription to be started. The Gal4 protein is expressed in a driver line under control of an endogenous promoter for example in the fly neurons or eyes. To activate the protein expression, the transgenic line is crossed with the driver line. In the resulting offspring the Gal4 protein is expressed and initiates the transcription by binding to the UAS sequence of the transgene (figure 1.5). Thus, the system allows a generation- and tissue-specific analysis of the effects of peptide or protein expression, such as A $\beta$ .

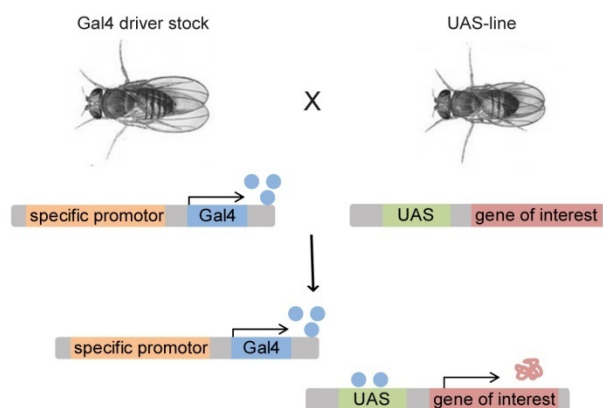


*Figure 1.5* Expression of transgenes in *Drosophila melanogaster* using the Gal4-UAS system. A fly expressing Gal4 under a tissue specific promoter is crossed with a fly that is made up with the transgene fused to the UAS sequence. The resulting offspring can express the transgene in the tissue determined by the Gal4 fly. Abbreviations: Gal4 = yeast Gal4 protein, UAS = Upstream Activating Sequence.

### 1.5 Treatment of Alzheimer's disease using drugs and immunisation

To date, no cure has been found to heal or stop the progress of AD. It thus remains necessary to develop tools to identify toxic species and get insights into the pathology of the disease. Fibrillisation studies on A $\beta$  revealed that small-molecule compounds like Ro 90-7501, HMP (hexadecyl-N-methylpiperidinium) or imidazopyridoindoles can inhibit the formation of mature amyloid fibrils, and in case of the last two compounds, can ameliorate A $\beta$ (1-42)-induced toxicity in a rat cell culture model <sup>[100-102]</sup>. Additionally, several approaches like drug development or immunotherapy (overview in table 1.2) are under investigation, but so far only drugs approved by the US Food and Drug Administration (FDA) for AD treat only the symptoms of the disease <sup>[103, 104]</sup>. A number of synthetic drugs have been developed and tested for the treatment of AD <sup>[105-112]</sup>. Within those drugs a first promising, and FDA-approved pharmaceutical was the N-methyl-D-aspartate (NMDA) receptor antagonist memantine, which inhibits the overstimulation of a cell by blocking the NMDA receptor and preventing excessive Ca<sup>2+</sup> influx, resulting in beneficial effects on behaviour and cognition <sup>[105]</sup>. Reduction of A $\beta$ (1-42) levels and modulation of  $\gamma$ -secretase was seen when applying nonsteroidal anti-inflammatory drugs (NSAIDs), such as ibuprofen, to mice and cell culture systems <sup>[111]</sup>. Clinical studies suggest that NSAIDs can delay the progression of AD. Another compound which has completed phase II trials is the plant sugar alcohol scyllo-inositol (termed: ELND005), which was found to inhibit the aggregation of A $\beta$  in transgenic mice <sup>[112]</sup>.

Table 1.2: Overview of drugs in clinical trials. Abbreviations: FDA = U.S. Food and Drug Administration

name	mechanism	company	FDA phase	status
AN1792	active immunisation	Elan Pharmaceuticals	phase II	failed
Bapineuzumab	passive immunisation	Elan Pharmaceuticals & Wyeth	phase III	ongoing
ELND005	A $\beta$ aggregation inhibitor	Elan Pharmaceuticals	phase II	ongoing
Galantamine	acetylcholinesterase inhibitor	Janssen-Cilag AG	FDA approved	
Ibuprofen	NSAIDS		phase IV	discontinued
Memantine	NMDA receptor antagonist	Merz & Co.	FDA approved	
Rivastigmine	acetylcholinesterase inhibitor	Novartis	FDA approved	
Simvastatin	HMG-CoA reductase inhibitor	Merck & Co.	phase II/III	ongoing
Tarenflurbil	modulation $\gamma$ -secretase activity	Myriad Pharmaceuticals	phase III	failed
Intravenous immunoglobulins	anti-A $\beta$ and anti-inflammatory properties	Baxter	phase III	ongoing

A second approach to AD treatment is the idea to use active and passive vaccination to create antibodies against A $\beta$  <sup>[113]</sup>. Two possible approaches were applied to animal models: active vaccination applying A $\beta$ (1-42) and the subsequent development of antibodies, and passive immunisation with anti-A $\beta$  antibodies. In both methods antibodies bind to A $\beta$  and induce its clearance (figure 1.6).

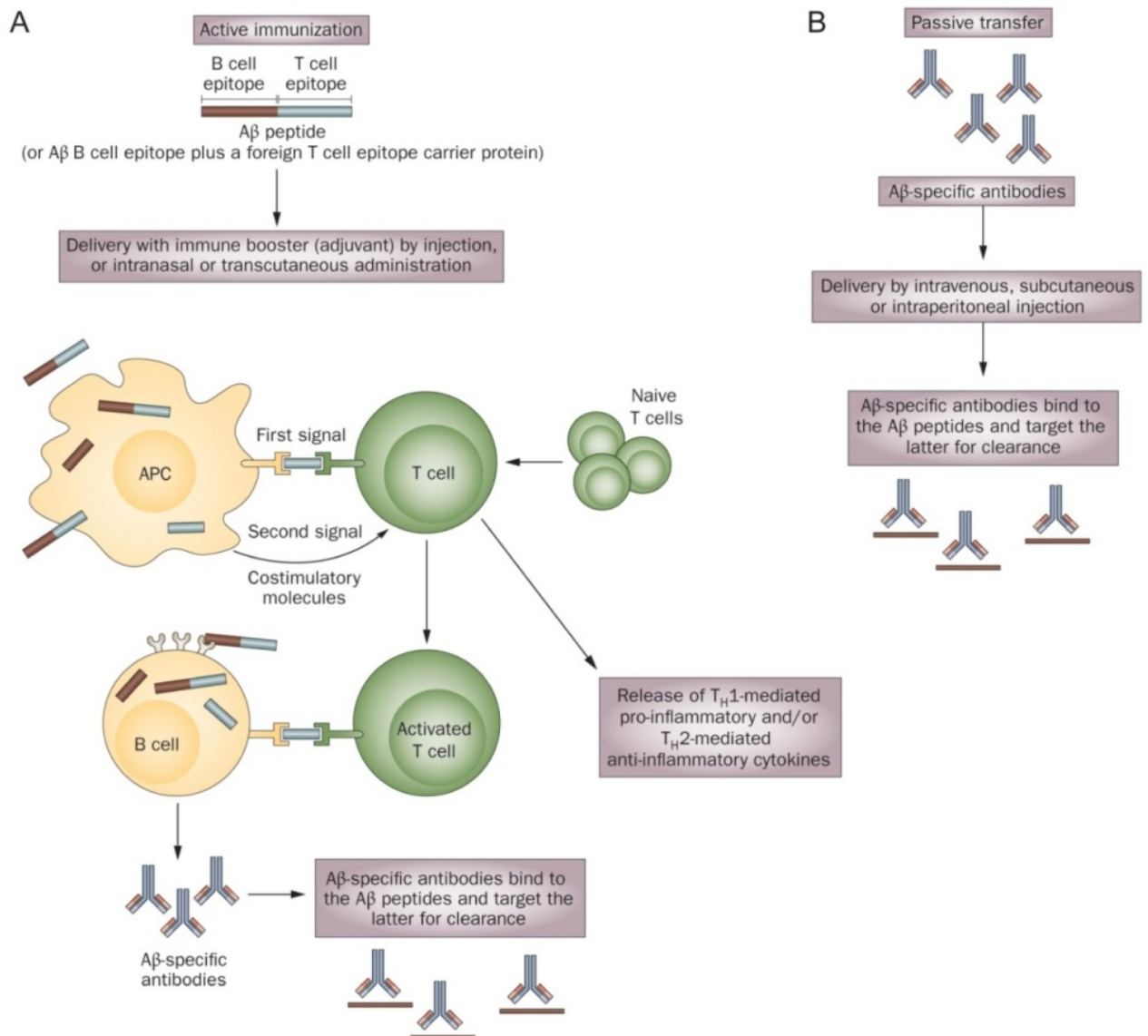


Figure 1.6 Comparison of active and passive immunisation (adopted from Lemere & Masliah, 2010 <sup>[114]</sup>).

Active A $\beta$ -immunisation studies demonstrated that generated anti-A $\beta$  antibodies are capable of reducing AD-like pathology and improving behavioural deficits in transgenic mice <sup>[115-118]</sup>. However, a clinical trial using active immunisation with AN1792 (synthetic A $\beta$ 1-42) was stopped in phase IIa due to the development of aseptic meningoencephalitis by some patients <sup>[119, 120]</sup>. Nevertheless, this

trial showed that immunotherapy is worth investigation. Petrushina *et al.* demonstrated that in mice with pre-existing AD pathology active vaccination selectively initiating B-cell response is able to prevent the adverse effects seen in the AN1792 trial <sup>[121]</sup>. A second approach using immunisation with keyhole limpet hemocyanin (KLH)-A $\beta$ <sup>37-42</sup> in mice models induced a high selective, non-inflammatory antibody response against A $\beta$ (1-42) <sup>[122]</sup>. The resulting IgG antibodies were also able to stain senile plaques in AD brains.

By 1996 and 1997 Solomon *et al.* had already demonstrated the ability of monoclonal A $\beta$  antibodies to dissolve A $\beta$  aggregates and also to prevent their formation <sup>[123, 124]</sup>. For example, the m266 antibody was tested in young PDAPP mice where it altered the level of A $\beta$  in the plasma and CNS, and reduced the deposition of A $\beta$  in the mouse brain <sup>[125]</sup>. Also, in another approach the plaque burden could be reduced due to administration of an antibody <sup>[126]</sup>. An approach using passive immunisation, led to reduced A $\beta$  deposition and improved learning and memory, despite development of angiopathy <sup>[127]</sup>. One passive immunisation study is currently in phase III trials, using the monoclonal antibody Bapineuzumab which targets the N-terminus of A $\beta$  and was designed to clear A $\beta$  from the brain.

Recently, endogenous antibodies against A $\beta$  were discovered in human blood pools <sup>[128-130]</sup>. These so-called autoantibodies have been found to be reduced in AD patients <sup>[130, 131]</sup>. Dodel *et al.* revealed that these autoantibodies bind preferentially to early A $\beta$  aggregation intermediates, thus leading to increased A $\beta$  clearance, reduced plaque formation and improved cognition <sup>[132]</sup>. Clinical trials into AD treatment are currently being run using human intravenous immunoglobulins (IVIGs) containing A $\beta$ -autoantibodies. IVIGs may promote A $\beta$  clearance and improve cognitive function, as well as decelerating cognitive decline.

### **1.5.1 Conformation-sensitive antibodies against A $\beta$**

Another approach to the question of A $\beta$  dependent neurotoxicity is the use of conformation-sensitive antibodies. Compared with common, sequence-specific antibodies a conformation-sensitive antibody recognises an epitope that is formed while folding or misfolding of a protein into its 3 dimensional structure (figure 1.7). Conformation-sensitive antibodies can be used to target specific intermediates of the amyloid formation and provide information about the pathogenicity of specific aggregation intermediates *in vivo*.

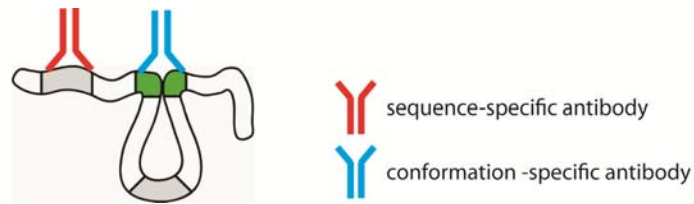


*Figure 1.7* Epitope recognition by conformation-sensitive versus sequence-specific antibodies. A sequential epitope results from the amino acid sequence while a conformational epitope is created when the protein folds into a secondary, tertiary or quaternary structure.

It has been shown previously that conformation-sensitive antibodies, either derived from vaccination or engineered, are able to recognise several A $\beta$  aggregation intermediates such as soluble oligomers <sup>[133-135]</sup> or fibrils <sup>[136-138]</sup>. Reduced A $\beta$  neurotoxicity was also found for other conformation-sensitive antibodies tested in cell culture or animal models <sup>[133, 134, 139]</sup>. Additionally, several antibodies do not recognise only the A $\beta$  oligomers or fibrils, but also bind to other disease-related amyloid intermediates suggesting common structural motifs <sup>[133, 136, 137]</sup>.

### **1.5.2 The camlid antibody domains B10 und KW1**

Camelid serum contains of a unique type of antibodies, so called heavy-chain antibodies. In comparison to ordinary mammalian antibodies, these antibodies are lacking the two light chains. This allows the heavy chains to attain a greater structural flexibility (figure 1.8). These heavy chains are referred to as VHHs and are small, functional antigen binding domains <sup>[140, 141]</sup>. Consequently, the antigen binding specificity is restricted to the hypervariable region of the heavy chain, especially as the complementary determining region 3 (CDR 3) is statistically longer compared to conventional antibodies allowing a broad antigen-binding repertoire <sup>[142, 143]</sup>. In contrast, the smallest functional antigen binding fragment of conventional antibodies is the Fv region, containing only one variable heavy and light chain (~30 kDa). Compared to common antibodies, VHH domains can be expressed recombinantly as single-domain antibodies, leading to small molecules (~15 kDa) with better solubility due to their extended CDR 3 folding around the hydrophobic part of the domain <sup>[142]</sup>. Furthermore, VHH domains do not activate the complement system because of the missing Fc part.

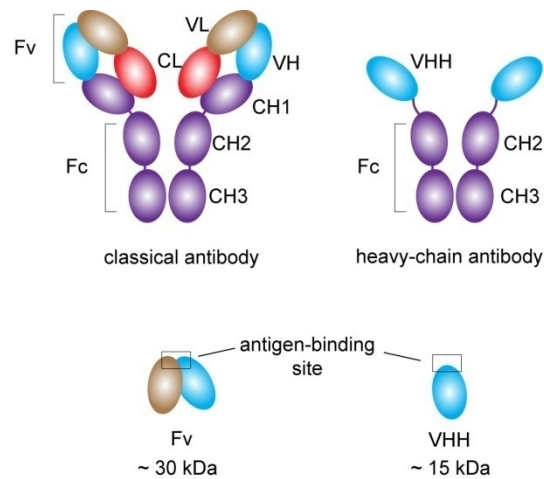


*Figure 1.8* Camelid antibodies (right) compared to ordinary mammalian antibodies (left). The antigen-binding side of camelid antibodies is formed by the VHH domain whereas in mammalian antibodies both the VL and VH are required (modified from Muyldermans *et al.*, 2001<sup>[142]</sup>). The boxes mark the antigen binding sites.

B10 and KW1 are two conformation-sensitive antibody domains that were selected from a camelid VHH domain library using phage display targeted against A $\beta$  species<sup>[135, 138]</sup>. In this technique, the VHH domains are presented on the phage surface and the phages are allowed to bind to immobilised antigens. To prevent the selection of sequence-specific antibodies, a competitive assay was applied where the phage library was mixed with disaggregated A $\beta$  during the process of incubation with the immobilised antigens.

After three panning rounds using immobilised A $\beta$ (1-40) fibrils, one VHH domain was selected which showed high specificity to A $\beta$  fibrils. The resulting VHH domain, B10, is a high selective fibril binder that can prevent the formation of mature A $\beta$  fibrils at substoichiometric concentrations. It acts by stabilising A $\beta$  protofibrillar intermediates, as shown by ThT kinetics and electron microscopy (figure 1.9A)<sup>[138]</sup>. Additionally, its selectivity enables B10 to discriminate amyloid fibrils from oligomeric or disaggregated A $\beta$ . B10 also binds to amyloid plaques in human AD brain slices, whereas no binding was observed in non-demented control brains<sup>[138, 144]</sup>. Furthermore, the B10 antigen binding site is strongly positively charged and recognises an acidic moiety that is common on the surface of a wide number of amyloid fibrils<sup>[145, 146]</sup>.

A second VHH domain was selected which acted against immobilised A $\beta$ (1-40) oligomers. After four panning rounds, five clones with similar CDR sequences were found to be specific to A $\beta$ (1-40) oligomers. The resulting VHH domain was termed KW1. It binds selectively to A $\beta$ (1-40) oligomers without recognising A $\beta$  fibrils or disaggregated A $\beta$ <sup>[135]</sup>. Furthermore, KW1 is able to retard the formation of ThT positive species in a substoichiometric manner leading to the aggregation of non-fibrillar species (figure 1.9B). It was found to neutralise the oligomer-dependent LTP reduction

on hippocampal slices of mice. KW1 is also able to discriminate between different types of oligomers. It does not bind to any A $\beta$ (1-42) oligomer preparation or oligomers derived from peptides other than A $\beta$ . The encountered selectivity of KW1 differs drastically from the widely used polyclonal A11 antibody serum, which recognises soluble oligomers independent from their amino acid sequence. The specificity of KW1 could arise from its monoclonal nature, which is consistent with the higher selectivity of A11-like monoclonal antibodies<sup>[147]</sup>.

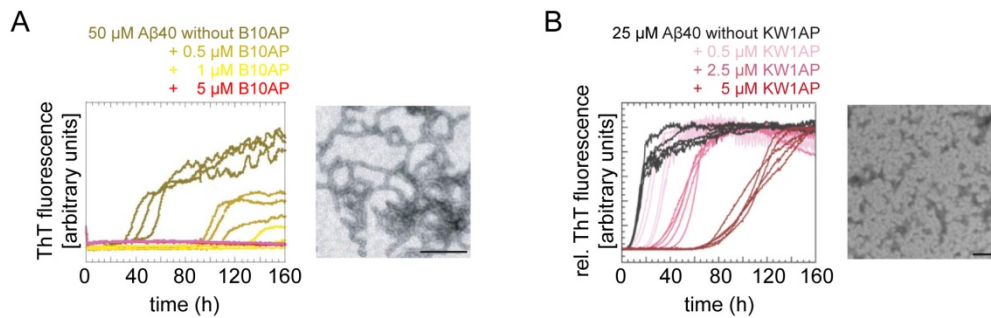


**Figure 1.9** Characterisation of the conformation-sensitive VHH domains B10 (A) and KW1 (B). Both antibody domains inhibit the formation of mature amyloid fibrils by stabilising A $\beta$  protofibrils (A) or non-fibrillar aggregates (B). Picture is modified from Habicht *et al.*, 2007<sup>[138]</sup> and Morgado *et al.*, 2012<sup>[135]</sup>.

## **1.6 Aims of the thesis**

B10 and KW1 are both able to interfere in the A $\beta$  aggregation process *in vitro*. Thus, both antibody domains are powerful tools to get further insights into the aggregation mechanism of A $\beta$ . To date, it remains elusive if a single A $\beta$  aggregation species is responsible for causing AD. The activities of A $\beta$  aggregates, ranging from differently shaped oligomers and protofibrils to mature amyloid fibrils<sup>[14, 62, 148, 149]</sup>, could be demonstrated by intra-cerebral injections into AD mouse models<sup>[150]</sup>, cellular assays for toxicity or neuronal dysfunction, LTP and synaptic plasticity measurements<sup>[14, 150-152]</sup>. However, all these attempts to identify a critical species of AD development *in vivo* have been invasive, that is involved an external interference, and have not considered the natural environment occurring in the brain. This thesis presents a unique approach to this challenge by endogenously targeting single A $\beta$  aggregation species using conformation-sensitive antibody fragments. The fibril binder B10 and the oligomer binder KW1 were used to examine the pathogenic role of A $\beta$  fibrils and oligomers *in vivo*. Investigations using endogenously expressed B10 and KW1 were carried out in a *Drosophila melanogaster* model of AD, to conformationally target the respective A $\beta$  aggregation species and address the following questions:

- 1) Can antibody domains, conformationally targeting specific A $\beta$  aggregates *in vivo*, alter the AD phenotype in *Drosophila melanogaster*?
- 2) What is the pathogenic relevance of A $\beta$  fibrils?
- 3) Does targeting of A $\beta$  oligomers affect the AD pathology?
- 4) Do conformation-sensitive antibodies have a therapeutic potential for AD?

## 2. Material & methods

### 2.1 Material:

#### 2.1.1 Chemicals

name	company
Hexamincobalt(III) chloride,	Applichem
Acc65I, EcoRI, HindIII, NdeI, XbaI, XhoI	Fermentas
Boric acid, Coomassie Brilliant Blue R-250, Copper chloride dihydrate, Hexafluoro-2-propanol	Fluka
Agarose, Blasticidin, DEPC-treated water, Dynabeads® Protein A, Hoechst 33342 (DAPI), Normal goat serum (NGS), PCR SuperMix, Propidium iodide, SYBR® Safe DNA Gel Stain, TRIzol®	Invitrogen
Chloroform	Merck
MSD Blocker A, MSD Read Buffer	Meso Scale discovery
Fetal bovine serum (FBS), Sf9-S2 medium	PAA
Uranyl acetate dihydrate	Plano
Sodium molybdate	Riedel de Haën
Acetic acid, Agar-Agar, Ammonium chloride, 30 % Ammonium hydroxidesolution, Ampicillin, Chloramphenicol, Dimethylsulfoxide, Di-Sodium hydrogen phosphate dodecahydrate, EDTA, Ethanol, Glucose, Guanidinium hydrochloride, HEPES, Imidazol, Isopropyl β-D-1-thiogalactopyranoside, Isopropanol, LB medium, Lithium chloride, magnesium sulphate, Manganese(II)chloride, Methanol, Milk powder, Potassium acetate, Potassium chloride, Potassium hydrogen phosphate, Sodium chloride, Trichloroacetic acid, Trifluoroacetic acid, Tris, Tween-20, Urea, Zinc Acetate	Roth
Cacodylic acid, Glutaraldehyde	Serva
Copper(II) sulphate, Ponceau S, Sodium dodecyl sulfate, Thioflavin T, TritonX-100	Sigma-Aldrich
Vectashield mounting medium	Vector Laboratories

#### 2.1.2 Kits and readymade solutions

name	company
SensoLyte® Homogeneous Rh110 Caspase - 3/7 Assay Kit	Anaspec
DC™ Protein Assay	Biorad
LDH-Cytotoxicity Assay Kit II	Biovision
RevertAid™ First Strand cDNA Synthesis Kit	Fermentas
PCR SuperMix	Invitrogen
NucleoBond® PC 100 kit	Macherey & Nagel
NucleoSpin® Extract II gel extraction kit	Macherey & Nagel
QIAprep Spin Miniprep Kit	Qiagen
SuperSignal West Pico Chemiluminescent Substrate	Pierce
SuperSignal West Femto Chemiluminescent Substrate	Pierce
NBT/BCIP -1-Step Substrat	Pierce
Cell Proliferation Kit I (MTT)	Roche
FuGENE® HD Transfection Reagent	Roche
QuikChange II XL Site-Directed Mutagenesis Kit	Stratagene

**2.1.3 Equipment**

name	company
Sonorex Digital 10P ultrasonic bath	Bandelin
CPD 030 Critical Point Dryer	BAL-TEC
SCD 005 Sputter Coater	BAL-TEC
Trans-Blot SD Semi-Dry Transfer Cell	Biorad
PowerPac HC Power Supply	Biorad
GelAir Drying System	Biorad
FLUOstar Omega reader	BMG Labtech
Freeze dryer	Martin Christ GmbH
Mastercycler personal	Eppendorf
Cooling microcentrifuge 5415 R	Eppendorf
Chromatographie System ÄKTAexplorer 100	GE Healthcare
Chromatographie System ÄKTApurifier 100	GE Healthcare
Cytoperm Incubator	Heraeus Instruments
HeraSafe Typ HS 12 flow cabinet	Heraeus Instruments
Cooling benchtop centrifuge Rotina 380R	Hettich
XCell SureLock™ Mini-Cell	Invitrogen
Laboport Vakuum pump N86KN.18	KNF Neuberger
Milli-Q Advantage A10 Water Purification System	Millipore
NanoDrop 2000	NanoDrop
ECLIPSE TE3000-E confocal microscope	Nikon
Lambda 900 spectrometer	Perkin Elmer
LS 55 fluorescence spectrometer	Perkin Elmer
UV transilluminator	Raytest
Helios Gamma UV-Vis Spectrophotometer	Thermo Scientific
Unitherm WA25 incubator	Uniequip
AGT2 submarine gel tank	VWR
Spot-Blot Apparatur Minifold I System	Whatman
EM 900 transmission electron microscope	Zeiss
LEO-1450 VP scanning electron microscope	Zeiss

**2.1.4 Programs**

name	company
Adobe Illustrator CS2	Adobe
Adobe Photoshop CS	Adobe
BioEdit	Ibis Therapeutics
Clone Manager 7	Sci-Ed Software
GraphPad Prism	GraphPad Software
ImageJ	nih.gov
KaleidaGraph	Synergy Software
Microsoft Office 2007	Microsoft
Sigma Plot 11	Systat Software Inc
TotalLab 100	Nonlinear Dynamics

**2.1.5 *E. coli* strains**

strain	genotype	source
XL10-Gold	Tet <sup>r</sup> , $\Delta(mcrA)183$ , $\Delta(mcrCB-hsdSMR-mrr)173$ , <i>endA1</i> , <i>supE44</i> , <i>thi-1</i> , <i>recA1</i> , <i>gyrA96</i> , <i>relA1</i> , <i>lac Hte</i> , [F', <i>proAB</i> , <i>lacIqZΔM15</i> , Tn10 (Tet <sup>r</sup> ) Amy Cam <sup>r</sup> ]	Stratagene
RV308	( $\Delta(lac)\chi74$ <i>galPO-308::IS2 rpsL</i> )	Maurer <i>et al.</i> <sup>[153]</sup>

### 2.1.6 Plasmids

name	usage	source
pGA4_B10	vector for synthetic B10	GeneArt
pGA18 KW1	vector for synthetic KW1	GeneArt
pMK-RQ_AP-Nullmut	vector for synthetic AP	Geneart
pUASTattB	basis vector for expression in <i>Drosophila melanogaster</i> ( <i>D.mel</i> )	L. Luheshi, Cambridge University
pUASTattB-B10	expression of B10 in <i>D.mel</i>	C.Haupt, HKI Jena
pUASTattB-KW1	expression of KW1 in <i>D.mel</i>	this thesis
pUASTattB-B10m	cloning of inactive B10(R39AR61A) for <i>D.mel</i>	this thesis
pUASTattB-B10APi	expression of B10AP in <i>D.mel</i>	this thesis
pUASTattB-KW1APi	expression of KW1AP in <i>D.mel</i>	this thesis
pUASTattB-B10mAPi	expression of inactive B10(R39AR61A)AP in <i>D.mel</i>	this thesis
pMA B10-myc	vector for synthetic B10-myc	GeneArt
p41 B10-myc	expression of B10-myc in <i>E. coli</i>	this thesis
pMT/V5-HisA	basis vector for transfection of S2 cells	Invitrogen
pMA-B10AP-S2	vector for synthetic B10AP for S2 cells	GeneArt
pMA-KW1AP-S2	vector for synthetic KW1AP for S2 cells	GeneArt
pMT/V5-HisA-B10AP-S2	expression of B10AP in S2 cells	this thesis
pMT/V5-HisA-KW1AP-S2	expression of KW1AP in S2 cells	this thesis
pCoBlast	blasticidine selection vector for S2 cells	Invitrogen

### 2.1.7 Proteins

name	source	purity	
A $\beta$ (1-40)	chemical synthesis	> 96 % (RPC)	Dr. Sven Rothmund, University Leipzig
A $\beta$ (1-42)	chemical synthesis	> 96 % (RPC)	Dr. Sven Rothmund
A $\beta$ (1-42)arc	chemical synthesis	> 96 % (RPC)	Dr. Sven Rothmund
B10AP	recombinant expression	> 95 % (SDS-PAGE)	in house <sup>[138]</sup>
KW1AP	recombinant expression	> 95 % (SDS-PAGE)	in house <sup>[135]</sup>

### 2.1.8 *Drosophila melanogaster* strains, marker and balancer

#### 2.1.8.1 *Drosophila melanogaster* strains

name	genome	chromosome	source
white <sup>1118</sup> <sub>iso</sub>	white <sup>-</sup> wildtype	X	D.Crowther, Cambridge University
Gal4-elav <sup>c155</sup>	Gal4 gene	X	D.Crowther
51D	attP landing site	2	Bloomington
B10/CyO	B10	2	BestGene
KW1/CyO	KW1	2	BestGene
B10APi/CyO	B10AP	2	BestGene
KW1APi/CyO	KW1AP	2	BestGene
B10mAPi/CyO	B10mAP	2	BestGene
A $\beta$ 40-29.1	A $\beta$ 40	2	D.Crowther
A $\beta$ 40-51D	A $\beta$ 40	2	D.Crowther
A $\beta$ 40-29.3	A $\beta$ 40	3	D.Crowther
Alz8	A $\beta$ 42	3	D.Crowther
Arc10.2k	A $\beta$ 42E22G	3	D.Crowther

### 2.1.8.2 *Drosophila melanogaster* marker and balancer <sup>[154]</sup>

name	mutation	type	chromosome
<i>IF</i>	<i>Irregular facets</i>	marker	2
<i>CyO</i>	<i>Curly wings</i>	balancer	2
<i>MKRS</i>	<i>Stubble bristles</i>	marker	3
<i>TM6B</i>	<i>Hu; Humeral</i>	balancer	3

### 2.1.9 Used cell lines

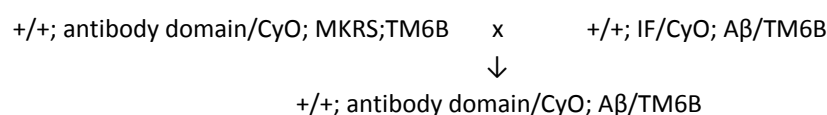
name	transgene	medium	source
S2	-	Sf9-S2	M. Heidler, Max-Planck Research Unit, Halle
S2-B10AP	antibody domain B10AP	Sf9-S2 + 20µg/ml Blastidine	this thesis
S2-KW1AP	antibody domain KW1AP	Sf9-S2 + 20µg/ml Blastidine	this thesis
SH-SY5Y	-	DMEM + 10 % FBS + 2 % Pen/Strep	DSMZ (no. ACC-209)

## 2.2 Methods

### 2.2.1 *Drosophila* work

#### 2.2.1.1 Husbandry of *Drosophila melanogaster* and generation of transgenic flies

Flies were cultured on standard fly food supplemented with dried yeast. Fly stocks were kept at 18 °C and crosses were set up at 25 °C, if not stated otherwise. *Drosophila melanogaster* transgenic for Aβ(1-40), Aβ(1-42), and Aβ(1-42)arc have been described in Crowther *et al.* (2005) <sup>[95]</sup>. *Drosophila melanogaster* transgenic for the antibody domains B10, B10APi, B10mAPi, KW1, KW1APi were received from BestGene Inc. (USA) created by embryo microinjection using the φC31 site-specific integration system <sup>[155]</sup>. In particular, one fly strain providing the landing site for the transgene on the second chromosome (51D) was chosen to create transgenic fly lines with similar expression levels. All transgenes were tracked using marker and balancer chromosomes (table 2.1.8.2) and the balancer chromosomes also inhibited recombination. To create stable double transgenic stocks *Drosophila* transgenic for the antibody domains were each crossed with *Drosophila* transgenic for Aβ(1-40), Aβ(1-42), and Aβ(1-42)arc:

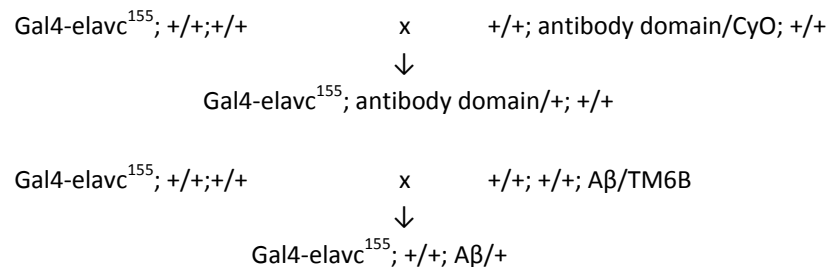


Each transgene was cloned with the same secretion signal peptide (MASKVSILLLLTVHLLAAQTFAQ), derived from the *Drosophila* necrotic gene <sup>[156]</sup> to equally target its expression to the secretory pathway. The expression was activated using the Gal4-UAS expressing system (1.4.2).

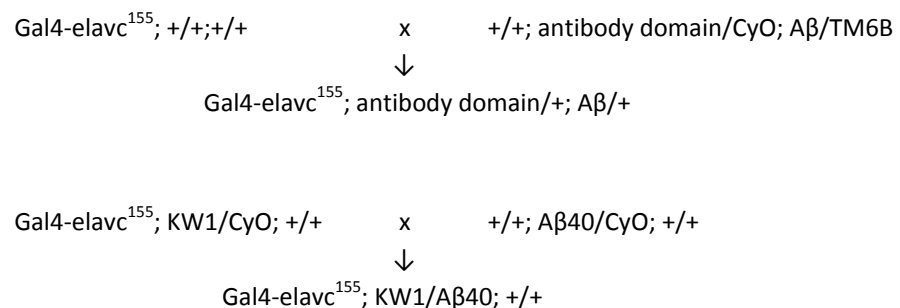
### 2.2.1.2 Gal4-UAS expression of *Drosophila* transgenes

The Gal4-UAS expression system is considered to be an easy handling method to study and control the expression of genes in the fruit fly <sup>[157]</sup>. The system is based on 2 parts: the Gal4 gene, coding for the yeast transcription activator protein Gal4, and the Upstream Activating Sequence (UAS), a short promoter section that is bound specifically by Gal4 to activate the gene transcription. There is a variety of Gal4 lines that express Gal4 specifically in fly tissue e.g. neuronal tissue or muscle cells. The fly analysis in this work is done with the neuronal Gal4 line *elav<sup>c155</sup>* and all transgenes are preceded with the UAS sequence. To express the antibody domains, A $\beta$  variants or RNAi the following crosses were set up to combine both parts of the Gal4-UAS system in offspring:

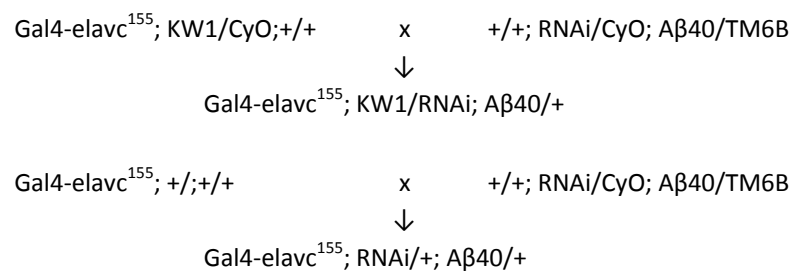
#### expression of the antibody domains or A $\beta$ :



#### expression of the antibody domain and the A $\beta$ peptides:



#### expression of RNAi with KW1 and A $\beta$ 40:



### **2.2.1.3 Survival and climbing assay**

The behaviour of *Drosophila* is measured in a negative geotaxis assay. After crossing the flies with Gal4-elav<sup>c155</sup> the offspring of all genotypes expressing A $\beta$  either alone or with an antibody domain was analysed in triplicates. Between the single analyses the flies were kept at 29 °C. For the analysis 15 flies ( $n_{\text{total}}$ ) were placed in 25 ml plastic tubes, tapped down to the bottom and allowed to climb for 45 sec. The number of flies above the 25 ml line ( $n_{\text{top}}$ ) and below the 2 ml line ( $n_{\text{bottom}}$ ) was counted and used to calculate the mobility index in the following equation:

$$CI = 0.5 \cdot \frac{n_{\text{total}} + n_{\text{top}} - n_{\text{bottom}}}{n_{\text{total}}}$$

To analyse the lifespan of the flies expressing A $\beta$  either with or without an antibody domain a survival assay was done at 29 °C. 100 flies per genotype were divided in groups of ten and placed in glass vials with fresh food every second day. The number of living flies was counted daily or every second day and finally the survival curves and median survivals of each genotype were analysed using Kaplan-Meier estimator, including confidence intervals and a Log-rank test (Sigma Plot or GraphPad Prism).

To examine the effect of MK-801 on the lifespan the drug was dissolved at a concentration of 3  $\mu\text{M}$  in pure water. 2 ml of the drug solution or pure water was added on top of the fly food and dried over night at room temperature.

## **2.2.2 Molecular biology methods**

### **2.2.2.1 Cloning : digestion, ligation, transformation**

The expression of the antibody domains in *Drosophila melanogaster* or cell culture required the sub cloning of the synthesised genes into the appropriate expression plasmids pUASTattB or pMT/V5-HisA, respectively. For expression in *E. coli* the synthetic gene B10-myc was sub cloned into the bacterial expression plasmid p41.

Therefore the genes were cut out of the customised vector using appropriate restriction enzymes. The reactions were set up in a total volume of 20  $\mu\text{l}$  and incubated for at least 2 hours at 37 °C:

0,5-1 $\mu\text{g}$ DNA	
2 $\mu\text{l}$	10 x buffer
1 $\mu\text{l}$	enzyme I
1 $\mu\text{l}$	enzyme II
add pure water up to 20 $\mu\text{l}$	

Afterwards the resulting fragments were separated by agarose gel electrophoresis, the bands were cut out of the gel under UV light and the DNA was eluted using the NucleoSpin® Extract II gel extraction kit (Macherey & Nagel). New plasmids were produced by cloning the gene fragments into the linear target plasmid. Therefore a ligation reaction was set up in a total volume of 20 µl:

20-100 ng linear plasmid DNA  
 5:1 insert DNA (molar ratio over vector)  
 2 µl 10x T4 DNA Ligase buffer  
 1 µl T4 DNA Ligase  
 add sterile pure water up to 20 µl

The mixture was incubated over night at 16 °C and 5 µl were used to transform 50 µl *E. coli* RV308 cells. Therefore the DNA was incubated with the chemically competent cells for 30 min on ice. A heat shock was applied for 90 sec at 42 °C and the cells were chilled for 2 min on ice before adding 500 µl prewarmed LB medium. After incubation for 1 hour at 37 °C the cells were plated on selective LB-agar and grown over night at 37 °C. Single clones were picked and grown in small cultures (5 ml) to amplify the plasmids before verification by restriction and sequencing. Positive clones were amplified in large cultures (100 ml) to obtain high concentrated plasmids.

The plasmids from small cultures were extracted using QIAprep Spin Miniprep Kit (Qiagen) and large cultures were handled with the NucleoBond® PC 100 kit (Macherey & Nagel).

### **2.2.2.2 Site-specific mutagenesis**

All amino acid exchanges or restriction site insertions were done using the QuikChange II XL Site-Directed Mutagenesis Kit (Stratagene). The QuikChange® Primer Design tool (Agilent Technologies) was used to generate appropriate primer with the optimal melting temperature (table 2.1). All mutants were cloned into *E. coli* RV308 cells and verified by sequencing.

Table 2.1: Primer for site-specific mutagenesis.

name	sequence
AP D51A	5' -TTT TGC TGA TTG GCG CTG GGA TGG GGG ACT C-3'
AP D51Arev	5' -GAG TCC CCC ATC CCA GCG CCA ATC AGC AAA A-3'
AP S102G	5' -GAC TAC GTC ACC GAC GGG GCT GCA TCA GCA AC-3'
AP S102Grev	5' -GTT GCT GAT GCA GCC CCG TCG GTG ACG TAG TC-3'
B10R39Afw	5' -CCA CCG CTA CCA CGC CTG GTT CCG CCA G-3'
B10R39Arev	5' -CTG GCG GAA CCA GGC GTG GTA GCG GTG G-3'
B10R61Afw	5' -CCA GAG CGG CAT GGC CAC CTA CTA CGC C-3'
B10R61Arev	5' -GGC GTA GTA GGT GGC CAT GCC GCT CTG G-3'
B10Kpnlfwd	5' -CAG CGA GGA AGA CCT GGG TAC CTA ATA GCT CGA GGG TA-3'
B10Kpnlrev	5' -TAC CCT CGA GCT ATT AGG TAC CCA GGT CTT CCT CGC TG-3'
KW1Kpnlfwd	5' -TCA GCG AGG AGG ATC TGG GTA CCT AAT AAC TCG AGG GTA C-3'
KW1Kpnlrev	5' -GTA CCC TCG AGT TAT TAG GTA CCC AGA TCC TCC TCG CTG A-3'

### **2.2.2.3 Isolation of genomic DNA**

The preparation of genomic DNA was done according to the method “Quick Fly Genomic DNA Prep” by E. Jay Rehm (Berkeley *Drosophila* Genome Project, BDGP). Briefly, 30 flies were homogenised in 200 µl buffer A (100 mM Tris-HCl pH 7.5; 100 mM EDTA; 100 mM NaCl; 0,5 % SDS) and after adding 200 µl buffer A the samples were incubated for 30 min at 65 °C. Subsequently, 800 µl LiCl/KOAc solution (6 M LiCl and 5 M KOAc in a ratio of 2,5 : 1) were added and the samples were incubated for 10 min on ice. After centrifugation for 15 min at 4 °C and 13000 *g* the supernatants were transferred into fresh tubes and the DNA was precipitated by adding 600 µl isopropanol followed by centrifugation for 15 min at room temperature and 13000 *g*. The pellet was washed with 70 % ethanol, air dried and resolved in 150 µl pure water. Afterwards the DNA was stored at -20 °C.

### **2.2.2.4 RNA extraction**

RNA was isolated from flies by using the TRIzol® Reagent (Invitrogen). 15-20 fly heads or 5 flybodies were homogenised in 100 µl TRIzol® using a plastic homogeniser. After centrifugation for 10 min at 13000 *g* and 4 °C the supernatant was transferred into a fresh reaction tube and after adding 50 µl TRIzol® the samples were incubated for 5 min at room temperature. The phase separation was done by adding 30 µl chloroform, vortexing the samples for 1 min and centrifugation for 15 min at 13000 *g* and 4 °C. The aqueous phase was transferred into a fresh reaction tube and 75 µl isopropanol were added to precipitate the RNA. After incubation for 15 min at -20 °C the samples were centrifuged for 10 min at 13000 *g* and 4 °C to pellet the RNA. The pellet was washed in 70 % ethanol, air-dried and dissolved in 20 µl DEPC-H<sub>2</sub>O.

### **2.2.2.5 Reverse transcription polymerase chain reaction (RT- PCR)**

The RNA concentration of each sample was determined on a Nano-Drop 2000 and 1 µg RNA was used for DNase (Fermentas) treatment to remove all DNA material following the manufacturer’s protocol. The RevertAid™ First Strand cDNA Synthesis Kit (Fermentas) was used to generate cDNA following the manufacturer’s protocol. The cDNA was stored at -80 °C and 2µl were used in subsequent analysis.

### **2.2.2.6 Polymerase chain reaction (PCR)**

All PCR’s were set up according to the method of Seiki (1990) <sup>[158]</sup> in a total volume of 50 µl. Table 2.2 specifies all primers used in this thesis. The PCR SuperMix (Invitrogen) including PCR buffer,

dNTPs and recombinant *Taq* DNA-polymerase was used to facilitate the set up of the following standard reactions:

	50-500ng	DNA	
	8pmol	forward primer	
	8pmol	reverse primer	
	45µl	PCR SuperMix (Invitrogen)	
Initial denaturing step:	95 °C	5 min	
Synthesis (28-32 cycles):	95 °C	30 sec	denaturing
	x °C	30 sec	primer annealing
	72 °C	x sec	extension time (1kb/min)
Final extension time:	72 °C	5 min	

All reactions were done in a Mastercycler personal (Eppendorf).

Table 2.2: RT-PCR primer.

name	sequence	annealing temperature
Aβ fwd	5' -CCA TCC TTC TCC TGC TAA CC-3'	52 °C
Aβ rev	5' -CAC CAT CAA GCC ATA ATC G-3'	52 °C
B10 fwd	5' -CTG GTG CAG CCG GGA GGC TCA-3'	57 °C
B10 rev	5' -GGC TCC GCT GGC GCT GCT CAC-3'	57 °C
KW1 fwd	5' -CGA GAG CGG AGG TGG AAG CGT GCA G-3'	60 °C
KW1 rev	5' -GGC TCC GCT GGC GCT GCT CAC-3'	60 °C
rp49 fwd	5' -GAT GAC CAT CCG CCC AGC ATA C-3'	57 °C
rp49 rev	5' -AGT AAA CGC GGT TCT GCA TGA GC-3'	57 °C
AP fwd	5' -GGC CCA GAT GAC CGA TAA GGC-3'	60 °C
AP rev	5' -CCT TCA TGG TGT AGA ACA GAT CGG-3'	60 °C
NMDA fwd1	5' -CGC GAA TTC TCG CAC TCG GAC AGC AAC GA-3'	55 °C
NMDA rev1	5' -CGC TCT AGA GGC GCA GGT CAG GTT CTC CA-3'	55 °C
NMDA fwd2	5' -ATT CCC GGC TGG TTG GCA GC-3'	53 °C
NMDA rev2	5' -CGC CTG GAC ATT GCC CGA CA-3'	53 °C

### **2.2.2.7 Agarose gel electrophoresis**

The separation of DNA-Fragments was carried out in 1 % agarose gels at 3-7 V/cm. The samples were mixed with 6x DNA Loading Dye (Fermentas) and equal amounts were loaded onto the gel. Additionally DNA ladders (GeneRuler™ 100bp DNA Ladder, GeneRuler™ 1kb DNA Ladder, Fermentas) were loaded to determine the band size. 1x Tris-acetate-EDTA (TAE; 40 mM Tris acetat, 1 mM EDTA) was used as running buffer and, supplemented with SYBR® Safe DNA Gel Stain (Invitrogen), to create the agarose gel. The separation of bands was analysed using a UV transilluminator (Raytest).

### **2.2.2.8 Protein synthesis in *E. coli***

The synthetic peptide B10-myc was cloned into p41 to be expressed in *E. coli* RV308 cells and purified using preparative chromatography. Briefly, to express the protein cells were grown in M9 minimal growth medium (composition below) at 26 °C until the OD reached 0.5. After adding 1mM IPTG the cells grew for 4 hours at 220 rpm and 16 °C while the expression took place. Cells were harvested by centrifugation (20 min, 15000 *g*, 4 °C) and the pellet was frozen at -80 °C.

composition of M9 minimal medium:

8.6 g Na<sub>2</sub>HPO<sub>4</sub> x 12 H<sub>2</sub>O; 0.5 g NaCl; 3 g KH<sub>2</sub>PO<sub>4</sub>; 1 g NH<sub>4</sub>Cl; 10 ml Eisen(III)-citrat (0.023 M); 0.1 ml EDTA (0.2 M); 0.1 ml CoCl<sub>2</sub> x 6 H<sub>2</sub>O (0.1 M); 0.1 ml MnCl<sub>2</sub> x 4 H<sub>2</sub>O (0.75 M); 0.1 ml CuCl<sub>2</sub> x 4 H<sub>2</sub>O (0.1 M); 0.1 ml H<sub>3</sub>BO<sub>3</sub> (0.5 M); 0.1 ml Na<sub>2</sub>MoO<sub>4</sub> x 2 H<sub>2</sub>O (0.1 M); 2 ml Zn(CH<sub>3</sub>COO)<sub>2</sub> x 2 H<sub>2</sub>O (0.018 M); add ddH<sub>2</sub>O to a total volume of 1 l  
before use add: 5 ml MgSO<sub>4</sub> (1 M). 20 ml Glucose (2.5 M)

### **2.2.3 Biochemical methods**

#### **2.2.3.1 Purification of B10-myc and B10APi**

To purify the proteins, the cell pellet was dissolved in ice cold resuspension buffer (50 mM sodium phosphate pH 8.0; 300 mM NaCl; 50 mM imidazol) and homogenised twice in the high pressure cell homogeniser NS1001-L2K (*Gea Niro Soavi*, 1000 bar). After adding 0.5 % Tween20 the solution was centrifuged for 90 min at 35800 *g* and 4°C and the supernatant was collected and filtered through a 1.2 µm membrane. The purification was carried out using two different chromatography techniques. The first step was an affinity chromatography using a Ni-NTA column and the proteins were eluted with an increasing concentration (5 % to 100 %) of elution buffer (50 mM NaPO<sub>4</sub> pH 8.0; 300 mM NaCl; 250 mM imidazol).

B10-myc was then cleaved with TEV protease and the protein was run again over the Ni-NTA column and the flow through was collected while the cleaved His-tag was bound to the column. In the second purification step B10-myc was trapped on a Source RPC column and eluted with increasing concentration of acetonitrile supplemented with 0.1 % TFA. The protein was lyophilised and stored at -80°C.

B10APi was after Ni-NTA affinity chromatography purified further with a Q-sepharose column and the protein was eluted with linear increasing concentrations of elution buffer (20 mM Tris pH 8.2; 0.5 M NaCl). The protein was stored at -80°C in elution buffer.

The purity of both proteins was analysed by SDS-PAGE, HPLC and ESI-MS.

### **2.2.3.2 Preparation of disaggregated A $\beta$ 1-40**

This protocol was used to create homogenous A $\beta$  that is supposed to be monomeric <sup>[159]</sup>. Briefly, 1 mg A $\beta$ (1-40) was dissolved in 2 ml 1,1,1,3,3,3-Hexafluoro-2-propanol (HFIP)-TFA (1:1) and incubated for 4 hours at room temperature. Afterwards the liquid was completely evaporated under a gently nitrogen stream and the resulting protein film was diluted in 1 ml 0.15 % ammonium hydroxide. The sample was frozen in liquid nitrogen and lyophilised over night. Until usage the lyophilised protein was stored at -80 °C.

### **2.2.3.3 Preparation of soluble A $\beta$ oligomers**

To prepare soluble A $\beta$ (1-40), A $\beta$ (1-42) and A $\beta$ (1-42)<sub>arc</sub> oligomers 1 mg peptide was dissolved in 400  $\mu$ l HFIP and incubated for 15 min at room temperature. The oligomers were formed by diluting the sample 1:10 in pure water followed by incubation for 15 min at room temperature. Larger aggregates were removed in a centrifugation step for 15 min at 13000 *g* and room temperature. The supernatant contained the soluble oligomers and was transferred into a new tube.

### **2.2.3.4 Preparation of A $\beta$ fibrils**

Fibril samples were generated by diluting 1 mg A $\beta$ (1-40), A $\beta$ (1-42) and A $\beta$ (1-42) in 1 ml 50 mM sodium borate buffer (pH 9.0). The protein concentration was determined by measuring the absorption of the sample at 280 nm in 6 M guanidinium hydrochloride and 20 mM sodium phosphate (pH 6.5). Using the Lambert-Beer law and the Gill & Hippel method <sup>[160]</sup> the extinction coefficient was estimated and the concentration was calculated. The sample was incubated for at least 1 week at 37 °C.

### **2.2.3.5 *Drosophila melanogaster* protein extraction**

For soluble protein extraction 15-25 fly heads or 5 fly bodies were homogenised in 20  $\mu$ l PBS (137 mM NaCl; 2.7 mM KCl; 8 mM Na<sub>2</sub>HPO<sub>4</sub>; 2 mM KH<sub>2</sub>PO<sub>4</sub>; pH 7.4) supplemented with 1 % SDS and protease inhibitor cocktail (cOmplete, Mini, EDTA-free; Roche) using a plastic homogeniser, sonicated for 480 sec and centrifuged for 7 sec at 13000 *g* at room temperature. The supernatants were stored at -20 °C or immediately used for a Bradford Assay and SDS-PAGE.

For sequential protein extraction into soluble and insoluble fraction the fly heads were homogenised in 20  $\mu$ l PBS supplemented with 1 % SDS and protease inhibitor cocktail and centrifuged for 7 sec at 13000 *g* at room temperature. The supernatant was stored at -80 °C as soluble fraction. The pellet was dissolved in 15  $\mu$ l urea buffer (9 M urea; 1 % SDS; 25 mM Tris; 1 mM EDTA), sonicated for

480 sec, followed by an incubation for 1 hour at 55 °C and centrifugation for 15 min at 13000 *g* and 4 °C. The supernatant was diluted in PBS supplemented with 1 % SDS and protease inhibitor cocktail to reach an urea concentration of 3 M and was stored as insoluble fraction at -80 °C. The soluble and insoluble fractions were analysed in a Bradford assay before loading onto a SDS gel.

#### **2.2.3.6 Bradford Assay**

The protein concentration was determined using the DC™ Protein Assay (Biorad) following the manufacturer's micro plate assay protocol. The standard curve was done with 5 different BSA concentrations from 2 mg/ml down to 0.01 mg/ml in PBS supplemented with 1 % SDS and protease inhibitor cocktail depending on the experiment. The samples were diluted 1:10 in PBS supplemented with 1 % SDS and protease inhibitor cocktail and analysed in duplicates. A FLUOstar Omega reader (BMG LABTECH) was used to read the absorbance of the 96-well plate at 750 nm. The protein concentration was equalised using Microsoft Excel and linear regression of the standard curve. The lowest protein concentration was set as 1 and the ratio of all other samples was calculated.

#### **2.2.3.7 Immunoprecipitation**

To precipitate target proteins from *Drosophila melanogaster*, magnetic Protein A beads (Invitrogen) were used according to the manufacturer's protocol with slight changes. Briefly, the beads were blocked in 2% BSA/PBST (PBS + 0.025 % TritonX-100) for 15 min at room temperature on a rotating wheel. Afterwards the beads were washed twice in PBST. If necessary the antibody was allowed to bind to the beads in PBST for 15 min. In between the fly heads were homogenised in PBST + proteinase inhibitor cocktail, sonicated for 1 min and spun down for 7 sec at 13000 *g*. An aliquot was taken out of the supernatant to present the 'before' sample. The homogenate was mixed with the beads and incubated for 20 min on the rotating wheel. Afterwards three washing steps in PBST were applied and the beads were transferred into a new tube. The proteins were eluted using 50 mM glycine (pH 2.8) and finally the beads were boiled in 1x NuPAGE® LDS Sample Buffer (Invitrogen). All fractions were analysed in a western blot.

#### **2.2.3.8 Quantification of B10 and A $\beta$**

To determine the ratio between antibody domain and A $\beta$ , the amount of the proteins was quantified by SDS-PAGE and subsequent western blot analysis. A standard curve was generated with increasing amounts of synthetic peptide and fly head homogenates were analysed. The blots were developed with three different development times and afterwards the intensity of the bands was

evaluated using 1D Gel Analysis from TotalLab 100 (Nonlinear Dynamics). The concentration was calculated referring to the linear regression of the standard curve.

### **2.2.3.9 SDS-polyacrylamid gel electrophoresis (SDS-PAGE)**

SDS-PAGE was done using the NuPAGE® MES buffer system (Invitrogen). The protein samples were prepared with 1x NuPAGE® LDS Sample Buffer (Invitrogen) and boiled for 10 min at 95 °C. For cysteine rich proteins 1x NuPAGE® Sample Reducing Agent (Invitrogen) was added additionally before boiling. The SDS-PAGE was done using precast NuPAGE® Novex 4-12 % Bis-Tris Gels (1 mm; 10 or 12 wells; Invitrogen) and NuPAGE® MES SDS Running buffer (Invitrogen) following the manufacturer's protocol. The further readout was done with Coomassie staining or western blot analysis.

### **2.2.3.10 Native Page**

For native PAGE analysis the Native PAGE® system (Invitrogen) was used. The protein samples were mixed with 5 µl of 4x NativePAGE® sample buffer (Invitrogen). Samples were separated without previous boiling on precast NativePAGE® 4-16 % Bis-Tris gradient gels (1 mm; 10 wells; Invitrogen) with NativePAGE® running buffer (Invitrogen) following the manufacturer's protocol. The further readout of the results was performed with western blot analysis.

### **2.2.3.11 Coomassie staining**

The gel was stained for 1 h in Coomassie solution (2.5 g Coomassie Brilliant Blue R-250; 10 % Acetic acid; 30 % Ethanol) and transferred into destain solution (10 % Acetic acid; 20 % Ethanol) until the protein bands are seen without background staining. All steps are carried out under gentle agitation. Coomassie stained gels were dried using the GelAir Drying System (Biorad).

### **2.2.3.12 Western blot analysis**

For western blot analysis the marker SeeBlue® Plus2 Pre-Stained Standard (Invitrogen) was used in the SDS-PAGE. The proteins were transferred on 0.45 µM nitrocellulose membranes by using the Semi-Dry Blotting System (Biorad). Briefly, two extra thick blotting papers and the membrane were soaked in transfer buffer (1x NuPAGE® Transfer Buffer [Invitrogen]; 20 % Methanol). The semi-dry blot was prepared by layering blotting paper, membrane, gel and a second piece of blotting paper onto the anode platform and closing the system with the cathode platform and the lid. Proteins were transferred for 35 min at 20 V.

After protein transfer the membrane was blocked in 5 % milk powder in PBST (PBS + 0.05 % TritonX-100) for 1 hour at room temperature under gentle shaking before adding the primary antibody (table 2.3) over night at 4 °C. Subsequently the membrane was washed for 3 x 5 min in PBST and the HRP-conjugated secondary antibody (table 2.3) was applied for 1 hour at room temperature. A second washing step of 3 x 5 min in PBST was applied and finally the proteins were visualised by incubating the membrane either with the SuperSignal West Pico Chemiluminescent Substrate (Pierce) or the SuperSignal West Femto Chemiluminescent Substrate (Pierce) and analysing the chemiluminescence with a CCD camera system (peqlab).

Table2.3: Antibodies used in western blots.

name	antigene	species	concentration	source
6E10	$\beta$ -amyloid (1-16)	mouse	1:1000	Covance
c-myc	myc-tag	rabbit	1:1000	Abcam
$\beta$ -actin	$\beta$ -actin	mouse	1:1000	Abcam
anti-His	His-tag	mouse	1:2000	Qiagen
anti-mouse-HRP	mouse IgG	goat	1:1000	DAKO
anti-rabbit-HRP	rabbit IgG	goat	1:1000	DAKO

### **2.2.3.13 Enzyme linked immunosorbant assay (ELISA)**

A sandwich ELISA was done to determine the total A $\beta$  concentration of fly samples. Therefore all samples were analysed in triplicates of 10 fly heads each with either synthetic A $\beta$ (1-40) or A $\beta$ (1-42) as standard protein. First all wells were blocked in 100  $\mu$ l 3 % MSD Blocker A in PBS for 1 hour at 600 rpm and room temperature. The wells were washed 5 times with PBS-Tween20 (0.05 %) and incubated with 25 $\mu$ l of biotinylated 6E10 (4  $\mu$ g/ml) in 1 % MSD Blocker A (table 2.4) for 1 hour at 600 rpm and room temperature. During this incubation triplicates of 10 fly heads per sample were homogenised in 5  $\mu$ l extraction buffer (50 mM HEPES pH 7.3; 5 mM EDTA; 5 M guanidine hydrochloride (GnHCl); protease inhibitor cocktail) using a plastic pistil. After sonication for 480 sec and centrifugation for 7 sec at 13000 *g* and room temperature 5 $\mu$ l of supernatant were transferred into a fresh reaction tube, diluted with 20  $\mu$ l dilution buffer (25 mM HEPES pH 7.3; 1 mM EDTA; 1 % MSD Blocker A) and stored on ice. The standard curve was prepared in triplicates by using fly juice (240 *white*<sup>1118</sup><sub>iso</sub> fly heads homogenised in 500  $\mu$ l extraction buffer) spiked with synthetic A $\beta$  in 1:5 dilution steps starting with 10  $\mu$ g/ml.

The plate was washed again 5 times with PBS-Tween20 (0.05 %) before adding the A $\beta$  standard and samples and incubation for 1.5 hours at 600 rpm and room temperature. An additional washing step was used to remove unbound A $\beta$  and then 25  $\mu$ l of 1 $\mu$ g/ml SULFO-tagged secondary antibody specific for A $\beta$ (1-40) or A $\beta$ (1-42) (2G3 and 21F12<sup>[161]</sup>, respectively, table 2.4) was added to each well

followed by incubation for 1 hour at 600 rpm and room temperature. The plate was washed again and 150  $\mu$ l of 1x MSD Read Buffer in water were added to each well.

Table 2.4: Antibodies used in ELISA.

name	antigene	species	concentration	source
6E10 biotinylated	$\beta$ -amyloid (1-16)	mouse	4 $\mu$ g/ml	D.Crowther
21F12 SULFO-tagged	A $\beta_{x-42}$	mouse	1 $\mu$ g/ml	D.Crowther, gifts of Elan
2G3SULFO-tagged	A $\beta_{x-40}$	mouse	1 $\mu$ g/ml	D.Crowther, gifts of Elan

The electrochemiluminescence of the plate was analysed using the SECTOR® Imager 6000 (Meso Scale Discovery) following the manufacturer's protocol. The samples as well as a synthetic protein standard (A $\beta$ (1-40) and A $\beta$ (1-42), respectively) were fitted automatically using the SECTOR® Imager 6000 software including a Four Parameter Logistic nonlinear regression model with the following equation:

$$y = \min + \frac{\max - \min}{1 + \left(\frac{x}{EC50}\right)^{HillSlope}}$$

#### **2.2.3.14 Spot Blot**

15 fly heads of each genotype were homogenised in 2 % SDS and centrifuged for 5 min at 5000 *g*. The supernatant was applied in triplicates on a 0.45  $\mu$ m nitrocellulose membrane using a pipette. To minimise the spot size, each sample was applied in three small aliquots to the same spot with air drying in between. Finally the membrane was dried for 10 min before blocking in 5 % milk powder in PBST for 1 hour at room temperature under gentle shaking. B10-myc was added over night at 4 °C. On the next day the membrane was washed 3 x 5 min in PBST before adding the primary antibody (table 2.5) followed by incubation for 1 hour at room temperature under gentle shaking. Again the membrane was washed 3 times in PBST before adding the HRP-conjugated secondary antibody (table 2.5). Finally the membrane was washed again 3 times in PBST and developed using the SuperSignal West Pico Chemiluminescent Substrate (Pierce).

Table 2.5: Antibodies used in spot blots.

name	antigene	species	concentration	source
B10-myc	A $\beta$ fibrils	<i>E. coli</i>	1 $\mu$ g/ml	<i>E. coli</i>
c-myc	myc-tag	rabbit	1:1000	Abcam
anti-B10	camelid	rabbit		C.Röcken <sup>[162]</sup>
anti-His	His-tag	mouse	1:2000	Qiagen
anti-mouse-HRP	mouse IgG	goat	1:1000	DAKO
anti-rabbit-HRP	rabbit IgG	goat	1:1000	DAKO

### **2.2.3.15 Dot Blot**

Proteins were applied twice in duplicates in increasing concentrations on a 0.45  $\mu\text{m}$  nitrocellulose membrane using the Minifold I <sup>TM</sup> system (Whatman). Afterwards each well was washed with TBST (50 mM Tris pH 7.4; 150 mM NaCl; 0.01 % (v/v) Tween20) and the membrane was cut. One half was stained with Ponceau S (2 % Ponceau S in 3 % TCA) to confirm the protein load and the other half was put in blocking buffer (2 % BSA in TBST) for 1 hour at room temperature. The membrane was washed in TBST followed by incubation with the primary antibody (table 2.6) in TBST over night at 4 °C. To increase the signal intensity the membrane was washed 3 x 5 min with TBST and an anti-AP antibody (in TBST, table 2.6) was applied for 1 hour at room temperature. Again 3 washing steps followed before adding the secondary anti-rabbit-AP antibody and incubation for 1 hour at room temperature. The blot was finally washed 3 times in TBST and developed using NBT/BCIP (Pierce) or SuperSignal West Femto Chemiluminescent Substrate (Pierce). The intensity of the Ponceau S and antibody staining was analysed using Array Analysis from Total Lab 100 (Nonlinear Dynamics).

Table 2.6: Antibodies used in dot blots.

name	antigene	species	concentration	source
B10AP	A $\beta$ fibrils	<i>E. coli</i>	4 $\mu\text{g}/\text{ml}$	recombinant
KW1AP	A $\beta$ (1-40) oligomers	<i>E. coli</i>	4 $\mu\text{g}/\text{ml}$	recombinant
B10AP-S2	A $\beta$ fibrils	<i>D. mel</i>	1 $\mu\text{g}/\text{ml}$	S2-cells
KW1AP-S2	A $\beta$ (1-40) oligomers	<i>D. mel</i>	1 $\mu\text{g}/\text{ml}$	S2-cells
anti-AP	alkaline phosphatase	rabbit	1:2000	Rockland
anti-rabbit-AP	rabbit IgG	goat	1:30000	Sigma
anti-rabbit-HRP	rabbit IgG	goat	1:1000	DAKO

## **2.2.4 Biophysical methods**

### **2.2.4.1 Thioflavin T (ThT) fluorescence spectroscopy**

ThT spectra were taken at room temperature using the LS 55 fluorescence spectrometer (Perkin Elmer). The samples were measured in a fluorescence ultra-micro cell (Hellma Analytics) with 5 mm path length and ThT was excited at 450 nm (slit 5 nm) and the emission spectrum was recorded from 460 to 700 nm (slit 5 nm). All samples were measured with 5 scan repeats.

### **2.2.4.2 8-Anilino-naphthalene-1-sulfonate (ANS) fluorescence spectroscopy**

ANS spectra were carried out using the LS 55 fluorescence spectrometer (Perkin Elmer). The samples were measured using a fluorescence ultra-micro cell (Hellma Analytics) with 5 mm path

length and ANS was excited at 374 nm (slit 5 nm) and the emission spectrum was recorded from 380 to 700 nm (slit 5 nm). All samples were measured with 5 scan repeats.

#### **2.2.4.3 Congo red (CR) absorption spectroscopy**

CR spectra were measured using the Lambda 900 spectrometer (Perkin Elmer). The samples were measured using an absorbance semi-micro cell (Hellma Analytics) with 10 mm path length and the absorption spectra were recorded from 400 to 700 nm (slit 2 nm). All samples were measured with 3 scan repeats.

#### **2.2.4.4 Aggregation kinetics**

Aggregation kinetic measurements are based on time-resolved ThT fluorescence measurements, carried out online in a 96-well plate and by using a FLUOstar OPTIMA (BMG Labtech) plate reader (37 °C). ThT fluorescence was recorded by using excitation and emission wavelengths of 482 nm and 490 nm, respectively. Each measurement cycle consisted of 30 min incubation followed by orbital shaking at 100 rpm for 10 seconds immediately before the measurement. Samples were prepared by dissolving disaggregated A $\beta$ (1-40)<sup>[159]</sup> in 100 % DMSO. Final sample volume in each well was 100  $\mu$ l and consisted of 25  $\mu$ M A $\beta$ (1-40), 20  $\mu$ M ThT, 50 mM HEPES (pH 7.4), 50 mM NaCl, a protease inhibitor cocktail (Complete mini, Roche) (1x) and, where appropriate, 5  $\mu$ M KW1.

#### **2.2.4.5 Transmission electron microscopy (TEM)**

The fibrillar and oligomeric morphology was assessed by negative stain TEM. TEM specimens were prepared by placing 5  $\mu$ l of each sample solution onto a Formvar carbon copper grid (200 mesh, Plano) followed by 1 min of incubation. The grid was washed by dipping it subsequently into 3 droplets of water (50  $\mu$ l) and counterstained with 3 droplets of 2 % (w/v) uranyl acetate (50  $\mu$ l). Specimens were examined using a Zeiss 900 electron microscope that was operated at an acceleration voltage of 80 kV. A magnification of 30 000  $\times$  was used for imaging.

#### **2.2.4.6 Scanning electron microscopy (SEM)**

To investigate the surface of the eye adult flies were anaesthetised and fixed in 2.5 % glutaraldehyde in 100 mM sodium cacodylate (pH 7.3) over night at 4 °C. The samples were sent to Dr. Martin Westermann (EMZ, Jena, Germany), who carried out the Critical Point Drying, gold sputtering and scanning electron microscopy.

## **2.2.5 Immunocytological methods**

### **2.2.5.1 Dissection and immunostaining of *Drosophila* brains (confocal microscopy)**

For fluorescence analysis the brains of anaesthetised flies were dissected in ice cold PBS and stored on ice. PBS was exchanged with fixative (4 % PFA in PBT [PBS + 0.5 % TritonX-100]) and the brains were shaken for 1 hour at 50 rpm and room temperature. Afterwards the blocking solution (5 % normal goat serum in PBT) was added followed by incubation for 30 min at 50 rpm and room temperature. The blocking solution was removed and the brains were incubated with the primary antibodies (table 2.7) in blocking solution over night at 50 rpm and 4 °C. On the next day 3 washing steps with PBT of 5 min were performed before adding the secondary antibodies (table 2.7) in blocking solution followed by incubation for 1 hour at 50 rpm and room temperature. Again 3 washing steps were applied followed by a final washing in PBS (+ Hoechst 33342). The brains were mounted using VECTASHIELD® mounting medium (Vector laboratory), sealed with nail polish and stored at 4 °C. The images were taken using a confocal laser scanning microscope (Nikon ECLIPSE TE2000-E).

Table 2.7: Antibodies used for immunofluorescence.

name	antigene	species	concentration	source
6E10	β-amyloid (1-16)	mouse	1:500	Covance
c-myc	myc-tag	rabbit	1:500	Abcam
elav-7E8A10	elav protein	rat	1:50	DHSB
anti-mouse-555	mouse IgG	donkey	1:200	Molecular Probes
anti-rabbit-488	rabbit IgG	donkey	1:200	Molecular Probes
anti-rat-TRITC	rat-IgG	goat	1:200	Jackson

## **2.2.6 Cytological methods**

### **2.2.6.1 Transfection and protein synthesis in insect cells**

The Schneider 2 (S2) insect cell line was isolated from late stage *Drosophila melanogaster* embryos<sup>[163]</sup> and is a suitable host for stable expression of recombinant proteins<sup>[164]</sup>. The antibody domains B10AP and KW1AP were expressed in S2 cells adapted to serum-free growth in Insect Express Sf9-S2 medium (PAA Laboratories). To create stable S2 cells expressing either B10AP or KW1AP the FuGENE® HD Transfection Reagent (Roche) was used. Briefly 3x10<sup>6</sup> S2 cells were seeded in 3 ml medium and grown for 5 hours at 28 °C. The following transfection mix was prepared in a total volume of 100µl: 0.4 µg pCoBlast (selection vector); 15 µl FuGENE® HD Transfection Reagent; 4 µg transgenic vector (pMT/V5-HisA-B10AP-S2 or pMT/V5-HisA-KW1-S2); sterile water. The solution was mixed, spun down and incubated for 15 min at room temperature. Under gentle shaking the

solution was added drop wise to the cells followed by incubation for 48 hours at 28 °C. Afterwards 30 µg/ml blasticidine were added to select stable transfected cells and monitored over the next days. When colonies started to form, the cells were moved into culture flasks and finally the selected cell lines were kept on 20 µg/ml blasticidine. From each stable cell line samples were frozen at a density of  $1 \times 10^7$  cells/ml in freezing medium (40 % fresh growth medium, 40 % conditioned growth medium, 10 % heat-inactivated FBS, 10 % DMSO) to maintain the stocks.

Proteins were expressed by adding 1mM  $\text{Cu}_2\text{SO}_4$  to the cells when they reached the log-phase and incubation for 36 hours at 28 °C. Afterwards the cells were spun down and the protein was purified from the medium. First the copper was removed using dialysis against resuspension buffer (50 mM sodium phosphate pH 8.0; 300 mM NaCl; 50 mM imidazol). An affinity chromatography was carried out using a Ni-sepharose column and the protein was eluted with an increasing concentration (5% to 100%) of elution buffer (50 mM sodium phosphate pH 8.0; 300 mM NaCl; 250 mM imidazol). The protein was dialysed against 50 mM sodium phosphate buffer (pH 7.4) to remove the imidazol and stored at -80 °C.

#### **2.2.6.2 Cultivation of human neuroblastoma cells**

The cell line SH-SY5Y is a subclone of the cell line SK-N-SH which was derived from a female human with metastatic neuroblastoma <sup>[165]</sup>. The cells were grown in Dulbecco's Modified Eagle Medium (DMEM, PAA Laboratories) supplemented with 10 % heat-inactivated FBS and 2 % Pen/Strep (PAA Laboratories) at 37 °C with 10 %  $\text{CO}_2$ . The cells grow adherent as monolayer. For splitting the cell layer was rinsed with PBS and the cells were treated with 1 ml trypsin/EDTA (PAA Laboratories) before they could be detached using DMEM.

#### **2.2.6.3 Toxicity assays**

To measure toxicity, cells were seeded into 96-well plates at a density of 50 000 cells/well in 100 µl cell culture medium and grown for 24 h at 37 °C. The medium was removed and new medium supplemented with the test substance was added and incubated for another 24 h at 37 °C.

The test substances included  $\text{A}\beta \pm \text{KW1}$ , a buffer control as well as a sample containing KW1 only. Therefore,  $\text{A}\beta$  was incubated at  $100 \mu\text{M} \pm 20 \mu\text{M}$  KW1 in 50 mM HEPES; 50 mM NaCl (pH 7.4) at 37 °C without shaking for four or five days.

The cell viability was assessed using the Cell Proliferation Kit I (MTT, Roche) according to the manufacturer's protocol. The colorimetric assay was analysed in a FLUOstar Omega reader (BMG LABTECH) reading the absorbance at 550 and 690 nm.

Secondly, the LDH-Cytotoxicity Assay Kit II (Biovision) was used according to the manufacturer's protocol to determine the release of the lactate dehydrogenase. The LDH assay was analysed by measuring the absorbance at 450 nm with a reference read at 650 nm using the FLUOstar Omega reader.

---

## 3. Results

---

### 3.1 Selectivity of B10 and KW1-binding to A $\beta$ (1-40), A $\beta$ (1-42) and A $\beta$ (1-42)arc peptides

It was previously described that B10 binds specifically to amyloid fibrils<sup>[138]</sup>, whereas KW1 recognises oligomers<sup>[135]</sup>. All *in vivo* studies described herein were carried out using *Drosophila melanogaster* transgenic for the three A $\beta$  variants A $\beta$ (1-40), A $\beta$ (1-42) and A $\beta$ (1-42)arc. It was, therefore, important to analyse first the binding of B10 and KW1 to fibrils and oligomers formed by each of these peptides *in vitro*.

Oligomers and fibrils of A $\beta$ (1-40), A $\beta$ (1-42) and A $\beta$ (1-42)arc were generated and characterised using fluorescence as well as absorption spectroscopy prior to assessment of their binding to B10 and KW1. Two fluorescent dyes are commonly used to study oligomer and fibril assemblies. The first fluorescent dye 8-Anilino-naphthalene-1-sulfonate (ANS, figure 3.1.1A) is a common marker of molten-globule states<sup>[166]</sup>. ANS interacts with hydrophobic protein surfaces resulting in increased fluorescence intensity and a blue shift of the emission maximum to 480 nm compared to the free dye (540 nm). It has been shown to bind to oligomeric aggregates<sup>[152, 167, 168]</sup>. The second dye, the benzothiazole Thioflavin T (ThT, figure 3.1.1B), binds to  $\beta$ -sheet rich structures and displays enhanced fluorescence intensity and a red shift of the emission maximum (482 nm) compared to the free dye<sup>[169]</sup>. ThT is widely used to monitor fibril formation. Furthermore the diazo dye Congo red (CR, figure 3.1.1C) is extensively used to characterise amyloid fibrils. It is not characterised by fluorescence intensity but rather shifted and increased signals of UV absorbance (from 490 to 540 nm)<sup>[170]</sup>.

Measuring the ANS fluorescence of A $\beta$ (1-40), A $\beta$ (1-42) and A $\beta$ (1-42)arc fibrils formed in 50 mM Na-borate buffer (pH 9.0) showed no increase in the signal intensity compared to buffer. In addition, no significant shift of the emission maximum was visible (figure 3.1.1D). In contrast, the ThT spectra of the same fibrils showed increased fluorescence intensity and an emission maximum around 480 nm that is characteristic of amyloid fibrils in all cases. Differences in the fluorescence intensity were, however, detectable for different peptides. A $\beta$ (1-42) fibrils showed the highest and A $\beta$ (1-42)arc fibrils the lowest intensity whereas A $\beta$ (1-40) fibrils were found between the other two A $\beta$  variants (figure 3.1.1E). The presence of fibrils was further confirmed using CR spectroscopy (figure 3.1.1F). Fibril preparations of all three peptides showed a shift of the absorbance maximum from 490 to 540 nm as well as an increase in the signal intensity compared to the buffer alone.

Oligomers of A $\beta$ (1-40), A $\beta$ (1-42) and A $\beta$ (1-42)arc peptides were formed in 10 % HFIP and analysed in the same manner described above. The ANS spectra of all three oligomer preparations resulted in increased fluorescence intensity compared to the buffer sample with clearly visible characteristic peak shifts from 540 to 480 nm (figure 3.1.1G). Differences occurred in the signal intensity with A $\beta$ (1-42)arc (green curve) showing the highest intensity, followed by A $\beta$ (1-40) oligomers (red curve) and

A $\beta$ (1-42) oligomers (blue curve) presenting the lowest fluorescence signal. Additionally, the curves of A $\beta$ (1-42) and A $\beta$ (1-42)arc oligomers showed a small shoulder around 540 nm which seems to be absent in the A $\beta$ (1-40) oligomer preparation but may originate from unbound ANS. The resulting ThT spectra showed only a minor intensification of the fluorescence signal (figure 3.1.1H) and also the CR absorbance did not reveal a peak shift or increase in the absorbance maximum (figure 3.1.1I). In summary, all three A $\beta$  oligomer preparations produced a strong fluorescence signal with ANS compared to the fibrils samples, indicating the presence of solvent-accessible hydrophobic patches. Contrastingly, A $\beta$  fibrils showed a much stronger binding to ThT and CR than A $\beta$  oligomers.

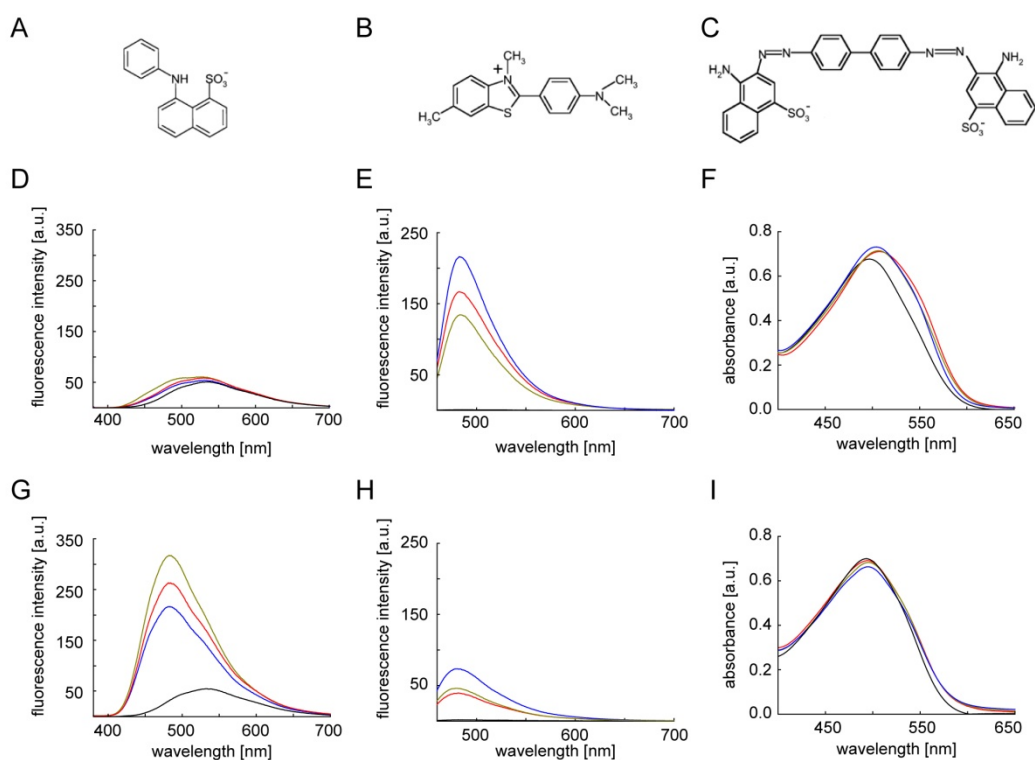


**Figure 3.1.1** Biochemical characterisation of A $\beta$  fibrils and oligomers formed from A $\beta$ (1-40), A $\beta$ (1-42) and A $\beta$ (1-42)arc peptides (A-C) Chemical structures of ANS (A), ThT (B) and Congo Red (C). (D,E) Fluorescence spectra of A $\beta$  fibrils grown in 50 mM Na-borate buffer (pH 9.0) using ANS (D) and ThT (E). (F) Absorption spectra of A $\beta$  fibrils determining the Congo red binding ability. (G,H) Fluorescence spectra of A $\beta$  oligomers formed in 10% HFIP using ANS (G) and ThT (H). (I) Absorption spectra of A $\beta$  oligomers using Congo Red. Black curves: buffer; red curves: A $\beta$ (1-40); blue curves: A $\beta$ (1-42); green curves: A $\beta$ (1-42)arc. The samples for recording ThT spectra contained 20  $\mu$ M and 15  $\mu$ M ThT. ANS samples contained 20  $\mu$ M A $\beta$  and 200  $\mu$ M ANS and CR samples contained 25  $\mu$ M A $\beta$  and 15  $\mu$ M CR.

The morphology of the A $\beta$  oligomers and fibrils characterised above was examined by negative-stain transmission electron microscopy (TEM). All three fibril samples contained large quantities of elongated, linear structures (figure 3.1.2C); while the three oligomeric samples comprised almost spherical structures (diameters of 10 - 60 nm) (figure 3.1.2D), consistent with an oligomeric morphology<sup>[152]</sup>.

In order to analyse B10 and KW1 (figure 3.1.2A,B) binding to the respective A $\beta$  assemblies spot blot assays with the dimeric versions B10AP and KW1AP were used. The alkaline phosphatase (AP) moiety, which enables dimerisation of the antibody domains and therefore increases their effective affinity, facilitates binding studies in the spot blot format. A $\beta$  oligomers and fibrils were spotted onto nitrocellulose membranes and equal protein loading was confirmed using Ponceau S stain before detection with the antibody domains. B10AP binding was detected with all amyloid fibril samples tested here (figure 3.1.2E) extending previous results and demonstrating that B10 displays poly-amyloid specific binding<sup>[171]</sup>. This broad specificity was in contrast to the highly selective binding of KW1AP, which was only able to recognise A $\beta$ (1-40) oligomers, while A $\beta$ (1-42) and A $\beta$ (1-42)arc oligomers were not bound (figure 3.1.2F). These data further underlined the argument that KW1 presents a strong preference for A $\beta$ (1-40) peptide-derived oligomers<sup>[135]</sup>.

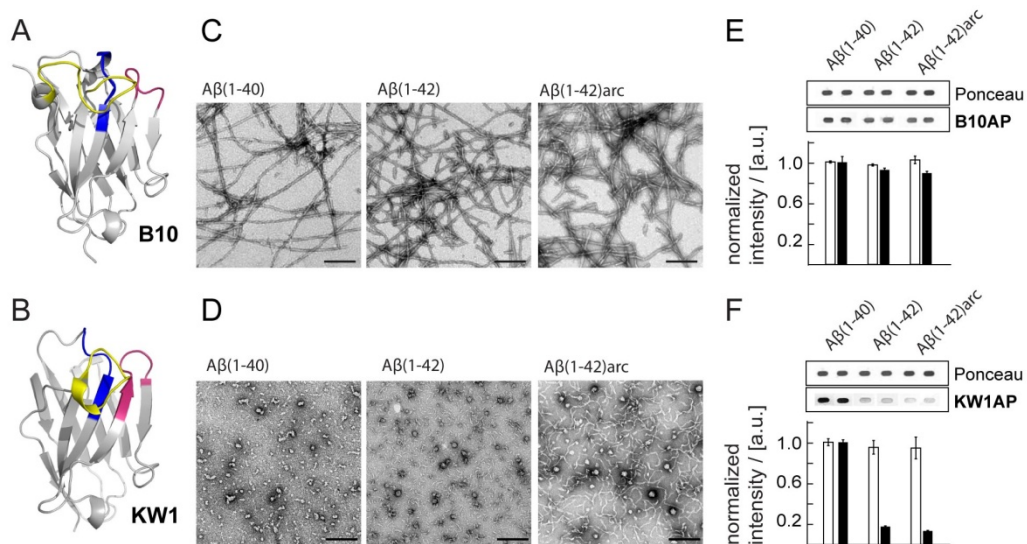


**Figure 3.1.2** Characterisation of B10AP and KW1AP binding towards different A $\beta$  variants. (A,B) X-ray structures of B10 (protein data base/PDB code: 3LN9<sup>[172]</sup>) (A) and KW1 (B) (PDB code: 3TPK<sup>[135]</sup>) (C,D) TEM analysis of A $\beta$  fibrils (C) or oligomers (D) formed from A $\beta$ (1-40); A $\beta$ (1-42) or A $\beta$ (1-42)arc peptides. Scale bar represents 200nm. (E,F) Spot blot data of B10AP binding to amyloid fibrils (E) as well as KW1AP binding to A $\beta$  oligomers (F). Ponceau S staining (upper panel) reveals equal protein loading and lower panel represents B10AP/KW1AP staining. Black bars: B10AP/KW1AP staining; white bars: Ponceau S staining. All bars have been normalised to A $\beta$ (1-40) fibrils or oligomers (n=2).

### **3.2 B10 and KW1 can be functionally expressed in *Drosophila melanogaster* cells**

So far, the camelid antibody domains B10 and KW1 were expressed in *E. coli* and characterised regarding to their conformation sensitivity to A $\beta$ (1-40) monomers, oligomers and fibrils as well as to their respective assemblies formed from A $\beta$ (1-42) and A $\beta$ (1-42)arc peptides. Nevertheless, it remained unclear if both antibody domains will be functional when expressed in *Drosophila melanogaster*. To test whether this was the case transformed *Drosophila Schneider S2*

cells (S2), which can be transfected and are suitable for stable expression of recombinant proteins, were transfected with the dimeric antibody domains B10AP and KW1AP cloned into the expression plasmid pMT/V5-HisA. This vector enabled protein expression in S2 cells under control of an inducible methallothionein promoter (figure 3.2A). The promoter is tightly regulated and easily activated through binding copper sulphate or cadmium chloride.

Upon induction of expression in S2 cells B10AP and KW1AP were secreted into the cell culture medium and purified via His-tag using Ni-chelate chromatography. All purification steps were analysed using SDS-PAGE and Western blot. In both Coomassie-stained SDS-gels a band was observed at 66kDa in the second elution step (E2) consistent with the presence of B10AP (67128.8 Da, figure 3.2B) and KW1AP (66301.9 Da, figure 3.2E). Western blot analysis using an anti-His antibody showed bands at the same size in the cell culture supernatant as well as in the second elution step confirming the successful expression and purification of B10AP and KW1AP.

Binding of cell culture derived dimeric B10AP or KW1AP fusion proteins to A $\beta$  monomers, oligomers and fibrils was assessed by spot blot analysis. All peptide aggregates were immobilised onto nitrocellulose membranes and equal protein loading was confirmed with Ponceau S staining (figure 3.2C,D,F,G) before the interaction with the two antibody fragments B10AP and KW1AP was assessed.

B10AP derived from S2 cells was able to bind to A $\beta$ (1-40) fibrils, but not to oligomers or disaggregated peptide (figure 3.2C). B10AP from S2 cells also reacted with A $\beta$ (1-42) fibrils (figure 3.2D), consistent with previous observations that many different amyloid fibrils are recognised by this antibody. As predicted, KW1AP bound A $\beta$ (1-40) oligomers, but not fibrils or disaggregated peptide (figure 3.2F). By contrast, KW1AP displayed no discernible binding to A $\beta$ (1-42) oligomers compared to A $\beta$ (1-40) oligomers (figure 3.2G), matching previous observations of its rather narrow antigen selectivity. All experiments led to the conclusion that B10 and KW1 can be expressed and secreted in functional form in *Drosophila melanogaster*.

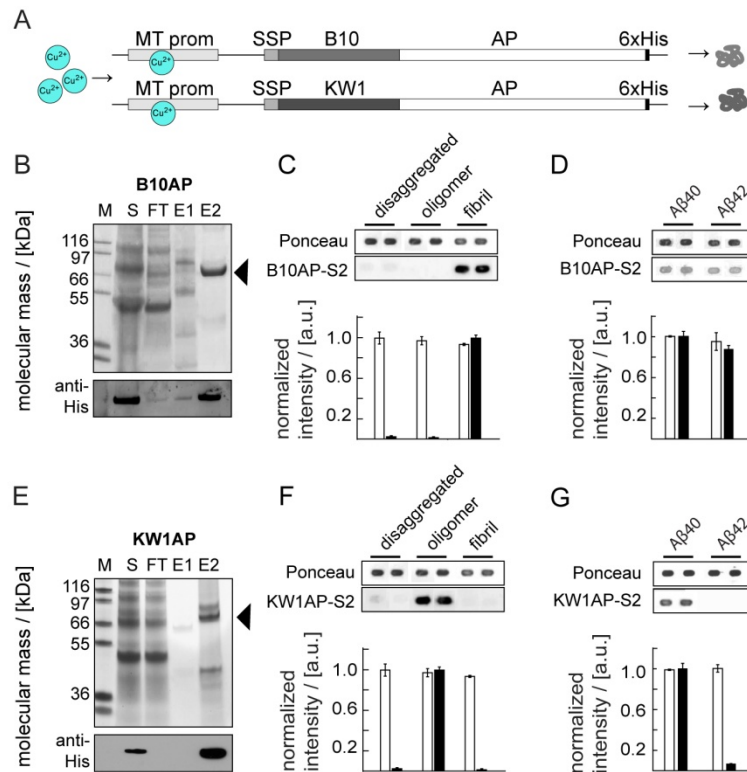


**Figure 3.2** Biochemical characterisation of B10AP and KW1AP expressed in *Drosophila* Schneider 2 cells. (A) Schematic representation of the gene constructs expressed in S2 cells as well as the binding of Cu<sup>2+</sup> ions to the methallothionein promotor (MT prom) to induce the protein expression (B, E) Coomassie stained SDS-PAGE (top) and western blot (bottom), following purification of B10AP (B) and KW1AP (E) from S2 cells. Western blots were developed using an anti-poly-histidine (anti-His) primary antibody. The bands shown in the western blots are indicated in the SDS-PAGE image by arrow heads. Abbreviations refer to molecular weight marker (M), supernatant of the S2 cell culture (S), which was applied onto the column, flow through (FT), and elution steps 1 (E1, 12.5 mM imidazole) and 2 (E2, 250 mM imidazole). (C, D) Spot blot analysis of S2-cell derived B10AP (black bars). B10AP binding to Aβ(1-40) fibrils, oligomers or disaggregated, i.e. mainly monomeric, peptide (C) and Aβ(1-40) or Aβ(1-42) fibrils (D). Ponceau S staining (white bars) served as a loading control. Densitometrically analyzed data were normalised to Aβ(1-40) fibrils. (n = 2-3). (F,G) Spot blot analysis of S2-cell derived KW1AP (black bars). KW1AP binding to Aβ(1-40) fibrils, oligomers or disaggregated peptide (F) and Aβ(1-40) or Aβ(1-42) oligomers (G). Ponceau S staining (white bars) served as a loading control. Densitometrically analyzed data were normalised to Aβ(1-40) oligomers (n = 2-3).

### **3.3 Generating *Drosophila melanogaster* lines transgenic for B10 and KW1**

In order to determine whether the conformation-sensitive antibody domains B10 and KW1 could be used as *in vivo* modifiers of Aβ aggregation and toxicity, *Drosophila melanogaster* transgenic for B10 and KW1 were created. Expression of the two antibody domains B10 and KW1 was achieved using the Gal4-UAS system and the pan neuronal expression driver Gal4-elav<sup>c155</sup>. To explore if B10 and KW1 can modify Aβ aggregation *in vivo* experiments were carried out with three different fly lines expressing the human peptide variants Aβ(1-40), Aβ(1-42) or the arctic mutation E22G (Aβ(1-42)arc). Hereafter, these three fly lines will be referred to as Aβ40, Aβ42 and Aβ42arc flies, respectively. The nontransgenic w<sup>1118</sup><sub>iso</sub> *Drosophila melanogaster* line was used as a wildtype (WT) control throughout.

### **3.3.1 Characterisation of B10-transgenic flies**

To characterise the function of the fibril binder B10 the gene for the antibody domain was cloned into the Gal4-responsive pUASTattB expression plasmid. The construct consisted of a secretion signal peptide (SSP) from the *Drosophila necrotic* gene<sup>[156]</sup>, the coding sequence for the antibody domain B10 and a C-terminal myc-tag that facilitates the detection in immunoblots and immunohistochemistry. The construct was cloned downstream of the UAS-sequence that is activated by Gal4 binding (figure 3.3.1A).

After crossing the flies with the neuronal driver line Gal4-elav<sup>c155</sup> the transcription of B10 was detected by reverse transcription polymerase chain reaction (RT-PCR) analysis (figure 3.3.1B). A control PCR using rp49 primers amplifying the gene for the large subunit of the ribosomal protein 49 was used to confirm equal cDNA amount in all PCR samples. RT-PCR using B10 specific primers revealed that B10 is strongly transcribed in the fly heads when the Gal4-elav<sup>c155</sup> driver was used and with lower amounts in the fly bodies or without the Gal4-elav<sup>c155</sup> driver suggesting that the promoter is leaky. Western blot analysis was carried out to investigate the translation of B10. Detection with an anti-myc antibody showed strong bands at around 17 kDa with almost identical distribution as the B10 mRNA (figure 3.3.1C). These data revealed that B10 is translated correctly in the fly brain.

Since both A $\beta$  and B10 are expressed under the control of the UAS-sequence western blot analysis was used to assess whether there is enough Gal4 protein to establish the same A $\beta$  expression level in A $\beta$  transgenic flies co-expressing B10 compared to transgenic flies expressing A $\beta$  alone. Head extracts from A $\beta$ 42 and B10;A $\beta$ 42 expressing flies were analysed using the monoclonal antibody 6E10 (figure 3.3.1D). Strong bands of similar intensity were found around 4 kDa for both genotypes and blotting for actin revealed equal protein loading.

The neuronal localisation of B10 was examined using immunofluorescence microscopy (IFM). Brains of adult flies were dissected and stained with anti-elav antibody to detect the neurons as well as with the anti-myc antibody to stain B10 (fig 3.3.1E). The cellular localisation of the elav protein is nuclear and the staining signals (red) were found in the cell nuclei of the neuronal cell bodies whereas no signal was visible in the neuropil. Anti-myc signals staining B10 were located intracellular. The merged picture demonstrated that the B10 signals were located around the cell nuclei of the neurons. Thus, B10 was expressed correctly in the nervous system of the fly brain.

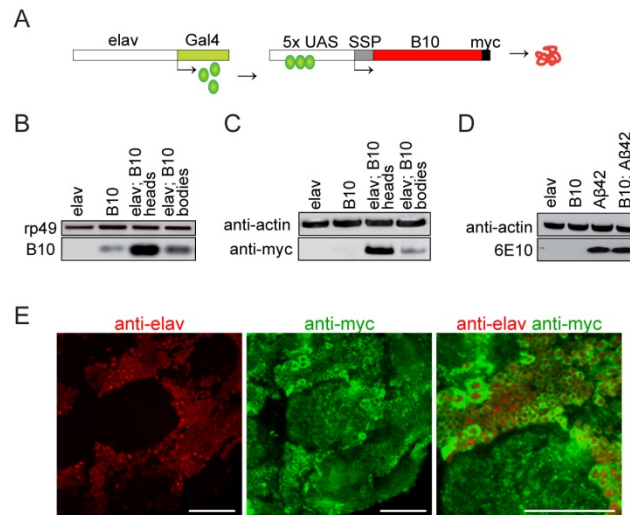


**Figure 3.3.1** Expression of B10 in *Drosophila melanogaster*. (A) Schematic representation of the expression construct. (B) RT-PCR analysis of B10 mRNA transcription in the head or remaining body; i.e. thorax and abdomen, of different fly lines as indicated in the panels. Constitutively transcribed rp49 mRNA served as a loading control. (C) Western blots with an anti-myc primary antibody showed a strong band at around 17 kDa with almost identical distribution as the B10 mRNA in panels (B). Anti-actin western blot served as loading control. (D) Western blot with 6E10 primary antibody to detect A $\beta$  displayed a strong band at around 4 kDa in A $\beta$  expressing *Drosophila melanogaster*. Anti-actin western blot served as loading control. (E) IFM of B10 expressing flies using anti-elav antibody (red) to stain neuronal cells and anti-myc antibody (green) to detect B10. The right picture is a magnified merge of both stainings. Scale bars represent 50  $\mu$ m.

### **3.3.2 Characterisation of KW1-transgenic flies**

The gene for the oligomer binder KW1 was also cloned into the Gal4-responsive pUASTattB expression plasmid. The construct is similar to the B10 expression plasmid (figure 3.3.2.A), except that the B10 antibody domain was replaced with KW1.

After crossing the flies with the neuronal driver line Gal4-elav<sup>c155</sup> the KW1 product was analysed by RT-PCR and western blot analysis (figure 3.3.2B). RT-PCR with KW1 specific primers revealed that KW1 is predominantly transcribed in the fly heads. There was no KW1-mRNA without the elav driver or in the fly bodies. A control PCR using rp49 primers confirmed equal cDNA quantities in all PCR samples. Western blot analysis using the anti-myc antibody showed a strong band at around 17 kDa in the fly heads and only a weak band in the fly body sample, with anti-actin staining confirming equal protein loading of the samples (figure 3.3.2C). Taken together these data demonstrated that KW1 is translated correctly in the fly brain. Next, the A $\beta$  level was analysed in presence of KW1. Western blot analysis using the monoclonal antibody 6E10 was carried out comparing A $\beta$  (A $\beta$ 40, A $\beta$ 42 and A $\beta$ 42arc) with KW1;A $\beta$  expressing flies (figure 3.3.2D). Strong bands reflecting A $\beta$  were found around 4 kDa in each case. Thereby similar amounts of A $\beta$  were found in the presence and absence of KW1. Anti-actin antibody staining of the membrane confirmed equal protein loading. The neuronal localisation of KW1 was assessed using IFM on adult fly brains (figure 3.3.2E). Staining with the anti-elav antibody (red) showed the nuclear localisation of the elav protein and the anti-myc staining signals (green) were found in the cytoplasm of the neurons. The

merged picture demonstrated that KW1 is located around the cell nuclei of the neurons. Thus, KW1 was expressed and secreted correctly in the nervous system of the fly brain.

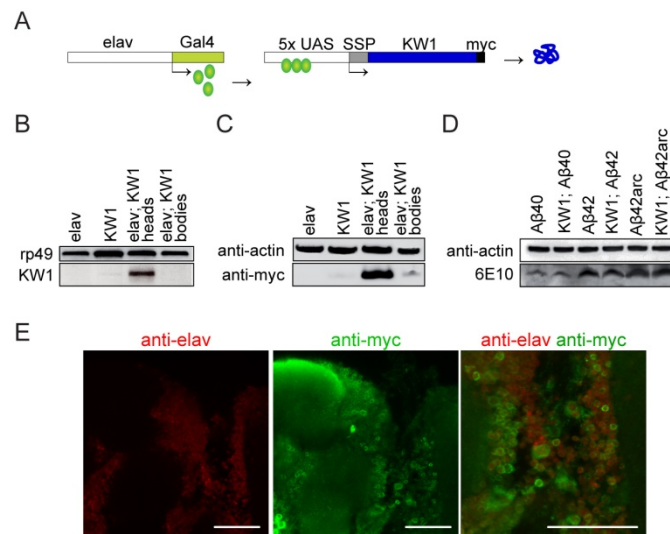


**Figure 3.3.2** Expression of KW1 in *Drosophila melanogaster*. (A) Schematic representation of the expression construct. (B) RT-PCR analysis of KW1 mRNA transcription in the head or remaining body; i.e. thorax and abdomen, of different fly lines as indicated in the panels. Constitutively transcribed rp49 mRNA served as a loading control. (C) Western blot with an anti-myc primary antibody showed a strong band at around 17 kDa with almost identical distribution as the KW1 mRNA in panels (B). Anti-actin western blot served as loading control. (D) Western blot with 6E10 primary antibody to detect A $\beta$  displayed a strong band at around 4 kDa in A $\beta$  expressing *Drosophila melanogaster*. Anti-actin western blot served as loading control. (E) IFM of KW1 expressing flies using anti-elav antibody (red) to stain neuronal cells and anti-myc antibody (green) to detect KW1. The right picture is a magnified merge of both stainings. Scale bars represent 50  $\mu$ m.

### **3.3.3 B10 and KW1 do not affect the overall expression of A $\beta$**

As the expression of both transgenes are regulated by the binding of Gal4 to a 5x UAS sequence, it could be possible that expression of Gal4 leads to different A $\beta$  levels in flies expressing A $\beta$  alone or together with an antibody domain. Qualitative analysis of western blots suggested that the A $\beta$  level is not altered in presence of B10 or KW1 (figure 3.3.1D and 3.3.2D). However, in order to determine the total A $\beta$  levels in the fly brain more quantitatively an A $\beta$ (1-40) and A $\beta$ (1-42)-specific sandwich enzyme linked immunosorbant assay (ELISA) assay was used. Head homogenates of A $\beta$ 42arc or A $\beta$ 40 flies were compared to B10; A $\beta$ 42arc and KW1;A $\beta$ 40 flies, respectively. After eclosing the flies were decapitated and total protein was extracted from the heads using a strong denaturing buffer (5 M guanidinium hydrochloride). ELISA experiments were carried out using the monoclonal antibody 6E10 to capture A $\beta$  and detection was performed using the A $\beta$ (1-40) specific antibody 2G3 as well as the A $\beta$ (1-42) specific antibody 21F12 <sup>[161]</sup>.

The A $\beta$ (1-40) concentration detected in the ELISA assay using the 2G3 antibody was  $40.47 \pm 0.6$  ng/ml. In presence of B10 and the A $\beta$ (1-40) concentration was  $42.48 \pm 0.46$  ng/ml and  $40.98 \pm 0.66$  ng/ml, respectively. ELISA assessment with the 21F12 antibody obtained an A $\beta$ (1-42)arc concentration of  $16.79 \pm 2.47$  ng/ml when no antibody was co-expressed. The A $\beta$ (1-42)

concentration was  $17.77 \pm 1.96$  ng/ml in presence of B10 and  $18.29 \pm 2.02$  ng/ml in presence of KW1. These data demonstrated that the expression of the antibody domains has no discernible effects on the total A $\beta$  expression level. However, since the measurement of A $\beta$ (1-40) and A $\beta$ (1-42) in this assay critically depended on the specificity of the monoclonal antibodies used in the detection step the results allow only conclusions about the total A $\beta$  level of one A $\beta$  variant and is not useful to compare A $\beta$ 40 and A $\beta$ 42 levels.

B10 and KW1 flies were then used to create double transgenic *Drosophila melanogaster* stocks that can co-express A $\beta$  and one of the antibody domains in the neurons. Therefore the flies were crossed with *Drosophila melanogaster* transgenic for A $\beta$ (1-40), A $\beta$ (1-42) and A $\beta$ (1-42)arc (see method 2.2.1.2). This led to the following fly lines:

Table 3.1 *Drosophila melanogaster* double transgenic for A $\beta$  and B10 or KW1.

+/+; B10/CyO; A $\beta$ 40/TM6B	+/+; B10/CyO; A $\beta$ 42/TM6B	+/+; B10/CyO; A $\beta$ 42arc/TM6B
+/+; KW1/CyO; A $\beta$ 40/TM6B	+/+; KW1/CyO; A $\beta$ 42/TM6B	+/+; KW1/CyO; A $\beta$ 42arc/TM6B

### **3.4 Quantification of B10 and KW1 expressed in *Drosophila melanogaster***

B10 and KW1 are known to inhibit fibril formation at substoichiometric concentrations. A ratio of one molecule of B10 per ten molecules of A $\beta$  was found to block the formation of mature A $\beta$  fibrils <sup>[138]</sup>, whereas one molecule of KW1 per five molecules of A $\beta$  is needed to prevent the transition of oligomers <sup>[135]</sup>. The nature of these ratios in the fly, however, remained to be determined.

First, B10 and KW1 expressing flies were analysed using western blot to investigate the expression level of both antibody domains. Fly heads were collected and proteins were extracted using PBS supplemented with 1 % SDS. The protein concentration to be loaded on a SDS-PAGE gel was equalised using a Bradford assay. After blotting the membrane was cut and stained with anti-myc and anti-actin antibodies. Upon the same genomic insertion of B10 and KW1 it was expected that the anti-myc signal reveals similar protein levels of B10 and KW1. This expectation was confirmed by western blot, whereas blotting for actin revealed equal protein loading (figure 3.4.1A).

For a quantitative measurement of B10 levels *in vivo* a B10 variant for expression in *E. coli* was generated with its amino acid sequence being identical to the antibody domain expressed in *Drosophila melanogaster* (B10-myc). It included the sequence for B10 as well as the C-terminal myc-tag and was cloned into the *E. coli* expression plasmid p41. After induction with IPTG B10-myc was expressed in *E. coli* and purified using the ÄKTAexplorer system (GE Healthcare). The purification using two nickel chelate chromatography (NiNTA) columns and one reversed phase chromatography (RPC) column led to pure B10-myc ( $\geq 95$  %), as shown by SDS-PAGE and a resulting band around

17 kDa (figure 3.4.1B). B10-myc was then utilised as a protein standard to determine the amounts of B10 and KW1 expressed in the fruit fly.

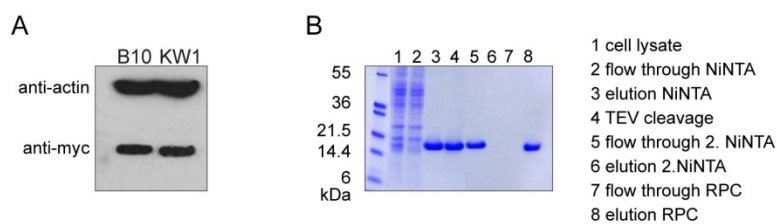


**Figure 3.4.1** Comparison of B10 and KW1 expression in *Drosophila melanogaster* and establishment of recombinant B10-myc. (A) Western blot analysis enabled the comparison of the expression levels of B10 and KW1. Using an anti-actin antibody equal protein loading was confirmed. (B) To quantify the protein amounts the *Drosophila* equivalent B10-myc was overexpressed in *E. coli* and purified using NiNTA and RPC chromatography with  $\geq 95\%$  purity.

To quantify the amount of the antibody domains *in vivo* head homogenates of three B10- and KW1-expressing flies each were analysed in a western blot. To create a standard curve B10-myc was prepared in increasing amounts (0,5 – 5 ng) and blotted together with the fly samples onto a nitrocellulose membrane (figure 3.4.2A). Afterwards all relevant bands were quantified densitometrically using the TotalLab 100 software and the amount of B10 and KW1 was calculated using linear regression of the standard curve (figure 3.4.2A bottom panel). To calculate the molarities of B10 and KW1 per fly head a head volume of 65 nl was assumed<sup>[173]</sup>. The following equation was used:

$$c (\mu\text{M}) = \frac{c (\text{ng})}{\text{head (65nl)}} \cdot \frac{1 \cdot 10^6}{\text{MW}} \quad \text{MW} = \text{molecular weight}$$

Analysing the fly sample in triplicates the following results were achieved: on average the B10 amount in three fly heads is  $2.48 \pm 0.59$  ng and there is slightly more KW1 ( $3.11 \pm 0.87$  ng). For one fly head this gives values of  $0.83 \pm 0.197$  ng/head (B10) and  $1.04 \pm 0.290$  ng/head (KW1) leading to a molarity of  $0.79 \pm 0.19$   $\mu\text{M}$  and  $1.05 \pm 0.29$   $\mu\text{M}$ , respectively. Comparable results were seen for expression of the human protein Transthyretin (TTR) in *Drosophila melanogaster* using expression based on the Gal4-UAS system in the neurons<sup>[173]</sup>. From the density of the TTR bands in a western blot Berg *et al.* estimated a TTR concentration of 0.23 mg/ml displaying a molarity of 16  $\mu\text{M}$  per fly head<sup>[173]</sup>.

Since the protein extraction using 1 % SDS might not pull out all proteins from the fly homogenate a second extraction protocol was applied using 9 M urea in parallel to the previous protocol and compared the band intensities after western blot analysis (figure 3.4.2B). Again three fly heads from B10 or KW1 expressing flies were extracted using either 1 % SDS or 9 M urea and after transferring the proteins on nitrocellulose membrane the blot was developed using the anti-myc

antibody. Densitometrical analysis revealed that both extraction methods result in similar amounts of protein. Thus, the SDS-extraction method is sufficient to estimate the protein concentration.

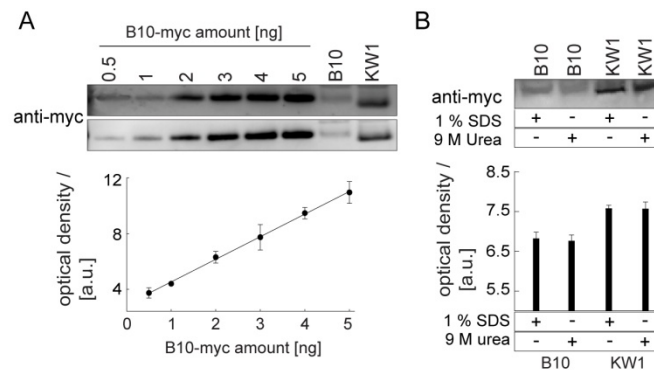


**Figure 3.4.2** Quantification of B10 and KW1 expression in *Drosophila melanogaster*. (A) Western blot of recombinant B10-myc as peptide standard to quantify the antibody domains. Detection was carried out using the anti-myc antibody. The band intensity was measured using TotalLab 100 software and plotted protein amount [ng] versus optical density [a.u.] of the respective band (n=3). Finally, a linear regression was applied (r = 0.9994). (B) Western blot to compare the protein amount of the antibody domains after SDS and urea extraction. The band intensities were measured using TotalLab 100 software (n=2).

### **3.5 Quantification of A $\beta$ peptides expressed in *Drosophila melanogaster***

In the *Drosophila melanogaster* model of AD used in this work each of the human A $\beta$  variants A $\beta$ (1-40), A $\beta$ (1-42) or A $\beta$ (1-42)arc are expressed in the fly neurons. In proportion to their aggregation propensity, the peptides have been shown to accumulate intracellular resulting in progressive decline and neurodegeneration<sup>[95]</sup>. To take a closer look into the expression pattern of the three A $\beta$  variants RT-PCR and western blot analyses were carried out using A $\beta$ 40, A $\beta$ 42 and A $\beta$ 42arc flies (figure 3.5.1A-B). RT-PCR analysis was done on 20 fly heads per genotype and the subsequent PCR using A $\beta$ -specific primers showed the same band intensity in all three samples (figure 3.5.1A). A second PCR using the primers for the ribosomal protein rp49 demonstrated identical cDNA concentrations in all samples. Thus, the three fly lines transcribed A $\beta$  in similar amounts.

Western blot analysis was carried out using 6E10 to detect the amount of A $\beta$  actually present in the fly lines. For this assay it was not possible to use equal amounts of fly heads, due to the enormous differences in the peptide level of A $\beta$  in these fly lines. Using the heads of 15 A $\beta$ 40 flies, 10 A $\beta$ 42 flies and 5 A $\beta$ 42arc flies led to a comparable result (figure 3.5.1B). The greatest A $\beta$  amount in the fly neurons was visible within the A $\beta$ 42arc flies whereas the A $\beta$ 40 flies had the lowest A $\beta$  concentration. Western blot using anti-actin demonstrated the differences in the protein concentration due to the different number of fly heads. These data indicated that on the one hand the genes are transcribed at similar levels but on the other hand the clearance and accumulation of these peptides rely on the aggregation propensity leading to different peptide amounts. The data

were further supported by IFM analysis determining the accumulation of A $\beta$  inside the fly brain. Adult fly brains were stained with 6E10 to image the A $\beta$  accumulation and the cell nuclei were detected using the dye Hoechst 33342 (figure 3.5.1C). The flies were aged at 29 °C before the brains were dissected (A $\beta$ 40: 20 days, A $\beta$ 42: 20 days, A $\beta$ 42arc: 3 days). With the 6E10 staining a similar accumulation pattern was seen as with the western blot analysis. After 20 days the brains of A $\beta$ 40 flies showed only background staining and no distinct signals. The brains of A $\beta$ 42 flies displayed some distinct signals indicative of A $\beta$  accumulation, though only a limited amount. In contrast, brains of A $\beta$ 42arc flies presented a great number of 6E10 positive signals indicating strong A $\beta$  accumulation. Additionally, the IFM pictures showed that the 6E10 signals generally occurred in the cell bodies and not in the neuropil.

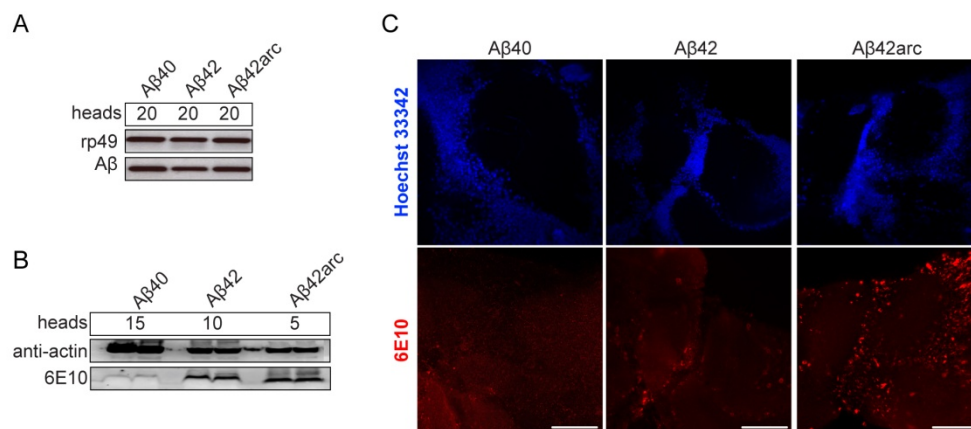


**Figure 3.5.1** Expression of A $\beta$  peptides in *Drosophila melanogaster*. (A) RT-PCR analysis of A $\beta$  mRNA in 20 fly heads of each A $\beta$ 40, A $\beta$ 42 and A $\beta$ 42arc flies. Ribosomal rp49 mRNA served as loading control. (B) Western blot with 6E10 antibody displayed A $\beta$  bands at around 4 kDa. Anti-actin western blot demonstrated differences in protein loading due to the different number of fly heads as indicated in the upper panel. (C) IFM with 6E10 antibody (red) to stain A $\beta$  distribution in the fly brain of aged A $\beta$  expressing flies. A $\beta$ 40: 20 days; A $\beta$ 42: 20 days, A $\beta$ 42arc: 3 days. Hoechst 33342 was used to stain the DNA in the nuclei. Scale bars represent 50  $\mu$ m.

To quantify the peptide concentration of all three A $\beta$  variants western blot analysis was performed. Since initial western blot analysis (figure 3.5.1B) demonstrated the presence of much more A $\beta$ (1-42)arc than A $\beta$ (1-42) and A $\beta$ (1-40) different amounts of fly heads were used in this assay. To determine A $\beta$ (1-40) seven fly heads were homogenised in PBS supplemented with 1 % SDS. In case of A $\beta$ (1-42) two fly heads were used and for A $\beta$ (1-42)arc one fly head led sufficient results. Synthetic A $\beta$ (1-40) or A $\beta$ (1-42) was used to prepare the standard curves with increasing peptide concentrations varying from 5 – 1000 pg.

Figure 3.5.2A presents the western blot using A $\beta$ 40 flies as well as B10;A $\beta$ 40 and KW1;A $\beta$ 40 flies. The standard ranged from 5 – 500 pg synthetic A $\beta$ (1-40). Using a linear regression and the formula shown in chapter 3.4 an A $\beta$ (1-40) concentration of  $0.19 \pm 0.025 \mu$ M per fly head was

determined. In presence of B10 the A $\beta$ (1-40) value was  $0.11 \pm 0.41 \mu\text{M}$  and  $0.17 \pm 0.59 \mu\text{M}$  in presence of KW1. The concentration of A $\beta$ (1-42) was determined in figure 3.5.2B again in the presence and absence of the two antibody domains. The peptide standard of synthetic A $\beta$ (1-42) was increased from 25–750 pg. The resulting concentration for A $\beta$ (1-42) was  $0.47 \pm 0.15 \mu\text{M}$  per fly head. Neither B10 ( $0.39 \pm 0.15 \mu\text{M}$ ) nor KW1 ( $0.32 \pm 0.07 \mu\text{M}$ ) altered the A $\beta$ (1-42) concentration significantly. As expected, the highest values were reached with A $\beta$ (1-42)arc flies (figure 3.5.2C). Referring to a synthetic A $\beta$ (1-42) standard varying from 50 – 1000 pg an A $\beta$  concentration of  $2.46 \pm 0.22 \mu\text{M}$  was determined per fly head. In the B10;A $\beta$ 42arc flies the concentration was  $2.47 \pm 0.46 \mu\text{M}$  and in KW1;A $\beta$ 42arc flies  $2.4 \pm 0.5 \mu\text{M}$  A $\beta$ (1-42)arc were present.

The quantification was completed with a western blot determining the A $\beta$  concentration upon SDS and urea extraction. The same amounts of fly heads as described above were used in parallel extractions. On one hand the heads were homogenised in PBS containing 1 % SDS and on the other hand 9 M urea buffer was used. Densitometrical analysis of the bands displayed that both extraction methods led to similar peptide concentrations (figure 3.5.2D).

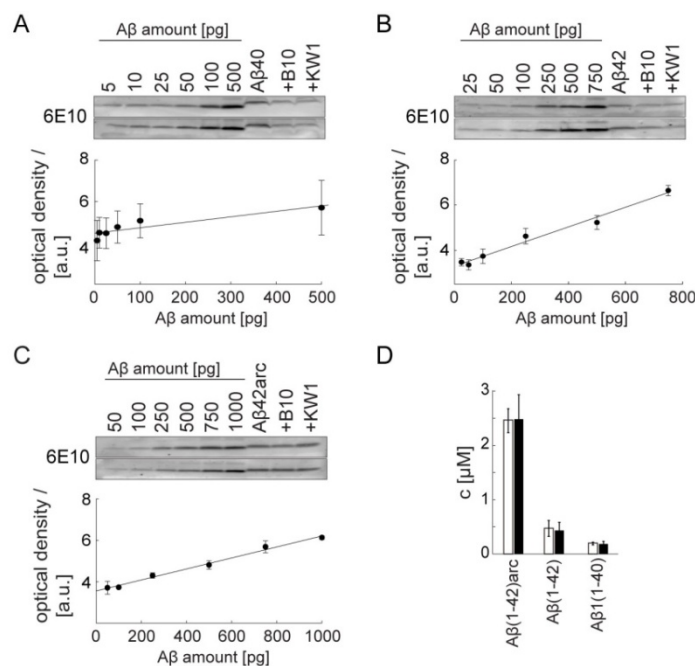


**Figure 3.5.2** Quantification of A $\beta$  peptide expression in *Drosophila melanogaster* in presence or absence of B10/KW1. (A) Western blot of recombinant A $\beta$ (1-40) as peptide standard to quantify the A $\beta$ (1-40) concentration in seven fly heads. (B) Western blot of recombinant A $\beta$ (1-42) as peptide standard to quantify the A $\beta$ (1-42) concentration using two fly heads. (C) Western blot of recombinant A $\beta$ (1-42) as peptide standard to quantify the A $\beta$ (1-42)arc concentration using one fly head per genotype. In all blots detection was carried out using 6E10. The band intensity was measured using TotalLab 100 software and plotted protein amount [pg] versus optical density [a.u.] of the respective band (n=3). Finally, a linear regression was applied ( $r \geq 0.99$ ). (D) Graphical comparison of A $\beta$  concentration upon SDS (white bars) and urea (black bars) extraction.

Taken together the data above demonstrated that A $\beta$  levels decline dependent on the expressed variant in the following way: A $\beta$ (1-42)arc > A $\beta$ (1-42) > A $\beta$ (1-40). A graphical comparison of the peptide concentration of all three A $\beta$  variants and the two antibody domains (figure 3.5.3A) led to the *in vivo* A $\beta$ -antibody domain ratios shown in figure 3.5.3B. Comparing A $\beta$  and B10 levels the data implied a molar stoichiometry that exceeds the molar ratio of 1:10 (B10:A $\beta$ ) which was found to inhibit the formation of mature fibrils *in vitro*<sup>[138]</sup>. The molar ratio of KW1 and A $\beta$  seen *in vivo* significantly exceeded the 1:5 (KW1:A $\beta$ ) stoichiometry that was found to prevent fibrillation *in vitro*<sup>[135]</sup>.

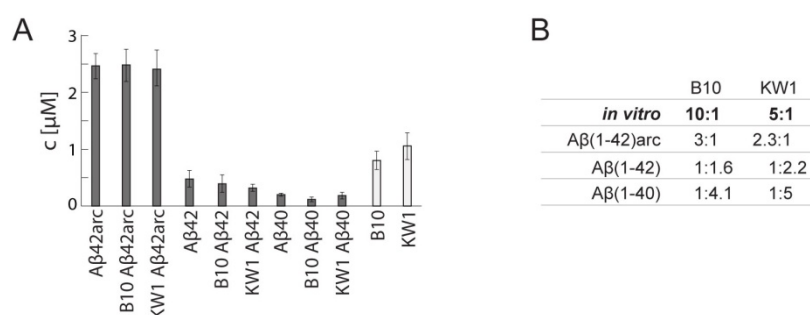


Figure 3.5.3 Comparison of A $\beta$  peptide and antibody domain levels in *Drosophila melanogaster*. (A) Graphical overview about peptide concentrations [ $\mu$ M] in *Drosophila melanogaster* (n=3). Grey bars: A $\beta$  concentration, white bars: B10 and KW1 concentration. (B) Determination of the molar ratio between A $\beta$  and B10 or KW1 calculated using the values in (A).

### **3.6 In vivo interactions of B10 and KW1 with A $\beta$**

#### **3.6.1 Immunofluorescence studies on adult fly brains suggest co-localisation**

B10 and KW1 are known to interfere with the *in vitro* process of A $\beta$  aggregation. It is however unknown whether both antibody domains were able to interact with A $\beta$  *in vivo*. The strategy of fly construction already suggested that the two polypeptide chains are likely to interact *in vivo*. A $\beta$  and B10 were both expressed through the neuron-specific Gal4-UAS system, and they were targeted to the secretory pathway. Confocal IFM was applied to study the protein localisation in the fly brain. Fly brains of adult aged flies were infiltrated with 6E10 and anti-myc antibodies to stain A $\beta$  and the antibody domains, respectively, while the DNA in the cell nuclei was stained using Hoechst 33342 (figure 3.6.1). To study the protein localisation the focus was pointed on the cell bodies of the neurons between the optical lobes and protocerebra indicated in figure 3.6.1A which have been shown to stain for A $\beta$  and the antibody domains (figures 3.3.1, 3.3.2 and 3.5.1). IFM of non-transgenic 20-day old WT flies showed only diffuse background staining (figure 3.6.1B) with 6E10 (red) and anti-myc (green). By contrast, 3-day old *elav;B10;Aβ42arc* flies showed punctuate 6E10

staining and also similar signal responses to the anti-myc antibody (figure 3.6.1C). An overlay of both 6E10 and anti-myc staining indicated co-localisation of B10 and A $\beta$ 42arc. Comparable results were seen with 20-days old KW1;A $\beta$ 40 flies (figure 3.6.1D). A weak, but distinct 6E10 signal was seen in the cell body region with a similar fluorescence pattern by the anti-myc antibody. Furthermore, these signals overlaid in the merged picture indicating that KW1 is able to co-localise with A $\beta$ 40.

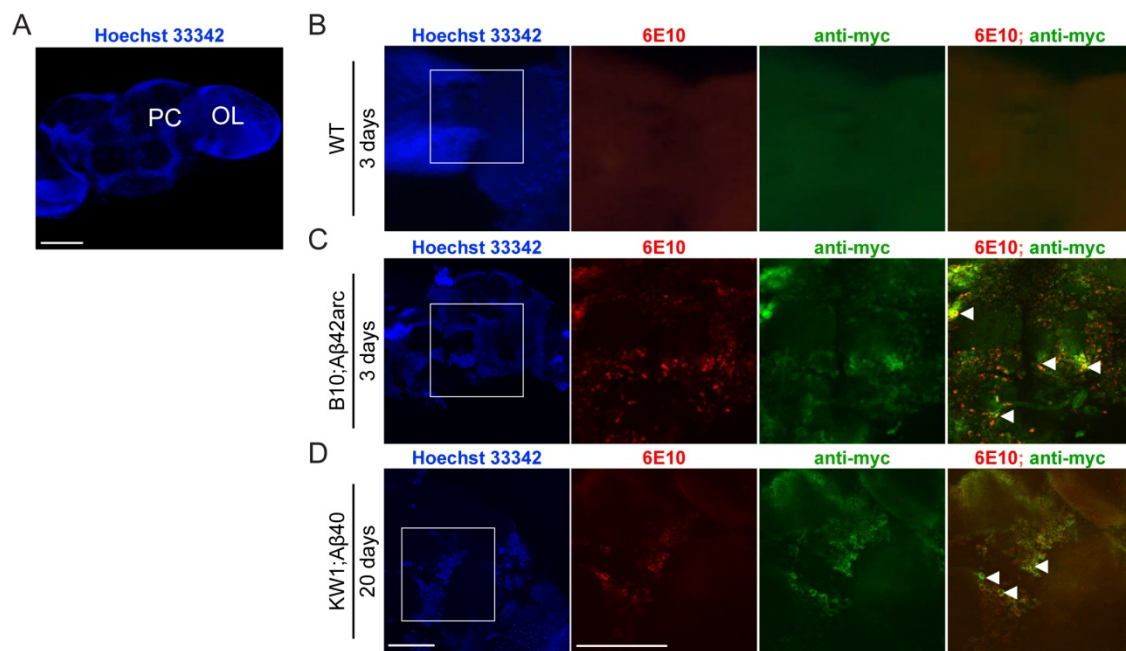


**Figure 3.6.1** Evidence for *in vivo* interactions of A $\beta$  and the two antibody domains using immunofluorescence (IFM). (A) Confocal IFM image of a WT brain stained with Hoechst 33342 to visualise the cell nuclei. The optical lobes (OL) and protocerebra (PC) of the right hemisphere are indicated. (B-D) IFM images of adult brains from 20-days old WT (B), 3-days old B10;A $\beta$ 42arc (C) and 20-days old KW1;A $\beta$ 40 flies (D). Left column (blue): Hoechst 33342 staining of the cell nuclei. The white box is enlarged in the following columns.; second column (red): A $\beta$ -staining with 6E10 antibody; third column (green): staining of myc-tagged B10 or KW1 with anti-myc antibody; right column shows an overlay of the 6E10 and anti-myc signals. All preparations are fly brain whole mounts viewed frontally with dorsal on top. Scale bars represent 50  $\mu$ m.

Whilst the IFM data demonstrated that from their cellular localisation B10 and KW1 may have the ability to bind to A $\beta$ , they are unable to prove a direct physical interaction due to the low resolution of the microscope relative to the size of the protein molecules.

### **3.6.2 Spot blot assay demonstrate the presence of the B10 epitope in *Drosophila***

To demonstrate the presence of the B10 epitope in the fly a spot blot assay was carried out. Head homogenates of WT, A $\beta$ 40, A $\beta$ 42 and A $\beta$ 42arc flies were spotted onto a nitrocellulose membrane together with *in vitro* formed A $\beta$ (1-40) fibrils (figure 3.6.2A). Ponceau S staining revealed equal protein loading in each spot (left membrane). The second membrane was incubated with

B10-myc and stained with the anti-myc antibody (right membrane). Clear signals were seen with the synthetic A $\beta$ (1-40) fibrils demonstrating the binding ability of B10-myc. Analysis of the fly samples demonstrated that B10-myc binds strongly to extracts of A $\beta$ 42 flies and more weakly to A $\beta$ 42arc and A $\beta$ 40 flies. This data suggested that the B10-epitope is present in the fly brain, however, a weak signal was also seen with B10-myc blotting of WT fly extracts. This could result from cross reaction of the anti-myc antibody with endogenous *Drosophila melanogaster* proteins. This assumption was confirmed by anti-myc western blot of head homogenates from WT and B10 expressing flies (figure 3.6.2B). 11 extra bands were visible on the anti-myc western blot, in addition to the B10 band. These data confirmed that protein homogenates from WT flies were also stained with the polyclonal anti-myc antibody.

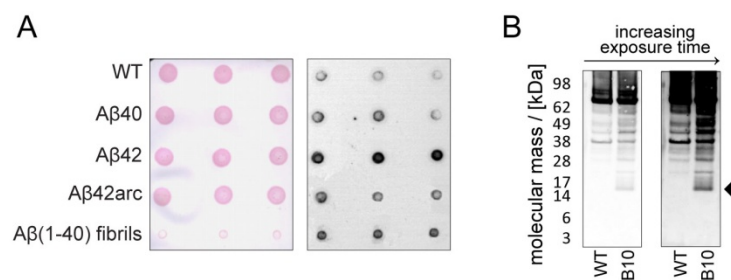


**Figure 3.6.2** The B10 epitope is present in *Drosophila melanogaster*. (A) Spot blot analysis of head homogenates of WT, A $\beta$ 40, A $\beta$ 42 and A $\beta$ 42arc flies stained with Ponceau S (left, loading control) and B10-myc (right). (B) Western blot analysis of WT and B10-expressing flies stained with anti-myc antibody displaying several extra bands despite the respective band for B10 (arrowhead).

Similar results to the anti-myc staining were seen when the membrane was incubated with *E. coli* B10 and KW1 followed by detection with the polyclonal antibodies anti-His or anti-B10<sup>[162]</sup> (figure 3.6.2.1). Both antibodies bound with no discernible differences to all four fly homogenates. Taken together these data revealed that, due to unspecific binding, spot blot is not applicable for a precise enough assay to demonstrate the presence of the B10 epitope from tissue samples.

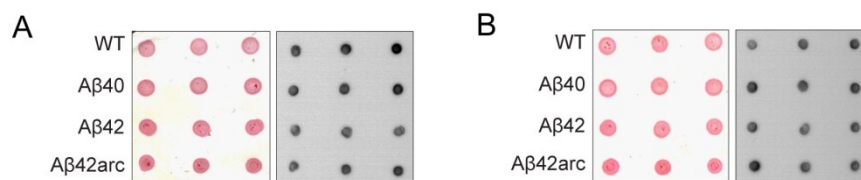


**Figure 3.6.2.1** Polyclonal antibodies in spot blot assays with *Drosophila melanogaster* homogenate. Spot blot analysis of head homogenates of WT, A $\beta$ 40, A $\beta$ 42 and A $\beta$ 42arc flies (A) stained with Ponceau S (left, loading control) and the polyclonal anti-His antibody (right) or (B) stained with Ponceau S (left) and the polyclonal anti-B10 antibody (right, gift from C.Röcken<sup>[162]</sup>).

### **3.6.3 B10AP and KW1AP do not cross-react with *Drosophila melanogaster* proteins**

The data in section 3.6.2 raised the question of whether B10 and KW1 also bind non-specifically to *Drosophila melanogaster* proteins. To address this question WT flies were homogenised and equal protein amounts were separated using SDS-PAGE and native PAGE. B10 and KW1 binding to endogenous *Drosophila melanogaster* proteins was analysed using western blot followed by incubation with B10AP and KW1AP and detection via their AP moiety (figure 3.6.3). After transfer one membrane was stained with Ponceau S to visualise the protein transfer to the membrane. Another membrane was used as negative control and incubated without antibody (no ab) to make sure that no endogenous proteins develop a signal when incubated with the AP substrate. Two more membranes were stained with either B10AP or KW1AP. After denaturing SDS-PAGE the staining with B10AP and KW1AP did not raise any signals (figure 3.6.3.A). A similar result was obtained in the western blot analysis following native PAGE (figure 3.6.3B). All staining patterns were confirmed by spotting A $\beta$ (1-40) fibrils or oligomers onto a membrane and incubation in the same antibody solution as a positive control (figure 3.6.3C). Ponceau S staining revealed the presence of the *in vitro* formed A $\beta$  species. These data verified that B10AP and KW1AP do not cross-react with endogenous *Drosophila melanogaster* proteins.

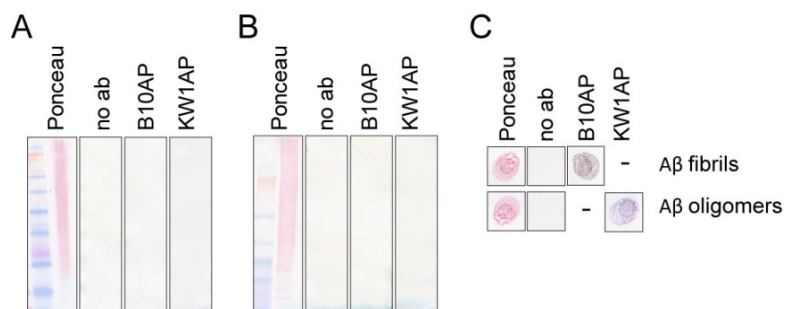


*Figure 3.6.3* Western blots of head lysates from WT flies probed with B10AP or KW1AP. Ponceau S staining served as a loading control. An additional control was carried out using no antibody (no ab) to exclude endogenous alkaline phosphatase activity. (A) Western blot after denaturing SDS-PAGE (B). Western blot after native PAGE (C). Positive controls with 20  $\mu$ g peptide A $\beta$ (1-40) fibrils or oligomers spotted on a membrane and stained with B10AP and KW1AP, respectively.

### **3.6.4. Immunoprecipitation analysis of A $\beta$ and B10 expressing flies**

Another approach to examine B10 and KW1 binding *in vivo* is immunoprecipitation (IP). IP analysis can determine explicitly whether two proteins are physically attached to one another. Several studies have established successful IP protocols for precipitating A $\beta$  out of mice or *Drosophila melanogaster* brain homogenates using the monoclonal antibody 6E10<sup>[174, 175]</sup>. Protein A is a cell surface protein originally found in the cell wall of *Staphylococcus aureus* that binds with moderate affinity to the Fc region of mouse IgG antibodies such as 6E10. Instead of slurry beads that are

separated from the solution by centrifugation or sedimentation, magnetic protein A beads displayed the advantage of easy solution changes such as washing and elution buffers. The general IP protocol used involved antibody binding to the beads, followed by incubation with brain homogenate, washing steps and elution of the target protein (figure 3.6.4A). The samples analysed using western blot were the total sample before IP (T), the supernatant after incubation with the beads (S), washing step 1 (W) and the final elution (E). Detection of A $\beta$  peptide in WB was carried out using the antibody 6E10. First, the antibody 6E10 was attached to the beads and A $\beta$  was precipitated from A $\beta$ 42arc flies (figure 3.6.4B). Western blot analysis displayed A $\beta$  in the total sample, supernatant and in the elution fraction. Afterwards, Non-specific A $\beta$  binding was excluded with an IP where no antibody was bound to the beads and in which A $\beta$ 42arc as well as A $\beta$ 40 flies were tested (figure 3.6.4.C). Western blot analysis demonstrates that all A $\beta$  was found in the supernatant in the fly homogenates which were incubated with the unconjugated beads. These data revealed that protein A beads are appropriate for A $\beta$  pull-down experiments.

In the next experiments direct precipitation of B10 and KW1 was tested using protein A beads without an additional antibody attached (figure 3.6.4D). The anti-myc staining after western blot of the B10 fly homogenate revealed that all B10 is found in the supernatant. In contrast, KW1 was seen in the supernatant but also in the elution fraction. Thus, KW1 can be precipitated directly using protein A beads whereas B10 cannot. This information led to the following experimental set ups:

1. For B10;A $\beta$ 42arc fly samples 6E10 was bound to the protein A beads to pull-down A $\beta$  and the fractions analysed by western blot are stained with anti-myc to visualise B10.
2. For KW1;A $\beta$ 40 fly samples no antibody was attached to the protein A beads and KW1 was precipitated. Western blot analysis of all fractions used 6E10 to detect A $\beta$ .

In figure 3.6.4E the western blot on B10;A $\beta$ 42arc flies is shown. As seen before, A $\beta$  is bound to the protein A beads and occurred in the elution fraction. Additionally, the anti-myc antibody detection demonstrated that B10 is reduced in the supernatant and occurred in the elution fraction together with A $\beta$ 42arc. This experiment indicated the binding of B10 to A $\beta$  *in vivo*. To exclude any nonspecific interactions between 6E10 and B10, the same experiment was done using B10 flies (figure 3.6.4F). Western blot analysis using anti-myc showed all B10 in the supernatant. Since the B10 flies did not express A $\beta$ , the western blot with 6E10 detected no bands at all. Taken together, these data led to the conclusion that due to an *in vivo* interaction B10 is co-precipitated together with A $\beta$ .

KW1;A $\beta$ 40 flies were used to demonstrate the *in vivo* interaction of KW1 and A $\beta$ 40 (figure 3.6.4G). Again western blot using anti-myc revealed that a good amount of KW1 is bound to protein A beads

and can be visualised in the elution fraction. The same fractions, stained with 6E10, show A $\beta$ 40 in both the supernatant and the elution fraction. Together with the information that A $\beta$ 40 does not bind to the protein A beads itself (figure 3.6.4C) this experiment proves the *in vivo* interaction of KW1 and A $\beta$ 40 in *Drosophila melanogaster*.

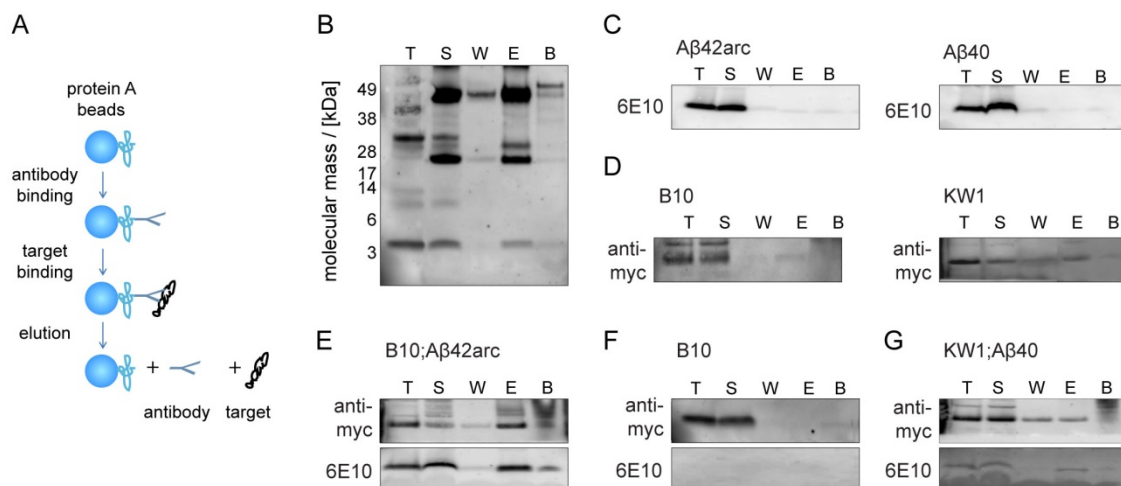


**Figure 3.6.4** Immunoprecipitation of *Drosophila* proteins using protein A beads. (A) Schematic draft of an IP including antibody binding, target binding and elution. Image was modified from Invitrogen. (B) IP on A $\beta$ 42arc flies. 6E10 was attached to the protein A beads. Western blot detection was carried out using 6E10. (C) IP on A $\beta$ 42arc (right) and A $\beta$ 40 (left) flies. Beads were not conjugated with an antibody before IP. Detection in western blot used 6E10. (D) IP on B10 (right) and KW1 (left) flies. No antibody was conjugated to the beads before IP and detection was carried out with anti-myc antibody. (E) IP on B10;A $\beta$ 42arc flies. 6E10 was bound to the beads to pull A $\beta$ . Anti-myc and 6E10 were used for detection in western blot. (F) IP on B10 flies with 6E10 attached to the beads. 6E10 and anti-myc were used for western blot detection. (G) IP on KW1;A $\beta$ 40 flies. Beads were not conjugated with an antibody before IP. Western blot detection was done using 6E10 and anti-myc. Abbreviations refer to total sample (T) before IP, supernatant after incubation with the beads (S), wash fraction (W), elution (E) and the beads after elution (B).

### **3.7 Phenotypic characterisation of A $\beta$ dependent neurodegeneration**

The expression of human A $\beta$  led to severe neurodegeneration in *Drosophila melanogaster* depending on the A $\beta$  variant<sup>[95]</sup>. The aggregation process developed an *in vivo* phenotype in the short lifespan of *Drosophila melanogaster*. This phenotype strongly correlated with the aggregation propensity of the A $\beta$  variant<sup>[51, 95]</sup>. In this thesis the effect of the antibody domains B10 and KW1 was assessed using A $\beta$ 40, A $\beta$ 42 and A $\beta$ 42arc flies. Three different assays were used to determine the phenotypic effects of A $\beta$  in comparison to WT flies: survival assay, climbing assay and scanning electron microscopy (SEM). Figure 3.7 gives an overview about the phenotypic changes observed upon expression of the three A $\beta$  variants A $\beta$ (1-40), A $\beta$ (1-42) and A $\beta$ (1-42)arc. To switch on the expression of the A $\beta$  variants, the transgenic A $\beta$  flies were crossed with the neuronal driver Gal4-elav<sup>c155</sup>. The flies were raised and after hatching kept at 29 °C. A survival assay was carried out to determine the lifespan of the A $\beta$  expressing flies. In this assay 100 flies per genotype were

counted every 2<sup>nd</sup> to 3<sup>rd</sup> day until all flies were dead and from this data the medium survival, where 50 % of the flies are dead was determined (figure 3.7.A, table 3.2). The WT showed a medium survival of  $43 \pm 0.1$  days (circles) and all flies died within 50 days. No difference from the WT was seen with A $\beta$ 40 flies (triangles, medium survival of  $43 \pm 0.6$  days). Upon expression of A $\beta$ (1-42) the lifespan of A $\beta$ 42 flies (diamonds) was reduced resulting in a medium survival of  $32 \pm 0.5$  days. The strongest phenotypic change was seen with A $\beta$ 42arc flies where all flies were deceased within 10 days (squares, medium survival of  $7 \pm 0.1$  days). This A $\beta$  dependent lifespan decline correlated well with previously observed results [95]. The second assay was a negative-geotaxis assay to estimate the climbing ability of the flies (figure 3.7B). Therefore, every 2<sup>nd</sup> day 15 flies per genotype were tapped down in a 25 ml plastic vial and the number of flies reaching the top and staying at the bottom was counted after 45 seconds. These data enabled the determination of the mobility index (see 2.2.1.3). Young flies usually are highly mobile and reach the top of the vial quickly. However, during ageing the mobility decreases and 60 % of the 20 day old WT flies do not reach the top within the time of the experiment. WT flies (circles) as well as A $\beta$ 40 flies (triangles) lost their climbing ability within 30 days. A $\beta$ 42 flies (diamonds) presented a reduced climbing ability and were immobile by day 22. As with the lifespan assay A $\beta$ 42arc flies produced the most severe phenotype and were immobile by day 6.

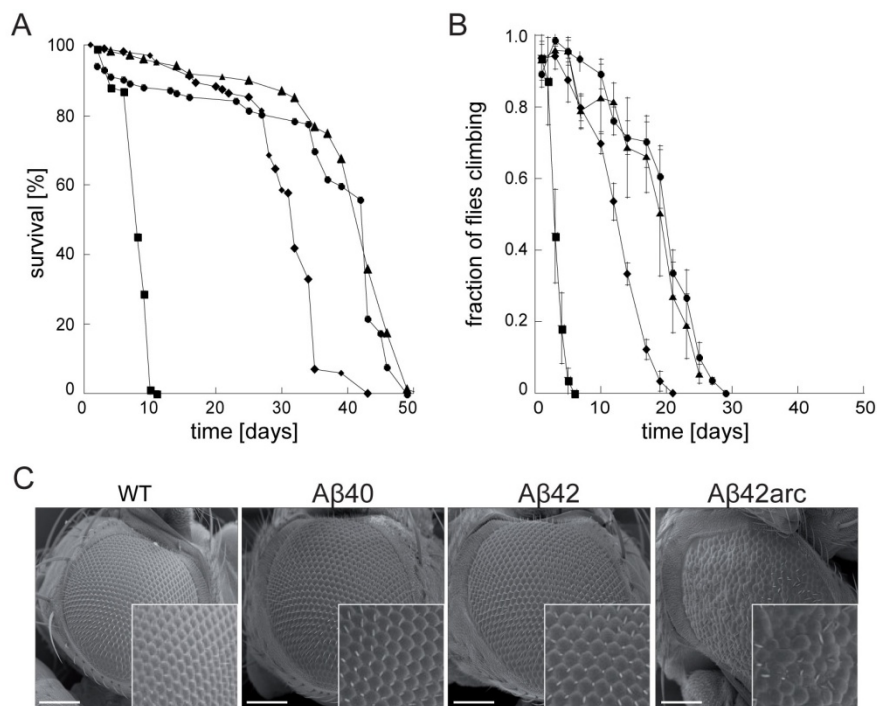


**Figure 3.7** Phenotypic characterisation of A $\beta$  expressing *Drosophila melanogaster*. (A,B) A $\beta$ 40 (triangles), A $\beta$ 42 (diamonds) and A $\beta$ 42arc (squares) flies were compared to WT flies (circles). (A) Viability of 100 flies per genotype was determined at 29° C. (B) Fraction of flies, reaching the vial top in a negative-geotaxis assay. Error bars represent standard deviation from three independent samples using 15 flies each. (C) Comparison of the eye morphology using SEM. All eye structures are shown enlarged (4x) in the boxes. Scale bars represent 20  $\mu$ m.

Table 3.2 Medium survival of A $\beta$  transgenic flies.

genotype	median survival	std.error	95 % lower confidence level	95 % upper confidence level
WT	43	0.1	42.767	43.233
A $\beta$ 40	43	0.6	41.8	44.2
A $\beta$ 42	34	0.3	33.393	35.607
A $\beta$ 42arc	7	0.1	6.846	7.154

The third assay allowed the investigation of the compound eye structure. Therefore scanning electron microscopy (SEM) was used to assess the morphology of the external eye. The external eye of the fly consists of regular, hexagonal arranged ommatidia including the photoreceptor cells surrounded by mechanosensory bristles<sup>[176]</sup> (figure 3.7.C). The eye morphology was assessed on flies directly after hatching. Highly regular ommatidia were visible with the WT, A $\beta$ 40 and A $\beta$ 42 flies. In contrast, the neuronal expression of A $\beta$ (1-42)arc resulted in a disruption of this geometrical array, known as *rough eye* phenotype<sup>[177]</sup>. This phenotype is characterised by fusion of ommatidia and loss inter-ommatidial bristles.

### **3.8 B10 does not alter the A $\beta$ dependent neurodegeneration**

Now the effect of the fibril binder B10 on *Drosophila melanogaster* that also express A $\beta$  was investigated. The double transgenic flies were crossed with the Gal4-elav<sup>c155</sup> driver line and the offspring was analysed regarding the lifespan, climbing ability and eye morphology (figure 3.8.1). For the lifespan and climbing ability assays the flies were kept at 29° C and transferred to fresh food every 2<sup>nd</sup> day. As seen before the median survival of the A $\beta$  flies (black curves) declined in the order WT = A $\beta$ 40 (43  $\pm$  0.6 days, triangles) > A $\beta$ 42 (32  $\pm$  0.3 days, diamonds) > A $\beta$ 42arc (7  $\pm$  0.1 days, squares). The expression of B10 (red curves) resulted in a medium survival of 41  $\pm$  0.9 days for B10;A $\beta$ 40 flies, whereas B10;A $\beta$ 42 flies had a medium survival of 31  $\pm$  0.6 days and the medium survival of the B10;A $\beta$ 42arc flies was 6  $\pm$  0.3 days (figure 3.8.1A; table 3.3). These lifespan measurements revealed no significant differences in the survival of the B10 flies compared to the respective non-B10 flies. Furthermore, when investigating the climbing ability (figure 3.8.1B) of B10;A $\beta$ 40, B10;A $\beta$ 42 and B10;A $\beta$ 42arc flies (red curves) identical results to the respective A $\beta$  expressing flies without co-expression of the antibody domain (black curves) were obtained. The eye morphology was then assessed on these B10;A $\beta$  flies (figure 3.8.1C). Flies expressing A $\beta$ 40 and A $\beta$ 42 showed a highly regular eye structure in presence and absence of B10 indistinguishable from WT flies. B10;A $\beta$ 42arc flies presented a strongly disturbed eye morphology similar to the one seen in A $\beta$ 42arc flies. In conclusion these data demonstrated that no discernible effect of B10 is seen on

A $\beta$ 40 flies and B10 was neither improving nor worsening the phenotype of flies expressing A $\beta$ 42 and A $\beta$ 42arc flies, although a definite *in vivo* interaction was demonstrated (figure 3.6.4).

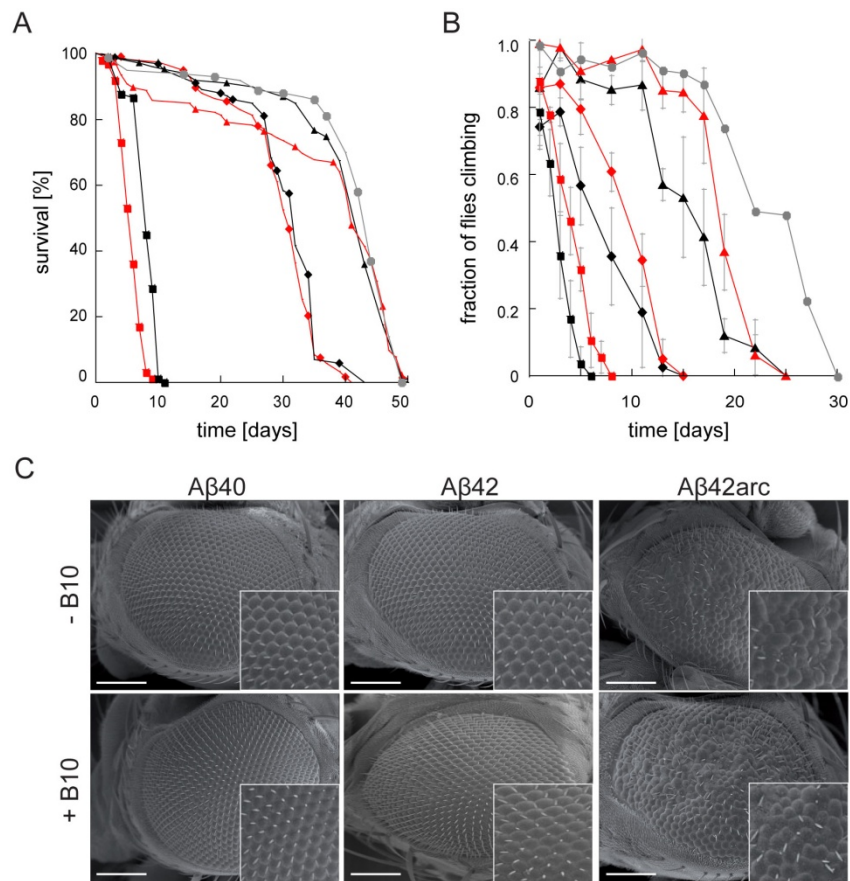


**Figure 3.8.1** B10 does not alter A $\beta$  expressing *Drosophila melanogaster*. (A,B) Phenotypic comparison of A $\beta$  (black) and B10;A $\beta$  (red) expressing flies. The following symbols were used: A $\beta$ 40 = triangles, A $\beta$ 42 = diamonds and A $\beta$ 42arc = squares. The grey curve represents the WT. (A) Determination of the viability. (B) Fraction of flies, reaching the top after 45 seconds. Error bars represent standard deviation from three independent samples. (C) Comparison of the eye morphology in absence (top row) and presence (bottom row) of B10 using SEM. All eye structures are shown enlarged (4x) in the boxes. Scale bars represent 20  $\mu$ m.

**Table 3.3** Median survival of B10 and A $\beta$  double-transgenic flies.

genotype	median survival	std.error	95 % lower confidence level	95 % upper confidence level
A $\beta$ 40	43	0.6	41.8	44.2
B10;A $\beta$ 40	41	0.9	39.328	42.672
A $\beta$ 42	34	0.3	33.393	35.607
B10;A $\beta$ 42	33	0.6	31.901	34.099
A $\beta$ 42arc	7	0.1	6.846	7.154
B10;A $\beta$ 42arc	6	0.3	5.491	6.509

Afterwards the effect of B10 on the SDS-solubility of A $\beta$  was assessed. Fly heads of all three A $\beta$  variants (A $\beta$ (1-40), A $\beta$ (1-42) and A $\beta$ (1-42)arc) were investigated in presence or absence of the antibody domain B10 using sequential protein extraction. First the proteins were extracted using 1 % SDS in PBS and after a brief centrifugation the pellet was dissolved in a buffer containing 9 M urea to denature and extract all remaining proteins. The SDS-soluble and insoluble fractions were analysed by western blot (figure 3.8.2). Equal protein loading was confirmed by probing the membranes with an anti-actin antibody. Comparing the SDS-soluble and insoluble fractions of A $\beta$ 42arc with B10;A $\beta$ 42arc flies (figure 3.8.2A) showed no differences in the band intensity of A $\beta$ , observed by probing the membrane with 6E10. The densitometric analysis of the bands revealed A $\beta$  levels that were not significantly different with or without B10 present. A $\beta$ 42 and A $\beta$ 40 flies also showed no differences in presence or absence of B10 (figure 3.8.2B-C). Comparison of the distribution of the A $\beta$  peptides into SDS-soluble and insoluble fractions showed effectively the same A $\beta$  levels, irrespective of whether or not B10 is present *in vivo*. Hence, B10 did not notably increase or decrease the solubility of any of the three A $\beta$  peptides.

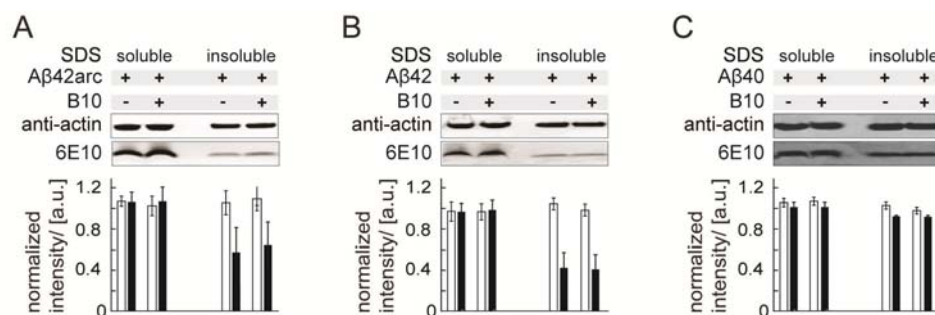


**Figure 3.8.2** B10 has no influence on the distribution of A $\beta$ . Proteins were extracted in a two step protocol to determine the SDS soluble and insoluble amount of A $\beta$  in the fly brain in presence or absence of B10. Fractions were analysed by western blot using anti-actin to ensure equal protein loading and 6E10 to detect A $\beta$ . Western blot and graphical comparison of A $\beta$ 42arc flies (A), A $\beta$ 42 flies (B) and A $\beta$ 40 flies (C). All graphs were normalised to the actin bands. Colour coding in all graphs: white bars = actin, black bars = A $\beta$ .

### **3.9 KW1 potentially effects the lifespan of A $\beta$ -transgenic flies**

Next, the *in vivo* effect of the oligomer binder KW1 was investigated. After crossing the flies with the neuronal driver line Gal4-elav<sup>c155</sup> KW1;A $\beta$  expressing flies (blue curves) were compared to A $\beta$  (black curves) expressing flies as regards their lifespan, climbing ability and eye morphology (figure 3.9.1). For the measurement of the lifespan (figure 3.9.1A, table 3.4) and climbing ability (figure 3.9.1B) the flies were kept at 29° C, whereas the eye morphology was examined after hatching (figure 3.9.1C). The neurotoxicity of the A $\beta$  peptides was again seen in the order A $\beta$ 40 (triangles) < A $\beta$ 42 (diamonds) < A $\beta$ 42arc (squares). KW1;A $\beta$ 42 flies corresponded to A $\beta$ 42 flies regarding their lifespan (medium survival of 32 ± 0.3 days), climbing ability and eye morphology.

Furthermore, KW1 had no discernible effect on A $\beta$ 42arc flies showing a similar medium survival of  $7 \pm 0.2$  days, identical decline of the climbing ability and a *strong rough* eye phenotype. By contrast, KW1 showed a significant effect on A $\beta$ 40 expressing flies. A $\beta$ 40 flies (without KW1) had a medium survival of  $43 \pm 0.6$  days. Additional expression of KW1 led to a significant decrease to  $28 \pm 1.1$  days (figure 3.9.1A). These observations showed that KW1 increased toxicity in KW1;A $\beta$ 40 flies compared to A $\beta$ 40 flies alone. Further it showed that KW1 specifically targets A $\beta$ (1-40) and does not bind to A $\beta$ (1-42) or A $\beta$ (1-42)arc *in vivo* were in accordance with the *in vitro* data <sup>[135]</sup>. Interestingly, neither the climbing ability nor the eye morphology of A $\beta$ 40 flies was affected by KW1 (figure 3.9.1B,C). Taken together, these data demonstrated that KW1 can induce A $\beta$ (1-40) dependent neurotoxicity *in vivo* but has no effect on A $\beta$ 42 or A $\beta$ 42arc flies.

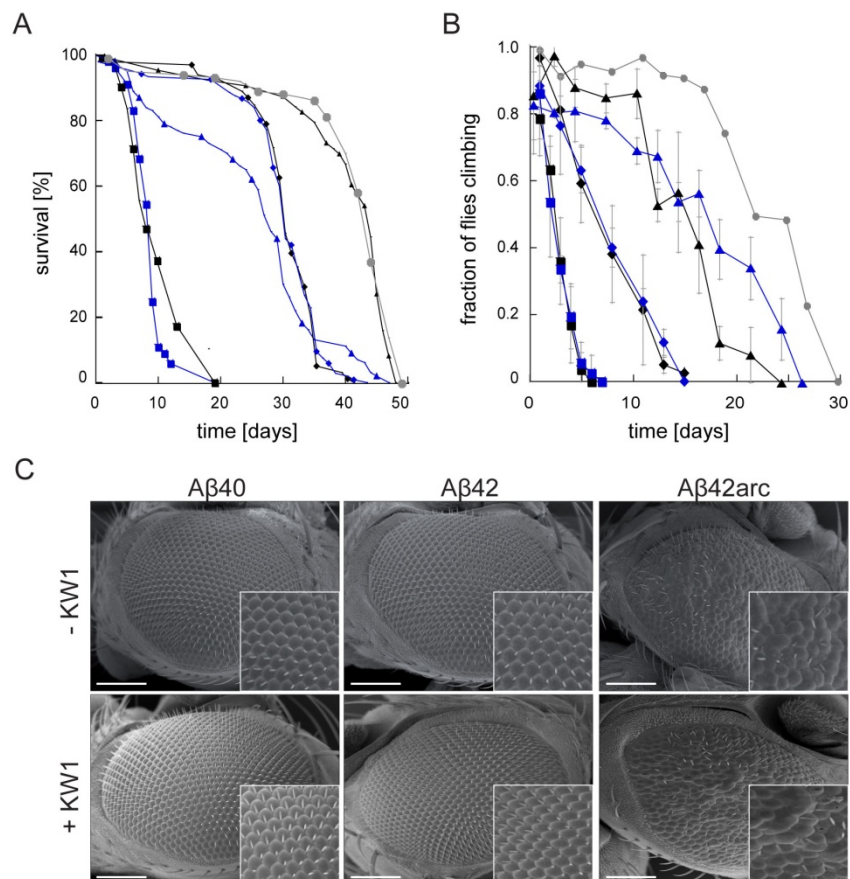


**Figure 3.9.1** KW1 selectively affects the lifespan of A $\beta$  expressing *Drosophila melanogaster*. (A,B) Phenotypic characterisation of A $\beta$  expressing flies (black) in comparison to KW1;A $\beta$  expressing flies (red). The A $\beta$  variants are represented using triangles (A $\beta$ 40), diamonds (A $\beta$ 42) and squares (A $\beta$ 42arc). The WT (grey) is shown for comparison. (A) Assessment of the viability. (B) Fraction of flies climbing top the top of the vial. Error bars stand for standard deviation of three independent measurements using 15 flies each. (C) Analysis of the eye morphology using SEM. A $\beta$  flies (top row) are compared to KW1;A $\beta$  flies (bottom row). White boxes represent enlarged pictures (4x) of the eye structures. Scale bars represent 20  $\mu$ m.

Table 3.4 Medium survival of KW1 and A $\beta$  double-transgenic flies.

genotype	median survival	std.error	95 % lower confidence level	95 % upper confidence level
A $\beta$ 40	43	0.6	41.8	44.2
KW1;A $\beta$ 40	28	1.0	26.046	29.954
A $\beta$ 42	34	0.3	33.393	35.607
KW1;A $\beta$ 42	35	0.3	34.414	35.586
A $\beta$ 42arc	7	0.1	6.846	7.154
KW1;A $\beta$ 42arc	7	0.2	6.614	7.386

The KW1 induced neurotoxicity of A $\beta$ (1-40) was examined in two independent repeats of the lifespan measurement using the same fly stocks of A $\beta$ 40 and KW1;A $\beta$ 40 transgenic flies (figure 3.9.2). The experimental set up of the repeat assays was analogue to the first one (100 flies per genotype, 29° C). The survival curves are shown in figure 3.9.2A in comparison to A $\beta$ 40 flies (black line). The medium survival was assessed for each tube of 10 flies per genotype and is compared in figure 3.9.2B. Additionally, the survival curve and medium survival of the first experiment using KW1;A $\beta$ 40 flies was added to the graphs (blue, solid line). The medium survival of KW1;A $\beta$ 40 flies in the first repeat resulted in a medium survival of  $30 \pm 1.4$  days (blue, dotted), whereas in the second repeat the medium survival was  $36 \pm 1.7$  days (blue, dashed). Although differences are seen within the three repeats all values are significantly lower than A $\beta$ 40 flies without KW1 present. Thus, the KW1 induced A $\beta$ (1-40) dependent neurotoxicity is a reproducible effect.

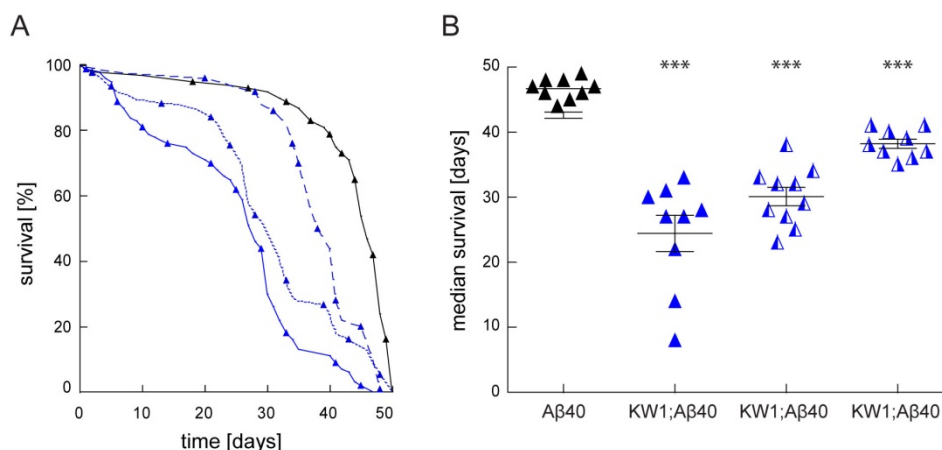
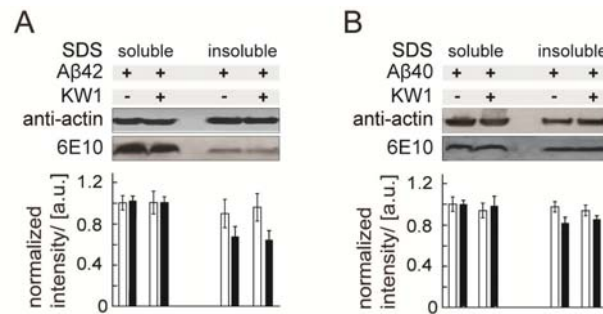


Figure 3.9.2 The KW1 dependent reduction of viability of A $\beta$ 40 flies can be repeated. (A) Graphical illustration of three independent survival assays using A $\beta$ 40 (black) and KW1;A $\beta$ 40 (blue) flies (B) medium survival of the flies determined from each of the 10 tubes per genotype tested in (A). Statistical analysis was performed using Mann-Whitney test (GraphPad Prism).\*\*\*:p<0.001.

The effect of KW1 on the distribution of A $\beta$  into SDS-soluble and insoluble fraction was examined to gain insights into the mechanism of the A $\beta$ (1-40) induced neurotoxicity. A sequential

protein extraction was applied on A $\beta$ 40 and A $\beta$ 42 fly heads in presence or absence of KW1. All fractions were analysed by western blot using 6E10 to detect A $\beta$  and an anti-actin antibody to confirm equal protein amounts in each sample (figure 3.9.3). Visual and densitometric analysis of the band intensity of A $\beta$ 42 flies showed no influence of KW1 on the distribution of A $\beta$ 42 (figure 3.9.3A). With A $\beta$ 40 flies KW1 also showed no effect on the distribution of A $\beta$ (1-40) (figure 3.9.3B).



**Figure 3.9.3** KW1 does not alter the distribution of A $\beta$ . A sequential protein extraction was carried out to determine if the distribution of A $\beta$  into SDS soluble and insoluble fraction is affected by KW1. All fractions were analysed by western blot using 6E10 to detect A $\beta$ . Anti-actin antibody was used to confirm equal protein loading. (A) Western blot and graphical comparison of A $\beta$ 42 flies. (B) Western blot and graphical comparison of A $\beta$ 40 flies. All graphs are normalised to the protein concentration determined by anti-actin staining. Colour coding in all graphs: white bars = actin, black bars: = A $\beta$ .

### **3.10 B10 and KW1 demonstrate no *in vivo* toxicity**

In order to investigate if B10 and KW1 alter the fly phenotype of WT flies independently of A $\beta$  expression the three different assays (survival, climbing and SEM) were employed. In the obtained survival plots (figure 3.10A, table 3.5) the WT flies presented a medium lifespan of  $43 \pm 0.1$  days, which is almost identical to the values obtained with B10 ( $43 \pm 0.2$  days) and KW1 flies ( $42 \pm 1.1$  days), showing that KW1 and B10 do not affect the lifespan.

The climbing assay revealed that all WT flies are immobile by day 30 (figure 3.10B). Upon expression of B10 or KW1 no discernible difference was observed and the flies showed an indistinguishable mobility and age-dependent decline compared to the WT flies (figure 3.10B).

SEM examination of B10- and KW1 expressing flies on day 1 after hatching revealed a highly regular eye morphology, which is similar to the WT and characterised by intact ommatidia and inter-ommatidial bristles (figure 3.10C). No signs of neurodegeneration were evident.

In conclusion, none of the assays provided evidence that B10 and KW1 expression in neurons led to adverse effects in *Drosophila melanogaster*. Thus, the observed phenotypic alterations are not caused by B10 or KW1.

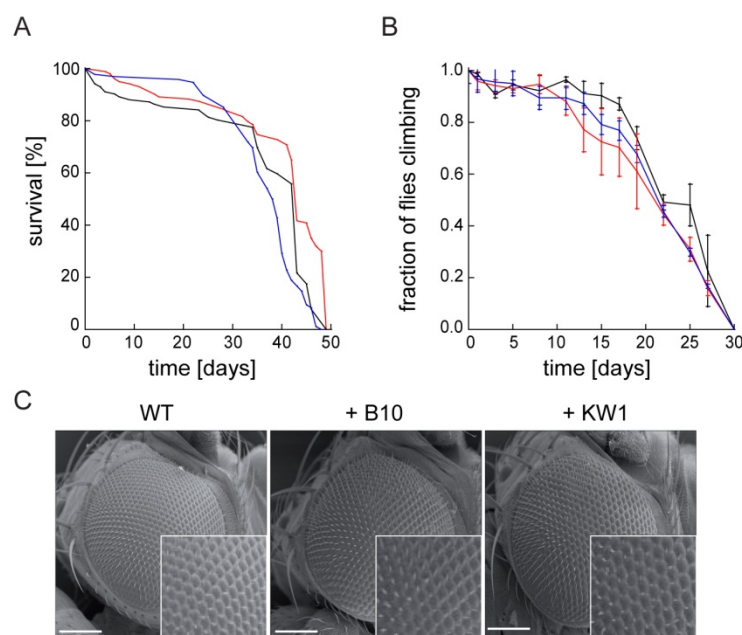


**Figure 3.10** Phenotypic characterisation of B10 and KW1 transgenes expressed in *Drosophila melanogaster*. (A) The viability of one hundred flies per genotype was analysed. The lifespan of B10 (red) and KW1 (blue) expressing flies is compared to non-transgenic WT flies (black). (B) Fraction of flies, reaching the vial top depending on fly age. Error bars show standard deviation from three independent experiments using 15 flies each. The climbing ability of B10 (red) and KW1 (blue) flies is shown in comparison to non-transgenic WT flies (black). (C) Scanning electron microscopy of the eye structure of WT, B10 and KW1 expressing flies. All eye structures are shown enlarged (4x) in the small boxes. Scale bars represent 20  $\mu$ m.

**Table 3.5** Median survival of B10 and KW1 transgenic flies.

genotype	median survival	std.error	95% lower confidence level	95% upper confidence level
WT	43	0.1	42.767	43.233
B10	43	0.2	42.591	43.409
KW1	40	1.1	37.765	42.235

### **3.11 KW1 positive A $\beta$ 40 aggregates accumulate in the fly brain while ageing.**

The experiments presented above have shown that A $\beta$ (1-40) dependent neurotoxicity only arises upon presence of KW1. It was therefore important to analyse whether KW1 altered the amount and distribution of A $\beta$ (1-40) peptide within the fly brain. IFM analysis enabled detailed information about the spatial localisation and amount of deposited A $\beta$ (1-40) in the adult fly brain. To study the effect of KW1, brains of 3- and 20-days old WT, A $\beta$ 40 and KW1;A $\beta$ 40 flies were dissected. The *ex vivo* brains were infiltrated with 6E10 to stain A $\beta$  and an anti-myc antibody to detect KW1. The cell nuclei were counterstained using Hoechst 33342 (figure 3.11) and the cell body region between the optical lobes and protocerebra was analysed (figure 3.11A). Independent of fly age the anti-myc antibody produced no distinct signal in WT and A $\beta$ 40 flies and the 6E10 staining revealed only a slight background noise

without any distinct signals (figure 3.11B top and middle panel). The expression of KW1 was visible in the 3- and 20-days old KW1;A $\beta$ 40 flies using the anti-myc antibody (figure 3.11B lower panel) resulting in distinct signals around the cell nuclei. The staining with 6E10 produced only a slight background in 3 day old KW1;A $\beta$ 40 flies, whereas in 20-day old KW1;A $\beta$ 40 flies clear signals were distinguishable from the background. A merge of the 6E10 image with the anti-myc image demonstrated that the signals of both stainings overlay indicating co-localisation of A $\beta$ (1-40) and KW1. These data indicated that KW1 accumulates A $\beta$ (1-40) in the fly brain during ageing. However, the presence of KW1 did not affect the concentration of A $\beta$ (1-40) peptide in the fly. RT-PCR and western blot analysis revealed similar levels of A $\beta$ (1-40) mRNA and peptide in 3-day and 20-day old A $\beta$ 40 and KW1;A $\beta$ 40 flies (figure 3.11C,D). Thus, KW1 alters the spatial distribution of A $\beta$ (1-40) without changing the protein concentration.

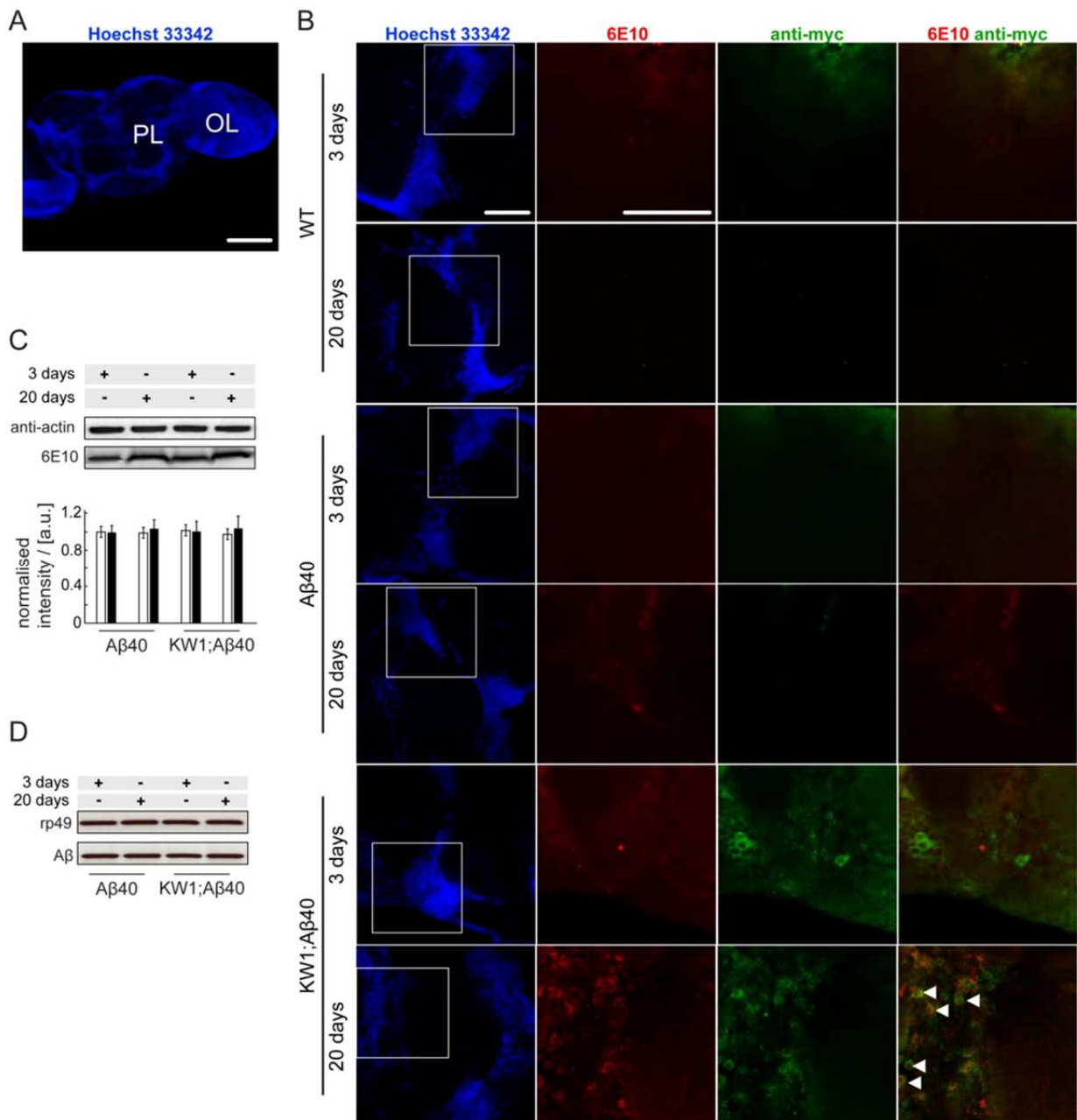


**Figure 3.11** IFM analysis displaying increasing amounts of KW1 positive A $\beta$ 40 aggregates during ageing. (A) IFM image of the protocerebral lobe (PL) and optical lobe (OL) regions of *Drosophila melanogaster* brain stained with Hoechst 33342. (B) Confocal IFM image of adult brain of WT (top), A $\beta$ 40 (middle) and KW1;A $\beta$ 40 (bottom) flies aged for 3 and 20 days. Left column (blue): Hoechst 33342 staining of the cell nuclei. The white boxes are enlarged in the following columns. Second column (red): A $\beta$ -staining with 6E10 antibody; third column (green): staining of myc-tagged B10 or KW1 with anti-myc antibody; right column shows an overlay of the 6E10 and anti-myc signals. All preparations are fly brain whole mounts viewed frontally with dorsal on top. Scale bars represent 50  $\mu$ m. (C,D) Western blot (C) and RT-PCR (D) analysis with heads from 3-day and 20-day old A $\beta$ 40 and KW1;A $\beta$ 40 flies. The samples in (C) were probed with 6E10 to detect A $\beta$  peptide (black bars). Anti-actin staining served as loading control (white bars). All bars were normalised to the 3 day old A $\beta$ 40 sample (n=2). The samples in (D) were probed for A $\beta$  mRNA. Constitutively transcribed rp49 mRNA served as a loading control.

### **3.12 KW1 induces neurotoxicity on two A $\beta$ (1-40) expressing fly lines**

To confirm that the previously seen neurotoxicity of A $\beta$ (1-40) induced by KW1 is reliable, two more A $\beta$ (1-40) transgenic fly lines were included in the examination. These two transgenic lines had the A $\beta$  transgene inserted on the second chromosome (A $\beta$ 40-29.1 and A $\beta$ 40-51D) instead of the third chromosome as was used for the earlier A $\beta$ 40 fly line. Of particular interest was A $\beta$ 40-51D, because the A $\beta$ (1-40) gene was inserted in the same genomic region (2R 51D) as KW1. To generate flies that express these two A $\beta$ 40 transgenes located on the second chromosome and KW1 together, a new driver line Gal4-elav<sup>c155</sup>/ Gal4-elav<sup>c155</sup>;KW1/Cyo was established (2.2.1.2). These flies were viable and showed no toxic effects as seen in figure 3.10 and were used for crosses with +/Y;A $\beta$ 40/CyO flies. The resulting offspring Gal4-elav<sup>c155</sup>/+;KW1/A $\beta$ 40 was analysed in a survival assay in comparison to Gal4-elav<sup>c155</sup>/+; A $\beta$ 40/+. All fly lines were raised at 29° C and kept at the same temperature during the analysis.

Figure 3.12.1 displayed the survival curves as well as the estimation of the medium survival of all three A $\beta$ 40 transgenes tested (table 3.6). The original A $\beta$ 40 line used is shown on the left side (A) in comparison to the new transgenes A $\beta$ 40-51D (B) and A $\beta$ 40-29.1 (C). Like the original A $\beta$ 40 flies, which survived  $43 \pm 0.6$  days, the lifespan of A $\beta$ 40-51D is indistinguishable from WT flies showing a medium survival of  $42 \pm 1.15$  days (black). KW1 significantly reduced this medium lifespan to  $36 \pm 0.83$  days (KW1, blue). Hence, KW1 also induced neurotoxicity in the A $\beta$ (1-40)-51D transgenic fly line. A $\beta$ 40-29.1 flies presented a medium survival of  $39 \pm 0.83$  days, showing a non-significant decrease in lifespan from WT flies. Upon co-expression of KW1 (blue) no significant change was seen in the medium survival ( $39 \pm 0.43$  days). Thus, KW1 was not able to induce neurotoxicity in the A $\beta$ (1-40)-29.1 transgenic fly line.

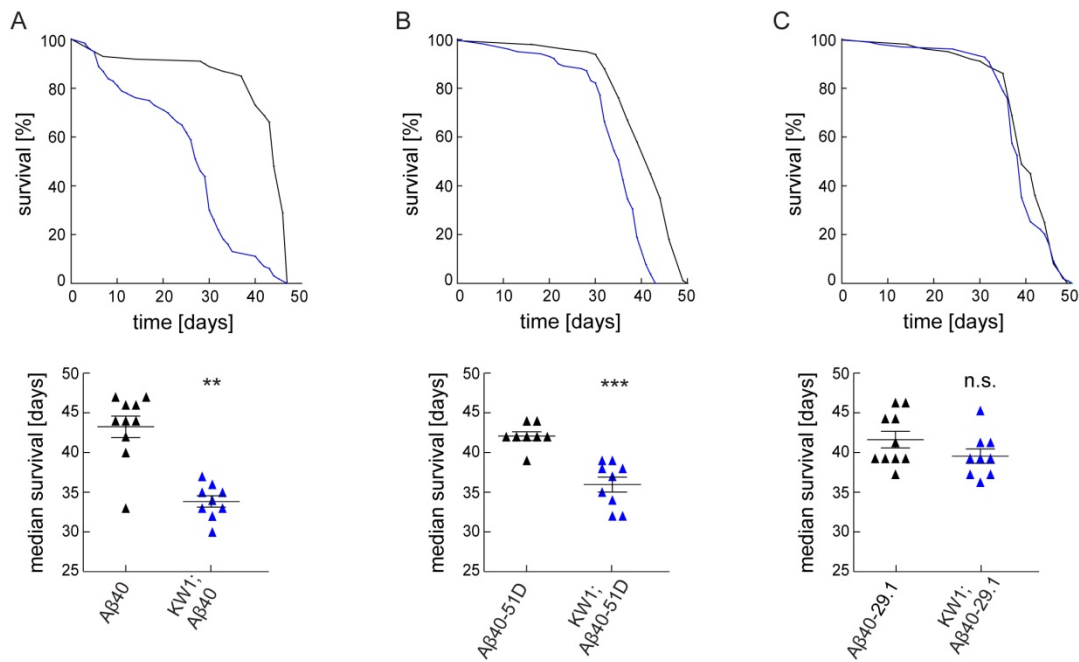


*Figure 3.12.1* KW1 affects the lifespan of different A $\beta$ 40 flies. (A-C) Lifespan measurement and comparison of medium survival including p-values of three A $\beta$ 40 expressing flies (black curves) with co-expression KW1 (blue). (A) A $\beta$ 40 flies. (B) A $\beta$ 40-51D (C) A $\beta$ 40-29.1. Statistical analysis was performed using the Mann-Whitney test. Therefore the medium survival was determined for each of the 10 tubes used per genotype. n.s.: non-significant, \*\*:  $p < 0.01$ , \*\*\*:  $p < 0.001$ .

*Table 3.6* Medium survival of different A $\beta$ 40 flies with or without KW1.

genotype	median survival	std.error	95 % lower confidence level	95 % upper confidence level
A $\beta$ 40-29.1	39	0.8	37.367	40.633
KW1.;A $\beta$ 40-29.1	39	0.4	38.152	39.848
A $\beta$ 40-51D	42	1.1	39.75	44.25
KW1;A $\beta$ 40-51D	36	0.8	34.377	37.623

The three A $\beta$ (1-40) transgenic fly lines were characterised further to assist in understanding the observed alterations in lifespan. Using RT-PCR and western blot analysis the transcription and translation level of each transgene were analysed (figure 3.12.2). The mRNA level was determined using A $\beta$  specific primers and the results were detected on an agarose gel. Similar band intensities were observed for all three fly lines (figure 3.12.2A) and a PCR using the ribosomal primers rp49 showed equal mRNA amounts were present in each sample. Next, the protein concentration was determined by western blot using the monoclonal antibody 6E10 to detect A $\beta$ . The band intensity indicated that the A $\beta$ (1-40) level is the highest in the original A $\beta$ 40 fly line (figure 3.12.2B) and that the concentration when compared to the original A $\beta$ 40 is lower in A $\beta$ 40-51D ( $64 \pm 1\%$ ) and again

lower in A $\beta$ 40-29.1 ( $51 \pm 0.5$  %). A control staining with the anti-actin antibody revealed equal protein concentrations on the membrane (figure 3.12.2B, upper panel). Taken together, the data indicated a correlation between the A $\beta$ (1-40) concentration *in vivo* and the observed reduction of the lifespan upon linear regression fit ( $r = 0.86$ , figure 3.12.2C).

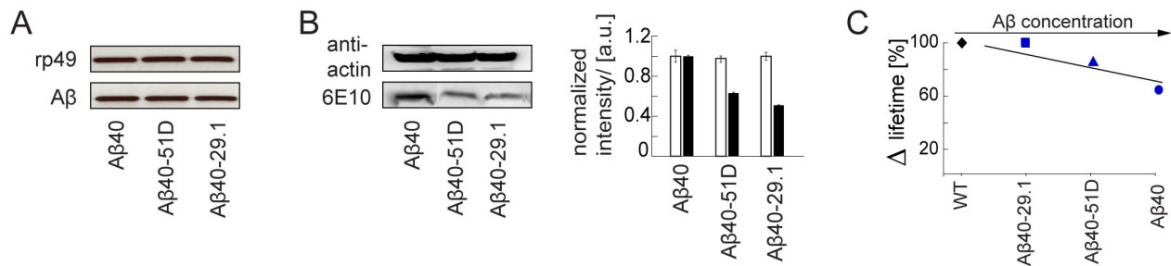


**Figure 3.12.2** KW1 dependent reduction of lifespan correlates with the A $\beta$ 40 concentration. (A) RT-PCR analysis of A $\beta$  mRNA in 20 fly heads of each A $\beta$ 40 29.3, A $\beta$ 40-29.1 and A $\beta$ 40-51D flies using A $\beta$  primers. Ribosomal rp49 mRNA served as loading control. (B) Western blot and graphical comparison of peptide level. 6E10 antibody displayed A $\beta$  bands at around 4 kDa. Anti-actin western blot served as loading control. Black bars display actin bands. White bars show A $\beta$  bands. All band intensities were normalised to the A $\beta$ 40 sample. (C) Reduction of the lifetime ( $\Delta$  lifetime) of KW1;A $\beta$ 40 flies in comparison to the obtained A $\beta$ 40 concentration. A linear regression was carried out to fit the data ( $r = 0.86$ ).  $\Delta$  lifetime = medium survival of KW1;A $\beta$ 40 flies subtracted from medium survival of A $\beta$ 40 flies.

### 3.13 Mechanism of A $\beta$ (1-40) mediated toxicity

The mechanism of A $\beta$  mediated neurotoxicity is not fully understood. There are studies suggesting that A $\beta$  interacts with several receptors such as scavenger receptor, Receptor for Advanced Glycation Endproducts (RAGE) or *N*-methyl-D-aspartate (NMDA) receptor<sup>[178-180]</sup> or with the cell membrane leading to the formation of pores<sup>[181]</sup>. Especially the NMDA receptor has been found to be involved in synaptic plasticity and synapse formation, playing a critical role in learning and memory<sup>[182-184]</sup> and the non-competitive NMDA receptor antagonist memantine has been shown to have beneficial effects in mice and rats as well as in human patients<sup>[185-189]</sup>. Studies using *Drosophila melanogaster* found that the non-competitive NMDR receptor antagonist MK-801 can also improve the fly phenotype upon expression of A $\beta$ (1-42) and A $\beta$ (1-42)arc<sup>[95]</sup>. The effects on the A $\beta$ (1-40) mediated neurotoxicity were tested by administering 3  $\mu$ M MK-801 in the fly food beginning from the embryonic stage. The flies were examined in a survival assay at 29° C in parallel, i.e. with (dashed line) or without (continuous line) MK-801 treatment (figure 3.13.1A). The WT flies (black circles) had a medium survival of around 46 days in presence or absence of MK-801. KW1 expressing flies (blue circles) as well as A $\beta$ 40 flies (black triangles) were used as further controls and MK-801 did not change the medium lifespan of these flies (figure 3.13.1B; table 3.7). KW1;A $\beta$ 40 flies presented a reduced lifespan as seen before (medium survival of  $30 \pm 1.4$  days). Nevertheless,

treatment with MK-801 did not significantly improve the phenotype ( $31 \pm 1.4$  days). These data suggested that either the NMDA receptor is not involved in the A $\beta$ (1-40) mediated neurotoxicity or the effect of MK-801 is too marginal to be detected under these assay conditions.

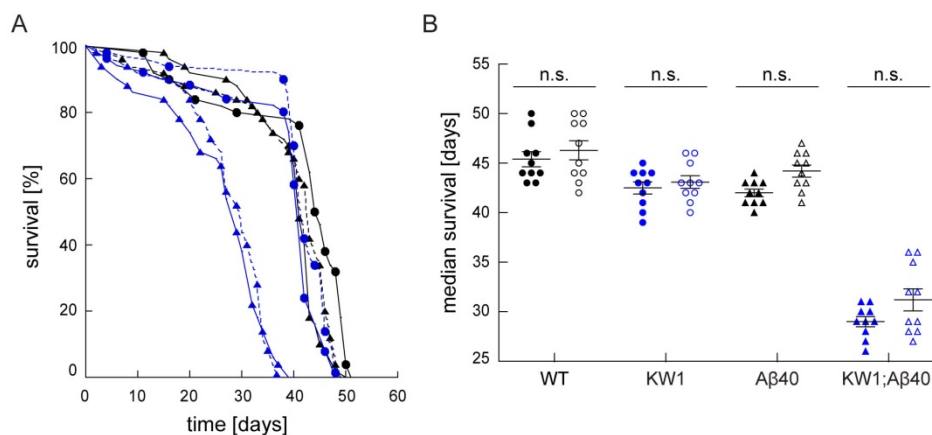


**Figure 3.13.1** MK-801 treatment to antagonise the NMDA receptor. (A) Lifespan measurement of flies treated with MK-801 or vehicle. The fly genotypes are represented using circles (WT), triangles (A $\beta$ 40), diamonds (A $\beta$ 42) and squares (A $\beta$ 42arc). Flies treated with MK-801 are shown by the dashed line and the vehicle control is displayed by the continuous line. (B) Median survival determined from 10 fly tubes per genotype used in graph (A). Flies on vehicle are represented by filled symbols and flies treated with MK-801 are displayed using open symbols. Statistical analysis was performed using Mann-Whitney test. n.s.: non-significant.

**Table 3.7** Median survival of flies treated without or without MK-801.

genotype	median survival	std.error	95 % lower confidence level	95 % upper confidence level
<i>no drug</i>				
51D	46	1.1	43.853	48.147
KW1	41	0.4	40.165	41.835
A $\beta$ 40	42	0.6	40.893	43.107
KW1;A $\beta$ 40	30	1.4	28.27	32.73
<i>3<math>\mu</math>M MK-801</i>				
51D	46	1.4	43.183	48.817
KW1	42	0.5	41.038	42.962
A $\beta$ 40	43	0.4	42.158	43.842
KW1;A $\beta$ 40	31	1.4	28.27	33.73

Another method to investigate the role of the NMDA receptor is the system of RNA interference (RNAi), which is used to target specific genes by interfering with the gene expression. The RNAi molecules bind to mRNA and form double-stranded RNA (dsRNA) molecules which are degraded by ribonucleases, thus leading to gene knock-out phenotypes. By targeting the gene *dNR1*, which is the homologue to the NMDA receptor subunit 1 located on the 3<sup>rd</sup> chromosome<sup>[190]</sup>, the NMDA receptor formation was inhibited. First the functionality of the RNAi system was tested by determining the transcription level of *dNR1* mRNA (figure 3.13.2A). RNA was extracted from

transgenic RNAi and A $\beta$ 40 flies in absence of Gal4 as well as in RNAi;A $\beta$ 40 flies upon expression of Gal4 in the neurons of Gal4-elav<sup>c155</sup> flies. Equal RNA amounts were confirmed in all samples using a control PCR with primers for the ribosomal protein (rp49). The first set of primers was designed across the nucleotide sequence of the *dNR1*-RNAi transgene. The PCR showed that a more intensive band is present in the elav;RNAi;A $\beta$ 40 flies compared to RNAi and A $\beta$ 40 flies proving the presence of both the *dNR1* and *dNR1*-RNAi mRNA (figure 3.13.2A, left). In a second PCR, a primer pair was used that amplifies the last exon of *dNR1*, which is not included in the *dNR1*-RNAi transgene (figure 3.13.2A, right). The result demonstrated that the expression of RNAi led to a lower amount of *dNR1* mRNA due to dsRNA mediated degradation. These data indicated that the RNAi system successfully decreased the amount of functional NMDA receptors.

Western blot analysis were carried out to exclude RNAi effects on the expression level of A $\beta$ (1-40) (figure 3.13.2B). The anti-actin antibody was used to prove equal protein concentrations on the membrane. Staining of the membrane with the monoclonal antibody 6E10 showed similar band intensities in the A $\beta$ 40 as well as in the RNAi;A $\beta$ 40 flies proving no influence of the RNAi molecules on the overall expression of A $\beta$ (1-40) *in vivo*.

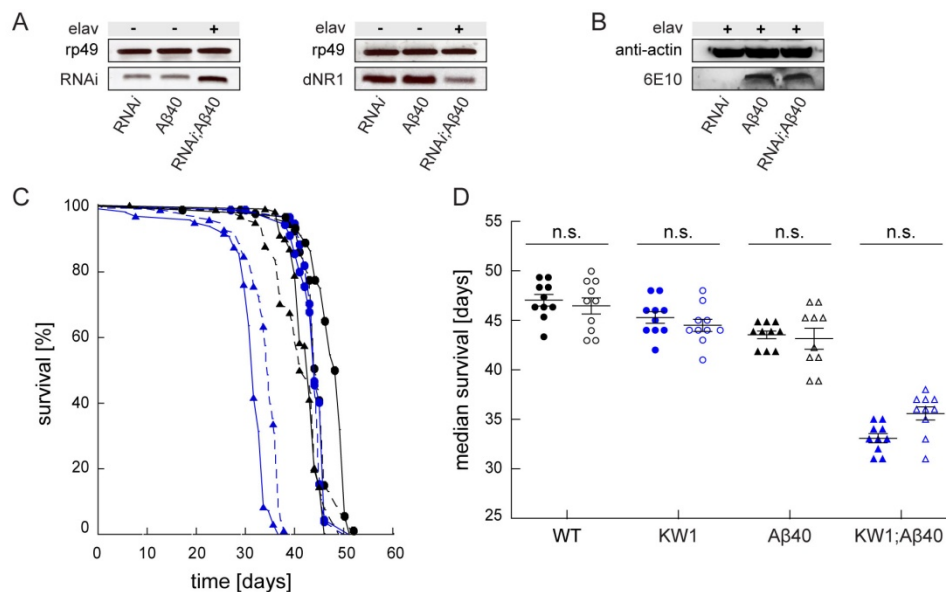


**Figure 3.13.2** NMDA receptor interference using the RNAi system. (A,B) RT-PCR and western blot of RNAi versus non-RNAi flies. (A) RT-PCR analysis of *dNR1* mRNA using 2 sets of primers. Left panel: primers are targeted to RNAi sequence. Right panel: primers are designed across the last exon of *dNR1*. Primers against the ribosomal rp49 mRNA served as loading control. (B) Western blot analysis of A $\beta$ 40 level in presence of RNAi. Detection of A $\beta$  was carried out using 6E10. Anti-actin antibody served as loading control. (C) Lifespan measurement of flies expressing RNAi in comparison to non-RNAi flies. The fly genotypes are represented using circles (WT), triangles (A $\beta$ 40), diamonds (A $\beta$ 42) and squares (A $\beta$ 42arc). Flies expressing RNAi are displayed by the dashed line whereas non-RNAi flies are represented by the continuous line. (D) Median survival from 10 flytubes per genotype used in graph (A). Flies expressing RNAi are shown by open symbols and non-RNAi flies are displayed using filled symbols. Statistical analysis was performed using Mann-Whitney test. n.s.: non-significant.

Flies expressing *dNR1*-RNAi (dashed line) were also analysed in a survival assay in comparison to non-RNAi flies (continuous line, figure 3.13.2C, D; table 3.8). WT flies (black circles) and KW1 flies (blue circles) served as negative controls. In both fly lines the expression of RNAi did not alter the medium survival. A similar result was seen with A $\beta$ 40 expressing flies (black triangles). The survival curve of RNAi/KW1;A $\beta$ 40 flies a slightly lesser decline compared to KW1;A $\beta$ 40 flies. The medium survival values showed an absolute difference of 3 days, but the value was not statistically significantly different from the non-RNAi fly line (figure 3.13.2D). In conclusion, the data from the MK-801 and the RNAi analysis indicated that the NMDA receptor is not involved in the A $\beta$ (1-40) mediated neurotoxicity emerged by KW1 stabilised toxic A $\beta$ (1-40) aggregates.

Table 3.8 Medium survival of non-RNAi flies in comparison to RNAi expressing flies.

genotype	median survival	std.error	95 % lower confidence level	95 % upper confidence level
51D	46	0.5	45.115	47.885
KW1	44	0.4	43.253	44.747
A $\beta$ 40	43	0.3	42.404	43.596
KW1;A $\beta$ 40	32	0.2	31.55	32.45
51D/ RNAi;	46	0.3	45.454	46.546
KW1/ RNAi	44	0.2	43.634	44.366
RNAi;A $\beta$ 40	43	0.5	41.982	44.018
KW1/ RNAi;A $\beta$ 40	35	0.3	32.632	35.368

### **3.14 KW1 stabilised A $\beta$ (1-40) aggregates are structurally different from A $\beta$ (1-40)**

#### **aggregates**

*In vitro* data suggested that KW1 is able to disturb the A $\beta$  assembly into mature amyloid fibrils. This effect was confirmed using ThT fluorescence spectroscopy of A $\beta$ (1-40) samples pre-incubated for five days with or without KW1 (figure 3.14A). At a molar ratio of 1:5 (KW1:A $\beta$ ) the KW1 stabilised A $\beta$ (1-40) aggregates displayed lower interactions with ThT than A $\beta$ (1-40) alone. A $\beta$ (1-40) alone led to a high increase in the ThT fluorescence intensity at 480 nm (black curve) whereas KW1 stabilised A $\beta$ (1-40) aggregates (blue curve) showed a significantly lower peak at the emission maxima. Furthermore, the presence of KW1 also delayed the aggregation of A $\beta$ (1-40). A $\beta$ (1-40) aggregated fast and ThT positive species occurred after 20 hours. Upon addition of KW1 the length of the lag phase was increased from  $5.6 \pm 0.5$  h to  $24 \pm 2.7$  h (figure 3.14B). By contrast, the antibody fragment induced the formation of hydrophobic surfaces as determined by ANS fluorescence spectroscopy (figure 3.14C). Aggregates formed by A $\beta$ (1-40) in absence of KW1 (black curve) did not lead to an increased fluorescence intensity and resulted only in a minor shift of the emission maxima of ANS. In contrast, KW1 stabilised A $\beta$ (1-40) aggregates (blue curve) showed a significant increase in the fluorescence intensity resulting in a high emission peak at 480 nm.

Negative stain TEM analysis revealed that within five days A $\beta$ (1-40) alone formed long, straight fibrils. In presence of KW1 small circular and short non-fibrillar A $\beta$  aggregation species were found (figure 3.14D).

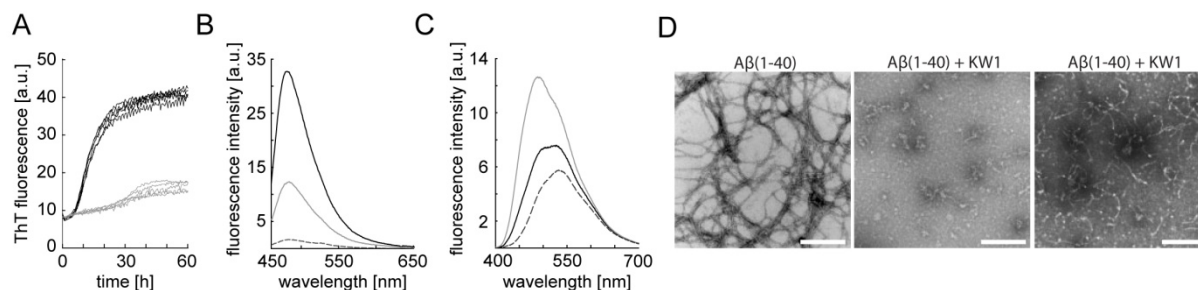


**Figure 3.14** Structural analysis of A $\beta$  aggregates. (A) Time-dependent ThT fluorescence at 490 nm using 25  $\mu$ M A $\beta$ (1-40) with (black) and without (grey) 5  $\mu$ M KW1 ( $n=5$ , 37  $^{\circ}$ C). (B) ThT fluorescence spectroscopy of A $\beta$ (1-40) pre-incubated with (grey) or without (black) KW1 for five days at 37  $^{\circ}$ C. The control contained dye without protein (dashed). The samples contained 15  $\mu$ M ThT and 20  $\mu$ M A $\beta$ . (C) ANS fluorescence spectroscopy of the samples used in (B). The spectra were recorded from 20  $\mu$ M A $\beta$  mixed with 200  $\mu$ M ANS. (D) Negative stain TEM analysis of the aggregation species. Scale bars represent 200 nm.

### **3.15 KW1 forms toxic aggregates *in vitro***

To gain further information on the nature of the A $\beta$ (1-40) aggregates formed in presence of absence of KW1 a cell culture model was used. The human neuroblastoma SH-SY5Y cells are adherent growing neuronal-like cells which are widely used to study A $\beta$  dependent neurotoxicity.

The neurotoxic effect was studied using two toxicity assays:

1. 3-(4,5-Dimethylthiazol-2-yl)-2,5-diphenyltetrazolium bromide (MTT) assay
2. Lactate dehydrogenase (LDH) assay

The MTT assay involves NADPH dependent reduction of the tetrazolium salt to purple formazan inside living cells. In the end, absorbance of the coloured solution was measured in a plate reader and the signal intensity allows conclusions to be drawn about the redox activity of the cells. The LDH assay is used to measure the amount of the enzyme lactate dehydrogenase released into the cell culture medium upon damage of the cell membrane. This enzyme catalyses a reaction in the medium which leads to the generation of a yellow dye whose absorbance was determined in a plate reader and the signal intensity is proportional to the number of dead cells.

A $\beta$ (1-40) was incubated *in vitro* in the presence or absence of KW1 or B10 (molar ratio of 5:1, A $\beta$ :B10/KW1) in 50 mM HEPES (pH 7.4) containing 50 mM NaCl at 37  $^{\circ}$ C for five days. Two additional

samples containing either buffer only or KW1 alone were incubated for the same time period serving as no-A $\beta$  controls while cells treated with 2  $\mu$ M of the toxin staurosporine served as positive control. The SH-SY5Y cells were seeded in 96-well plates at a density of 50 000 cells/well and after 24 hours the cell culture medium was replaced with medium containing the respective A $\beta$  samples. The assays were undertaken after an incubation period of 24 hours with the A $\beta$  or control samples. The MTT assay (figure 3.15A) displayed no decrease of the redox activity of cells incubated with medium, buffer or KW1 alone whereas treatment with staurosporine led to a nearly 100 % reduction of the cell viability. Cells treated with A $\beta$ (1-40) had a similar cell redox activity as untreated cells. In contrast, cells treated with the A $\beta$ (1-40) aggregates formed in presence of KW1 had a significant ~12% reduction of the metabolic activity. Thus by MTT analysis, the KW1 stabilised A $\beta$ (1-40) aggregates were more toxic to the cells compared to A $\beta$ (1-40) aggregates formed without KW1. However, the encountered effects were much smaller compared to the general cell toxin staurosporine. Additionally, the formation of these A $\beta$ (1-40) aggregates depended on incubation time. Their activity was most robustly seen if A $\beta$ (1-40) was co-incubated with KW1 for five to six days, whereas no significant difference was observed from day one to day four of the pre-incubation time (figure 3.15B). The lactate dehydrogenase (LDH) release that monitors cell death showed only mild, if any, toxic effects, and all tested A $\beta$  preparations were far less active than staurosporine (figure 3.15C). These findings provided *in vitro* evidence that the activity of KW1-induced aggregates disturbs neuronal activity without inducing apoptosis.

In consistency with these observations were also the results obtained with the LTP assay (figure 3.15D-F). This assay measures the disturbance of neuronal network functions upon application of potent disturbing compounds to mouse hippocampal brain slices. The addition of KW1 stabilised A $\beta$ (1-40) significantly impaired the measurable LTP response compared to the buffer sample, reflecting their synaptotoxic potential (figure 3.15D). By contrast, no effect on the LTP was seen when the hippocampal brain slices were incubated with A $\beta$ (1-40) pre-incubated without KW1 (figure 3.15E) and also KW1 alone did not cause any effects, displaying a nearly identical LTP trace when compared to buffer (figure 3.15F).

Finally, the KW1-induced A $\beta$ (1-40) aggregates were also less toxic than A $\beta$ (1-42) and A $\beta$ (1-42)arc-derived structures (figure 3.15E). Based on the MTT assay, A $\beta$ (1-42) aggregates reduced the metabolic activity by ~15%, whereas A $\beta$ (1-42)arc treatment induced a very dramatic ~70% reduction. However, the MTT reduction caused by A $\beta$ (1-42) and A $\beta$ (1-42)arc was not further influenced by the presence of KW1, consistent with the previously observed inactivity of this antibody fragment in KW1;A $\beta$ 42 and KW1;A $\beta$ 42arc flies (figure 3.9.1A, page 60). Moreover, there

was a good correlation between the *in vitro* effects measured by MTT and the mean lifespan of the flies obtained upon co-expression of these polypeptide chains (figure 3.15E).

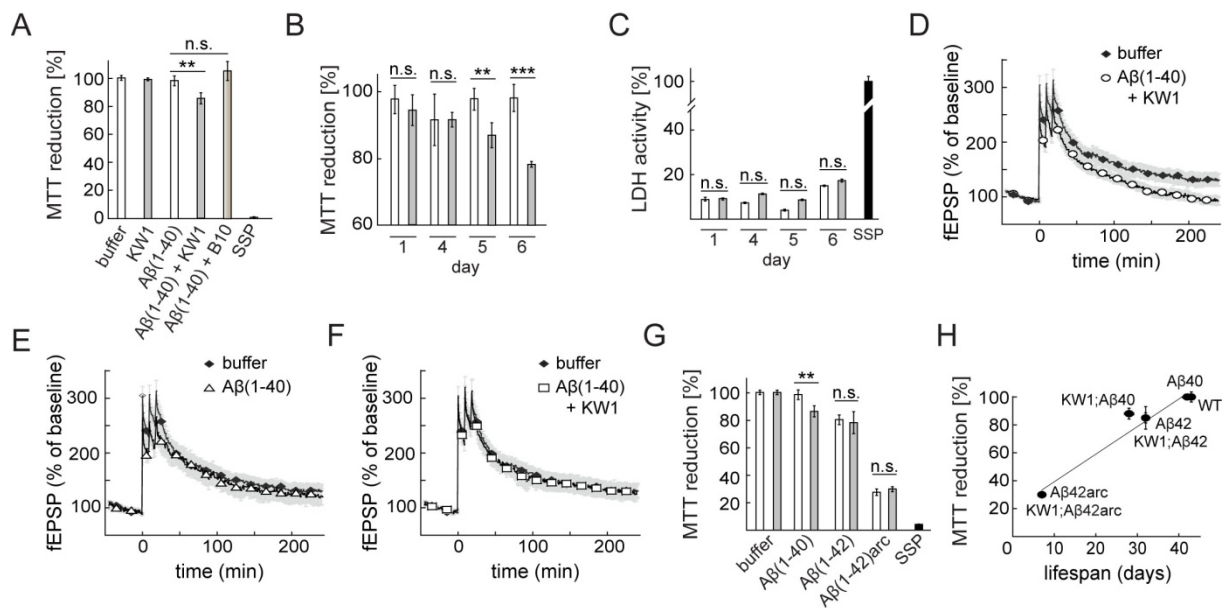


**Figure 3.15** Determination of Aβ(1-40) cytotoxicity. Throughout all SH-SY5Y experiments the cell toxin staurosporine (SSP, 2 μM, black bars) served as positive control. (A) MTT assay of SH-SY5Y cells treated with 1 μM Aβ(1-40) pre-incubated with KW1 or B10 for five days. Cells treated with buffer were normalised as 100 %. (B,C) SH-SY5Y cells treated with 1 μM Aβ(1-40) pre-incubated for one to six days alone (white bars) or with KW1 (grey bars). (B) MTT assay: Cells treated with buffer were normalised as 100 %. (C) LDH assay: The bars are normalised to LDH activity of the SSP treated cells. (D-F) LTP measurements on hippocampal slices incubated with 1 μM Aβ pre-incubated for five days at 37° C with KW1 (D) or alone (E). Control measurements were carried out with KW1 added after Aβ incubation (F) or sample solution containing only buffer (D-F). The LTP experiments were carried out by Dr. Raik Röncke (Leibniz Institute for Neurobiology, Madgeburg, Germany). (G) MTT assay of SH-SY5Y cells treated with 1 μM Aβ(1-40), Aβ(1-42) or Aβ(1-42)arc pre-incubated alone (white bars) or with KW1 (grey bars). Cells treated with buffer were normalised as 100 %. (H) MTT reduction plotted against the lifespan of the corresponding flies. Data were fitted by linear regression ( $r = 0.9796$ ). All error bars represent standard deviation of  $n=6$  (A-C,G) or standard error of mean  $n=10$  (D-F). n.s.: non-significant, \*\*:  $p < 0.01$ , \*\*\*:  $p < 0.001$ .

---

## 4. Discussion

---

### **4.1 *Drosophila melanogaster* models are appropriate for targeting A $\beta$ aggregates**

To date, the culprit of AD has not been definitively established. AD research is focused either on the Tau protein, which is found in neurofibrillary tangles, or the A $\beta$  peptide, which is found deposited in extracellular plaques in the brains of AD patients. To better understand the role of A $\beta$  in AD, experimental animal models have been developed that reproduce the pathological hallmarks of AD. It is known that several A $\beta$  peptide variants are present in the extracellular plaques of human brains [148, 191]. These variants display heterogeneity at both polypeptide chain ends, e.g. A $\beta$ (x-38), A $\beta$ (x-40) and A $\beta$ (x-42), with A $\beta$ (1-40) being the most commonly observed A $\beta$  species [192-194]. Nevertheless, *in vivo* studies have suggested that the A $\beta$ (1-42) variant is neurotoxic while A $\beta$ (1-40) does not play a toxic role [94, 195]. The reason for this may lay in the different aggregation behaviour of both peptide variants. Its extension by two C-terminal amino acids, Isoleucine41 and Alanine42, results in the dramatically increased aggregation propensity of A $\beta$ (1-42) compared to A $\beta$ (1-40) [196, 197]. Furthermore, the specific regions and residues controlling A $\beta$ (1-40) and A $\beta$ (1-42) oligomerisation differ, suggesting different toxicity mechanisms [198]. However, despite their distinct aggregation behaviour both peptides form amyloid fibrils as well as a range of differently shaped fibrillation intermediates, including oligomers and protofibrils [62, 148]. Several aggregation intermediate structures of A $\beta$  have been identified as able to trigger AD pathology, but so far this has only been observed *in vitro* or via injection into animal models [14, 199, 200]. The invasive nature of A $\beta$  infusion in model systems is inevitably accompanied by brain trauma which may complicate inflammatory reactions. To date, all such attempts lack a direct demonstration of the *in vivo* neurotoxic A $\beta$  species.

Within this thesis an approach was developed to explore the *in vivo* relevance of fibrillar and intermediate A $\beta$  structures by endogenous targeting of these species using conformation-sensitive antibodies. Throughout the experiments transgenic *Drosophila melanogaster* were used as a model organism. So far, various animal models have been used to investigate AD. These can be classified into spontaneous or induced models, but so far none of them recapitulates all aspects of AD [201, 202]. Mice models are the most widely used in current AD research, nevertheless, most studies undertaken in these models did not examine the toxicity of single A $\beta$  variants. This limitation occurs because these mouse models express the full-length APP, which after cleavage results in a mixture of APP fragments, including multiple A $\beta$  variants, comprising neurotoxic, neuroprotective or signalling functions that influence learning and memory. Moreover, in mouse models researchers have to wait for several months until the AD pathology develops.

Over the last decade, *Drosophila melanogaster* has become a widely used genetic model organism, used to screen medically relevant compounds for their treatment effects and to

investigate neurodegenerative diseases like AD <sup>[203-206]</sup>. The invertebrate is an ideal model organism, due to low costs and experimental set ups which provide results in short time periods. It also allows for genetic manipulations, like gene knock-down or transgenic insertion. Several *Drosophila* models were established that successfully reflect the AD phenotype, including showing intracellular A $\beta$  accumulation, extracellular A $\beta$  deposition and neurodegeneration accompanied by cognitive impairment, reduced locomotor behaviour and longevity <sup>[93-95]</sup>. These models enabled high throughput screens of potentially relevant compounds, as well as studies examining single A $\beta$  variants in parallel. Furthermore, one advantage of the *Drosophila* systems is the simple generation of transgenic organisms and the lack of a stringent blood-brain-barrier, which allows an easy access of compounds to the nervous system. Overall, *Drosophila melanogaster* is an appropriate model system to investigate AD allowing a broad range of experiments determining phenotypic alterations upon neuronal A $\beta$  expression.

One limitation of the *Drosophila melanogaster* model is its inability to determine the efficacy of compounds to treat AD like antibody-mediated A $\beta$  clearance upon T- or B-cell activation. Thus, the *Drosophila melanogaster* model is most appropriate for initial forward screenings of compounds for AD prior to testing in rodents. Its use results in significant reductions in the time and expense needed to check compounds for toxic side effects and to help identify the most promising candidates for further clinical trials. Transgenic *Drosophila melanogaster* have recently been generated expressing specific antibodies against neurodegenerative diseases and are being used to investigate their effects *in vivo*. The first antibody shown to be functional in *Drosophila melanogaster* is the single-chain Fv antibody fragment C4, which was efficacious against Huntington's disease <sup>[207]</sup>. Furthermore, an engineered small binding protein (affibody) was found to eliminate neurotoxicity of the A $\beta$  peptide in a *Drosophila melanogaster* model of AD <sup>[208]</sup>. These trials have proven the suitability of *Drosophila melanogaster* for A $\beta$  targeting and antibody screening *in vivo*.

#### **4.2 Antibody mediated A $\beta$ clearance of AD**

The steady-state level of A $\beta$  depends on a balance between its production and clearance. Thus a number of current intervention strategies focus on either blocking the formation of amyloid fibrils or degrading the existing plaques. Current approaches primarily involve A $\beta$  degradation using antibodies applied by active or passive vaccination <sup>[113, 114]</sup>. For the general clearance of A $\beta$  by antibodies three possible mechanisms have been proposed (figure 4.1): the toxic species can be disaggregated directly (A), removed via Fc receptor-mediated phagocytosis by microglial cells (B) or the equilibrium between plasma and central nervous system is altered, causing A $\beta$  efflux from the brain (peripheral sink hypothesis <sup>[125]</sup>, C).

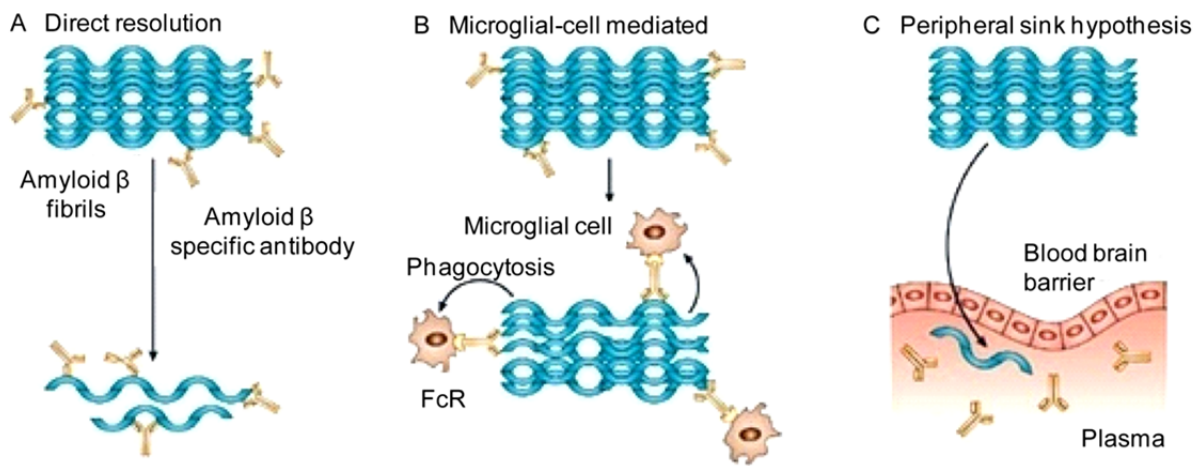


Figure 4.1 Antibody mediated A $\beta$  clearance from the brain. (A) Directed disaggregation of fibrils, (B) Fc-mediated phagocytosis through microglial cells and (C) decrease of plasma A $\beta$  levels causing A $\beta$  efflux from the brain. Figure adapted from Weiner & Frenkel 2006<sup>[209]</sup>.

Depending on the mechanism mentioned above, an A $\beta$ -specific antibody would require several features. Besides recognising A $\beta$  it needs to be small enough to penetrate the blood brain barrier (BBB) or must be engineered to be actively transported into the brain via a receptor or channel to be able to target A $\beta$  plaques directly. Small engineered antibody fragments which lack the Fc region may be able to enter the brain easily and have been shown to disrupt existing A $\beta$  fibrils<sup>[124, 209, 210]</sup>. Comparing the size of the VHH domains B10 and KW1 (~17 kDa) with single chain Fv antibodies (~25 kDa) it is anticipated that both antibody fragments have the ability to enter the brain and there bind to their respective A $\beta$  species. Both antibody fragments have been reported to stain brain slices derived from human AD brains<sup>[135, 138]</sup>, thus their respective epitopes occur during the aggregation process *in vivo*. However, *Drosophila melanogaster* has only an innate immune system and is therefore not suitable for antibody studies that involve the adaptive immune system.

In an alternative mechanism, anti-A $\beta$  antibodies that circulate in the blood can clear monomeric A $\beta$  by causing a shift in the concentration gradient of A $\beta$  across the BBB, which leads to a greater efflux from the brain<sup>[125]</sup>. So far passive immunisation attempts based on this peripheral sink hypothesis showed benefits in animal models, reducing the A $\beta$  burden without the need for antibodies to cross the BBB. One such monoclonal antibody, applied intravenously, is currently in phase III clinical trials to obtain information about its efficacy in human AD patients<sup>[211, 212]</sup>. The use of highly conformation-selective A $\beta$  binders within the *Drosophila* model provides an appropriate method to probe the pathogenic relevance of individual A $\beta$  aggregates and the antibody fragments B10 and KW1 are also used to perturb the aggregation process *in vivo*. The data obtained with *Drosophila melanogaster* can subsequently be related to biophysical and cell culture based

observations with pure polypeptide samples *in vitro*. Furthermore, if the endogenous targeting of A $\beta$  aggregates in *Drosophila melanogaster* would provide significant results, B10 and KW1 could be administered in other animal model systems such as mice to study their efficacy in clearing A $\beta$  from the brain. B10 might disaggregate existing fibrillar A $\beta$  plaques and indirectly increase the amount of misfolded A $\beta$  being cleared from the body, whereas KW1 could bind A $\beta$ (1-40) oligomers and inhibit their interaction e.g. with membrane receptors thus, decreasing their toxic potential. Thus, this thesis provides fundamental research results for the development of small antibody fragments that can subsequently be administered to human AD patients.

#### **4.2.1 Therapeutic benefits emerging from conformation- and sequence-sensitive antibodies**

In addition to the three suggested binding mechanisms new antibody based therapeutic approaches have to consider whether the antibody shall bind one specific aggregation species, identified *via* its conformation, or all A $\beta$  variants through a sequence-specific epitope. AD immunotherapy research intends to reduce the A $\beta$  burden in the brain by active or passive immunisation and the generated antibodies included both sequence- and conformation-sensitive anti-A $\beta$  antibodies. Both approaches have shown benefits in animal models and certain antibodies have been considered or used for clinical trials <sup>[114, 211, 213-215]</sup>. A broad specificity is expected from sequence-specific antibodies. These antibodies bind to a particular amino acid sequence within the peptide chain. Where this sequence is present on the surface of the A $\beta$  aggregation species the antibody can also recognise the aggregated structures. Monoclonal antibodies raised against the N-terminal region of A $\beta$  have been shown to recognise monomeric and fibrillar A $\beta$  as well as to disaggregate fibrils and block the amyloid dependent neurotoxicity <sup>[124, 216]</sup>. However, antibodies raised against the central or C-terminal part, which is buried within the  $\beta$ -sheet strands in A $\beta$  fibrils <sup>[217, 218]</sup>, may lack the potential of disassembling pre-existing aggregation species and are only effective in clearing monomeric or dimeric A $\beta$ . The efficacy of sequence-specific antibodies was published by Hoyer *et al.* who demonstrated that the affibody Z<sub>A $\beta$ 3</sub> inhibits A $\beta$  aggregation by stabilising monomeric A $\beta$  <sup>[219]</sup>. Furthermore, this affibody completely abolished A $\beta$  toxicity *in vivo* <sup>[208]</sup>. These data suggested that, as regards A $\beta$ , the major focus for AD treatment should be pointed towards blocking the fibril formation or dissolving oligomers and mature fibrils followed by clearing the A $\beta$  monomers (figure 4.2).

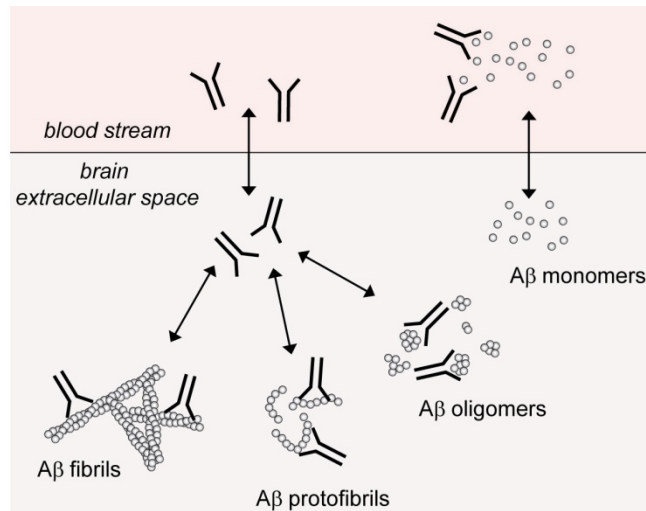


Figure 4.2 Mechanisms of antibody-mediated A $\beta$  clearance. Anti-A $\beta$  antibodies bind A $\beta$  either via a sequence- or conformation-sensitive epitope. The antibodies dissolve aggregates and clear monomeric A $\beta$  (modified from Schenk *et al.* 2004 <sup>[211]</sup>)

The first antibodies assessed in human AD trials were derived from active vaccination and stimulated the human T-cell response causing inflammatory reactions. AN1792 vaccination induced predominantly a pro-inflammatory T-helper 1 (T<sub>H</sub>1) mediated immune response, leading to adverse effects <sup>[220]</sup>. A significant number of patients developed autoimmune meningoencephalitis, caused primarily by the infiltration of autoreactive T lymphocytes into the brain in response to the active immunisation <sup>[221, 222]</sup>. A second active vaccination trial failed because the antibodies were not able to dissolve A $\beta$  plaques in the brain, although B- and T-cell responses were elicited <sup>[223]</sup>. Thus, to be beneficial for immunotherapy the antibodies have to overcome a number of different challenges. One possibility was developed after the identification of B-cell epitopes within the A $\beta$  sequence (A $\beta$ <sub>1-15</sub>) <sup>[224]</sup>. Petrushina *et al.* demonstrated that active vaccination with A $\beta$  segments, which exclude the T-cell epitope, could prevent the adverse effects by selectively initiating the B-cell response <sup>[121, 225]</sup>. An alternative, potentially non-inflammatory, approach is provided using single chain antibodies, which lack the F<sub>C</sub> part. These antibodies have been found to inhibit A $\beta$  aggregation *in vitro* as well as to prevent toxicity and reduce A $\beta$  burden *in vivo* <sup>[210, 226-228]</sup>. Furthermore, a recent study was published using V<sub>H</sub> antibodies that present a linear sequence epitope in the CDR 3 region that binds to A $\beta$  via hydrophobic interactions <sup>[229]</sup>. *In vitro* data demonstrated the inhibition of fibril formation, disruption of existing fibrils and elimination of A $\beta$  toxicity, suggesting the therapeutic utility of these antibodies <sup>[229]</sup>. For therapeutic approaches, the application of such antibodies via passive immunisation has several advantages over active vaccination, including greater safety, high efficacy and the possibility to target specific A $\beta$  aggregates via a conformation-sensitive epitope.

When amyloid fibrils were first identified in the extracellular plaques of AD brains, this species was thought to cause neurodegeneration. Antibodies were generated that specifically recognise amyloid fibrils, thus contributing to the understanding of these structures and the development of therapeutic agents <sup>[136-138]</sup>. Later, such conformation-sensitive antibodies were also raised against oligomers or protofibrils <sup>[133, 134, 214]</sup>. Based on data derived using these antibodies, it is now known that amyloid fibrils share a common structural motive <sup>[171]</sup>, whereas for oligomers various structures have been postulated <sup>[171, 199]</sup>. In general, conformation-sensitive antibodies enable specific targeting of A $\beta$  aggregation intermediates and subsequent analyses of their toxic properties. Recently, the two conformation-sensitive camelid antibody fragments B10 and KW1 were generated to recognise specific A $\beta$  aggregation intermediates *in vitro* <sup>[135, 138]</sup>. However, their therapeutic relevance *in vivo* remained elusive. Therefore the efficacy of B10 and KW1 was characterised in this thesis using a *Drosophila melanogaster* model of Alzheimer's disease. Generating *Drosophila melanogaster* animals transgenic for either B10 or KW1 allowed investigations regarding the consequences for *in vivo* neurotoxicity of both fibril and oligomer binding. Furthermore, the data allow conclusions about the suitability of conformation-sensitive antibodies for treating AD.

#### **4.3 Antibody domains B10 and KW1 are functionally expressed in *Drosophila melanogaster***

In order to determine whether B10 or KW1 can modify A $\beta$  aggregation *in vivo*, *Drosophila melanogaster* transgenic for B10 and KW1 were generated. To date, only one antibody derived from *Camelidae* has been endogenously expressed in *Drosophila melanogaster*. In the respective study, the efficiency of a monoclonal Llama anti-PABPN-1 intrabody was tested in a *Drosophila melanogaster* model of Oculopharyngeal muscular dystrophy <sup>[230]</sup> where it successfully suppressed muscle degeneration. Before characterisation of the two antibody fragments B10 and KW1 in *Drosophila melanogaster*, the genes for *B10AP* and *KW1AP* were cloned into a transfection vector for *Drosophila* S2 cells. After establishing stable transfected cells, both antibody domains termed as B10AP-S2 and KW1AP-S2, were synthesised and purified via their His-tag using Ni-chelate chromatography. The efficacy of the purified proteins derived from S2 cells was tested in spot blot analysis. B10AP-S2 recognised A $\beta$ (1-40) fibrils, whereas it did not bind to disaggregated or oligomeric A $\beta$ (1-40) (figure 3.2). Additionally, B10AP-S2 did not discriminate between A $\beta$ (1-40), A $\beta$ (1-42) and A $\beta$ (1-42)<sub>arc</sub> fibrils. On the other hand, KW1AP-S2 showed reactivity with A $\beta$ (1-40) oligomers but did not recognise disaggregated or fibrillar A $\beta$ (1-40) (figure 3.2). Furthermore, KW1AP-S2 was highly specific for A $\beta$ (1-40) oligomers and did not bind oligomers derived from A $\beta$ (1-42) or A $\beta$ (1-42)<sub>arc</sub> peptides. These results were in accordance with published results demonstrating the binding

characteristics of B10AP and KW1AP, expressed recombinantly in *E. coli*, where both presented a specific conformation-sensitive binding pattern <sup>[135, 138]</sup>.

These data revealed that the antibody domains B10 and KW1 are fully functional in *Drosophila melanogaster*. Thus, further investigations can be undertaken concerning the pathogenic role of A $\beta$  aggregation intermediates *in vivo*.

#### **4.3.1 A $\beta$ peptide variants are successfully expressed in *Drosophila melanogaster***

The efficacy of B10 and KW1 to modify A $\beta$  aggregation in *Drosophila melanogaster* was characterised using three fly lines, each with a different A $\beta$  variant: A $\beta$ 40, A $\beta$ 42 and A $\beta$ 42arc. The data in this study clearly demonstrate that the A $\beta$  burden is different depending on which A $\beta$  variant is expressed in the fly.

All previously established *Drosophila melanogaster* AD models demonstrated that A $\beta$ (1-42) is highly toxic, while A $\beta$ (1-40) shows no discernible effect on the organism <sup>[93-95]</sup>. Analysis of the A $\beta$  flies used in our study demonstrated that although A $\beta$ (1-40), A $\beta$ (1-42) and A $\beta$ (1-42)arc are transcribed at similar concentrations, the resulting protein quantities *in vivo* increased in the order A $\beta$ (1-40) < A $\beta$ (1-42) < A $\beta$ (1-42)arc (figure 3.5.1). Further, IFM images showed that no A $\beta$  aggregates are present in A $\beta$ 40 fly brains, while A $\beta$ 42 fly brains display some distinct A $\beta$  deposits and A $\beta$ 42arc fly brains contain high numbers of A $\beta$  plaques (figure 3.5.1). These data are fully in accordance with the previous *Drosophila melanogaster* models <sup>[94, 95]</sup>. Notably, similar results were demonstrated in a mouse model established to study the amyloid deposition of specific A $\beta$  variants *in vivo* <sup>[195]</sup>.

All three peptides, A $\beta$ (1-40), A $\beta$ (1-42) and A $\beta$ (1-42)arc, have been shown to form amyloid fibrils *in vitro*. Additionally, *in vitro* studies determined that the aggregation of these A $\beta$  peptides occurred via different intermediate species including oligomers and protofibrils <sup>[62, 100, 148]</sup>. A $\beta$  extractions from human AD patients, AD animal models and A $\beta$ -enriched cell lysates demonstrated the presence of soluble A $\beta$  structures ranging from dimers and trimers to high molecular weight oligomers and protofibrils <sup>[14, 200]</sup>. Many studies were carried out to detect the pathological impact of single A $\beta$  aggregation intermediate species, to establish the species responsible for the AD pathology. Taking all these studies together, there is evidence that each species may contribute to neurotoxicity <sup>[64, 161, 231]</sup>. For this reason, current understanding remains undecided whether a single toxic moiety is responsible for causing the AD pathology or if a number act synergistically. However, the A $\beta$  structures used in the assays so far were either *in vitro* prepared A $\beta$  conformers, derived from recombinant or synthetic A $\beta$  peptide, or derived from A $\beta$ -enriched cell lysates, brain homogenates or precipitates <sup>[199, 200]</sup>. Furthermore, all these studies used invasive injection procedures when applying

the A $\beta$  species, without reference to the natural environment of the organism. The establishment of a set of transgenic *Drosophila melanogaster* lines, which express the two camelid antibody domains B10 and KW1, has for the first time enable endogenous targeting of A $\beta$  fibrils and oligomers. These models will allow in depth analysis of the pathogenic role of A $\beta$  intermediate species within AD *in vivo*, without external influences to the organism.

#### **4.4 The pathogenic role of A $\beta$ fibrils characterised *in vivo* using the fibril binder B10.**

The conformation-sensitive antibody domain B10 was used to target A $\beta$  protofibrils and mature fibrils *in vivo*, to gain information regarding their pathogenic role in AD. In the brains of AD patients the extracellular plaques are primarily composed of A $\beta$  fibrils<sup>[14, 232]</sup> and these A $\beta$  fibrils were first thought to be responsible for causing the AD pathology. Several early studies identified A $\beta$  fibrils as a toxic species in cultured neuronal cell models<sup>[64, 233-236]</sup>. However, A $\beta$  peptides were found to form heterogeneous fibril species *in vitro*<sup>[237]</sup> suggesting that several fibril morphologies occur *in vivo*. Later research on human patients demonstrated that plaque counts, as determined histologically, do not correlate well with the degree of AD dementia<sup>[46]</sup>. It thus remains elusive, whether a general amyloid fibril dependent mechanism exists which causes neurotoxicity *in vivo*.

To help answer the question of A $\beta$  fibril pathogenicity, a conformation-sensitive fibril binder B10 was developed. This camelid antibody domain, B10, was previously found to bind to A $\beta$  fibrils *in vitro* as well as to inhibit the formation of mature fibrils by stabilising A $\beta$  protofibrils<sup>[138]</sup>. Protofibrils have been identified as a pathogenic species and have been shown to cause a decreased neuronal viability in primary cell culture models<sup>[65, 235]</sup>. Furthermore, research using human AD samples identified B10 positive A $\beta$  aggregates in brain samples of AD patients which were lacking in non-demented control patients<sup>[138, 238]</sup>. By using endogenous targeting of A $\beta$  with this conformation-sensitive fibril binder we can determine precise conclusions about the pathogenic role of A $\beta$  fibrils *in vivo*.

*Drosophila melanogaster* flies transgenic for A $\beta$ (1-40), A $\beta$ (1-42) and A $\beta$ (1-42)<sub>arc</sub> were used to test the *in vivo* ability of the fibril binder B10 to target A $\beta$  protofibrils and mature fibrils *in vivo*. This provided insights into the pathologic relevance of these species as well as into the potential therapeutic application of B10. Double-transgenic B10;A $\beta$  flies were crossed with the neuronal driver line Gal4-elav<sup>c155</sup> to enable the expression of both the A $\beta$  variants and the antibody domain B10. IFM and IP analysis demonstrated that B10 is physically attached to A $\beta$  *in vivo*. Thus, the overall presence of A $\beta$  fibrils in *Drosophila melanogaster*, as well as a B10-A $\beta$  interaction, was confirmed (figures 3.6.1 and 3.6.4).

All three lines of B10;A $\beta$  expressing flies were characterised phenotypically by measuring the lifespan, climbing ability and eye morphology. These tests determine if fibril targeting by B10 alters the A $\beta$  dependent neurotoxicity *in vivo*. In uncrossed flies, the lifespan and climbing ability of A $\beta$  expressing flies declines in the order WT = A $\beta$ 40 > A $\beta$ 42 > A $\beta$ 42arc. Upon expression of B10 this order was not altered, suggesting that B10 has no effect the neurotoxic properties of A $\beta$ (1-42) or A $\beta$ (1-42)arc (figure 3.8.1). Additionally, western blot studies displayed that B10 does not affect the SDS solubility of the A $\beta$  peptides (figure 3.8.2). Analyses of the neuronal expression of B10 alone revealed that the antibody domain does not modify the phenotype of WT flies (figure 3.10).

To summarise, the data demonstrated that B10 itself is not toxic to the fruit fly and has no significant effect on the neurotoxicity of any A $\beta$  variant when co-expressed in B10;A $\beta$  flies. However, B10 was able to interfere with the aggregation process, as demonstrated by IP analysis (figures 3.6.4). Since it is known that B10 perturbs the aggregation of A $\beta$  by stabilising protofibrils <sup>[138]</sup>, the lack of protective effect of B10 in A $\beta$  expressing flies implies that the debilitations in these flies are not caused by either protofibrils or mature amyloid fibrils. These data are consistent with other studies showing that A $\beta$  fibrils do not significantly contribute to AD pathology <sup>[14, 199]</sup>. For example, A $\beta$  fibrils have little effect the LTP of mouse neuronal cells <sup>[152, 239]</sup>. Instead, recent analyses have claimed that the deposited fibrils potentially play a detoxifying role, and are more likely to act in a neuroprotective role by binding, and therefore reducing the amount of, circulating toxic intermediates <sup>[14, 240]</sup>. Additionally, certain amyloid structures were found to have beneficial physiological functions in organisms such as bacteria, yeast and humans <sup>[2, 241-243]</sup>. The data presented herein, strengthens the theory that fibrils may adopt a non-toxic role *in vivo* and that amyloid fibril formation under physiological conditions is a common and potentially functional property of polypeptides <sup>[2, 244]</sup>.

#### **4.5 The pathogenicity of A $\beta$ oligomers is analysed *in vivo* using the oligomer-specific antibody domain KW1.**

The culprit of AD pathogenesis remains unclear. Current research has now established that A $\beta$  fibrils are unlikely to be the major pathogenic species, directing the research focus towards a role for earlier A $\beta$  aggregation intermediates. This has been fortified by a study demonstrating that A $\beta$  fibrils can be disaggregated into smaller aggregation intermediates <sup>[124, 228, 245]</sup> which leads to an increase in their toxicity <sup>[246]</sup>. Furthermore, *post mortem* analyses of human AD brains indicated that the levels of soluble non-fibrillar A $\beta$  aggregates correlate well with the extent of synaptic loss and cognitive decline <sup>[61, 161, 247]</sup>. These soluble aggregates can range from monomeric to dodecameric A $\beta$

species<sup>[199]</sup> and are known as low molecular weight oligomers. These species have been detected in brains of human AD patients and appear to occur at early stages of the aggregation process<sup>[248-250]</sup>.

The camelid antibody domain KW1AP was found to recognise A $\beta$  oligomers in human AD brains<sup>[135]</sup>. To determine whether the antibody domain KW1 can be used as an *in vivo* probe for targeting A $\beta$  oligomers an approach was set up by generating *Drosophila melanogaster* flies transgenic for KW1.

Phenotypic analyses of *Drosophila melanogaster* transgenic for KW1 revealed that KW1 alone does not modify the lifespan or behaviour compared to WT flies. Double-transgenic KW1;A $\beta$  flies, using the three A $\beta$  species: A $\beta$ (1-40), A $\beta$ (1-42) and A $\beta$ (1-42)arc, were then analysed to determine the efficacy of KW1 to target A $\beta$  oligomers *in vivo*. The presence of A $\beta$ (1-40) oligomers in the neurons of *Drosophila melanogaster* was characterised by IFM and IP analysis. IFM data suggested that KW1 is able to bind A $\beta$  *in vivo* and the co-precipitation of KW1 and A $\beta$  upon IP analysis revealed that KW1 is physically bound to A $\beta$  oligomers within the fly brain (figures 3.6.1 and 3.6.4). In conclusion, KW1 positive A $\beta$  oligomers are formed *in vivo*. Thus, *Drosophila melanogaster* transgenic for the oligomer binder KW1 and A $\beta$ (1-40), A $\beta$ (1-42) or A $\beta$ (1-42)arc can be used to determine firstly the pathogenic role of the three peptide variants, and secondly the potential pathogenic role of A $\beta$  oligomers, as demonstrated by the effects of KW1 targeting *in vivo*.

#### **4.5.1 A $\beta$ (1-40) is able to form neurotoxic aggregates in vivo**

Using *Drosophila melanogaster* transgenic for KW1 allowed studies regarding the pathogenic role of A $\beta$ (1-40) and A $\beta$ (1-42) *in vivo* due to the highly selective binding specificity of KW1 (figure 3.9.1). The phenotypic analysis revealed that KW1 has no discernible effects on A $\beta$ 42 and A $\beta$ 42arc flies. By contrast, KW1 showed a definite effect on the medium survival of A $\beta$ 40 flies. Surprisingly, the A $\beta$ 40 flies died earlier in presence of KW1 when compared to A $\beta$ 40 flies without co-expression of KW1. These data underscore the high selectivity of conformational targeting and show that KW1 recapitulates its biophysical specificity for A $\beta$ (1-40) *in vivo*.

No phenotypic changes between A $\beta$ 40 flies with or without KW1 were visible when measuring the climbing behaviour, which is an early indicator for neurodegenerative impairment. These findings are in contrast to earlier observations demonstrating that A $\beta$ (1-40) impairs the cognitive function, leading to age-dependent learning defects, but did not cause extensive neurodegeneration in *Drosophila melanogaster*<sup>[94]</sup>. To clarify how A $\beta$ (1-40) toxicity arises in this study, neuroblastoma cells were used to compare the synaptotoxic potential of A $\beta$ (1-40), A $\beta$ (1-42) and A $\beta$ (1-42)arc when incubated alone or in presence of KW1. The cell culture experiments

confirmed the results described above, revealing that KW1 stabilises A $\beta$ (1-40) aggregates *in vitro* which disturb the redox activity of neuronal cells while fibrillar A $\beta$ (1-40) does not interfere with this redox activity (fig.3.15A,B). Cells treated with A $\beta$ (1-42) showed a greater disruption of redox activity and the even more aggregation prone A $\beta$ (1-42)arc presented the highest reduction of the cellular metabolic activity (fig.3.15G). However, KW1 did not alter the cellular impairments caused by A $\beta$ (1-42) or A $\beta$ (1-42)arc. When comparing the cell culture data with the *Drosophila melanogaster* results, it was clear that the influence of the three A $\beta$  variants on the redox potential of the neuroblastoma cells correlated strongly with the decreased lifespan of *Drosophila melanogaster* (fig.3.15H).

Taken together, the foremost finding of this data is the proof that under certain circumstances A $\beta$ (1-40) leads to neurotoxicity *in vivo*. Previous research claimed only low levels of toxicity for this A $\beta$  variant<sup>[251]</sup> and A $\beta$ (1-40) was thought to play a protective role by inhibiting A $\beta$ (1-42) aggregation and its subsequent neurotoxic effects<sup>[252, 253]</sup>. However, upon KW1 targeting of A $\beta$ (1-40) there is a strong proof that A $\beta$ (1-40) contributes to pathogenicity *in vivo*. It was also shown earlier that A $\beta$ (1-40) is able to cause neurotoxicity itself in cell culture models<sup>[251]</sup> and that mutations are sufficient to transform A $\beta$ (1-40) into a more aggregation prone form that causes toxicity in *Drosophila melanogaster*<sup>[149]</sup>. However, KW1 did not increase the overall amount of the A $\beta$ (1-40) but instead altered its spatial distribution, thus confirming the capability of A $\beta$ (1-40) to form toxic aggregates *in vivo* (figure 3.11).

Earlier studies suggested that A $\beta$  toxicity depends on its aggregation on the cell surface, showing that toxicity correlates well with the presence of aggregates on cell surfaces<sup>[251]</sup>. Although many studies still claim that A $\beta$ (1-42) aggregation is essential for causing AD<sup>[195, 254]</sup>, it is not possible to state whether A $\beta$ (1-40) or A $\beta$ (1-42) alone are responsible, but rather that multiple A $\beta$  variants contribute to neurotoxicity. There is a clearly demonstrated influence of the C-terminal length of the A $\beta$  peptide on the AD phenotype<sup>[95, 255]</sup>. However, other post-translational modifications have also been shown to play relevant roles in AD. These modifications include N-terminal truncation, pyroglutamination, phosphorylation, isomerisation and racemisation of the A $\beta$  peptide<sup>[256-259]</sup>. The toxicity of these was demonstrated *in vivo* using transgenic *Drosophila melanogaster* or mice<sup>[191, 259]</sup>. For example, the pyroglutamate (pGlu) modification of N-terminally truncated A $\beta$  peptide led to an enhanced aggregation propensity and toxicity, demonstrating the neurotoxic potential of such post-translational modifications<sup>[260]</sup>. In the brains of AD patients pGluA $\beta$  is highly abundant and represents approximately 25 % of total deposited A $\beta$ <sup>[261]</sup>. An increasing effect of this modification was seen in the order pGluA $\beta$ (3-42) > pGluA $\beta$ (3-40)<sup>[262]</sup>, suggesting an additional effect of the N-terminal modification on the C-terminal influence, regarding the aggregation and neurotoxicity potential of the A $\beta$  peptide. Thus, due to post-translational modifications the variety of A $\beta$

aggregates contributing to AD is much higher and different aggregates can also interact *in vivo*, leading to enhanced neurotoxic effects and a more severe disease progression.

The influence of the antibody domains B10 and KW1 on the post-translational modifications and the interaction of different A $\beta$  aggregates could not be measured in the used *Drosophila model* and demonstrate the major limitation of our system. Additionally, the mechanism of A $\beta$  toxicity in *Drosophila melanogaster* remained elusive. As A $\beta$ (1-42) aggregation intermediates do not interfere with KW1, the conclusion is drawn that these intermediates structurally differ from A $\beta$ (1-40) aggregation intermediates. Thus, the data presented here suggest that the mechanism behind A $\beta$ (1-40) toxicity might be completely different from that of A $\beta$ (1-42) species.

#### **4.5.2 Oligomer targeting *in vivo* leads to increased neurotoxicity**

*In vitro* studies have indicated that soluble A $\beta$  oligomers are toxic to cultured neurons<sup>[133, 263, 264]</sup> and there is growing evidence that A $\beta$  oligomers are also neurotoxic *in vivo*<sup>[151, 265, 266]</sup>. However, it remains elusive if a specific size or conformation of these oligomers represents the main culprit in AD. In one case, Tomiyama *et al.* generated transgenic mice carrying an APP mutation that lead to an enhanced formation of A $\beta$  oligomers<sup>[267]</sup>. These mice displayed cognitive impairment and neuronal cell death without fibrillar A $\beta$  deposits. In a second study, the application of A $\beta$  oligomers onto living brain tissues lead to an impairment of the LTP and memory and also affected the synaptic plasticity<sup>[14, 151, 161, 268]</sup>. Additionally, A $\beta$  oligomers were found to decrease the number of synaptic spines of cultured neurons and the effect could be rescued by using monoclonal anti-A $\beta$  antibodies<sup>[264, 269]</sup>. Other studies further demonstrated that oligomer-specific antibodies inhibit the toxicity of A $\beta$  oligomers in cell culture systems and were able to detect these oligomers in human and mouse AD brains<sup>[133, 270]</sup>. Our use of the bivalent antibody domain KW1AP, generated against A $\beta$  oligomers, showed to be highly specific for A $\beta$ (1-40) oligomers. Additionally, the camelid antibody domain KW1AP was able to prevent the formation of mature amyloid fibrils *in vitro* and was also found to recognise A $\beta$  oligomers in human AD brains. Furthermore, it was demonstrated that A $\beta$  oligomers bound by KW1AP restore the LTP effects, as measured with mouse hippocampal slices<sup>[135]</sup>. These data imply a protective effect of KW1 by targeting A $\beta$  oligomers *in vivo*.

Although recent *in vitro* data suggested that KW1AP can inhibit the oligomer dependent toxicity<sup>[135]</sup>, the current data demonstrated that targeting A $\beta$ (1-40) with KW1 *in vivo* leads to the formation of neurotoxic aggregates. This conclusion is drawn from the observation that *Drosophila melanogaster* expressing KW1 and A $\beta$ (1-40) die significantly faster than A $\beta$ (1-40) expressing flies (figure 3.9.1-2). IFM analysis revealed that during ageing KW1 redirects the spatial distribution of

A $\beta$ (1-40) and causes accumulation of A $\beta$ (1-40) within the cell, leading to the formation of A $\beta$  deposits (figure 3.11). This is consistent with the general finding that A $\beta$ (1-42) and A $\beta$ (1-42)<sub>arc</sub>, which are more aggregation prone than A $\beta$ (1-40), are also usually found accumulated within the cell. However, the presence of KW1 does not affect the steady state concentration levels of A $\beta$ (1-40), compared to normally secreted A $\beta$ (1-40) alone.

The analysis of several A $\beta$ (1-40) fly lines displayed a good correlation between the initial A $\beta$ (1-40) concentration and the medium survival rates (figure 3.12.2). In conclusion, the current *in vivo* data demonstrated a toxic effect of oligomer-specific targeting that is age-dependent and critically depends on the A $\beta$ (1-40) peptide. These results were strengthened by toxicity analysis on a cell culture model and using hippocampal brain slices (figure 3.15). A $\beta$ (1-40) incubated alone neither affected the redox activity of neuroblastoma cells nor impaired the LTP of mice hippocampal brain slices. By contrast, the presence of KW1 during the aggregation of A $\beta$ (1-40) led to significant disturbance of the redox activity of neuroblastoma cells and impairment of the LTP, confirming the presence of neurotoxic A $\beta$  aggregates.

In contrast to previous expectations no neutralisation of A $\beta$  toxicity by KW1 was observed. An explanation for this contradiction would be that KW1 does not trigger an immune answer in *Drosophila melanogaster*. It is known that A $\beta$  activates inflammatory pathways in the brain of AD patients. A $\beta$  is theorised to stimulate microglia, which constitute the innate immune system of the brain<sup>[271, 272]</sup>. Microglia were also found to accumulate around A $\beta$  plaques in the brain and to exhibit chemotaxis towards aggregated A $\beta$ <sup>[273, 274]</sup>. The innate immune defence of *Drosophila melanogaster* has similarities to the human innate immune defence<sup>[275]</sup>. It has been published that in *Drosophila melanogaster* glia cells also play a role in the innate immune response and that they occasionally accumulate A $\beta$  intracellularly<sup>[174, 276]</sup>. The neurotoxic A $\beta$  aggregates bound by KW1 could be internalised into glia cells and cause cytotoxic reactions that is by activating pro-inflammatory cytokines. In summary, against all expectations KW1 was not able to sequester A $\beta$  from the aggregation pathway but instead it caused the accumulation of toxic A $\beta$ (1-40) aggregates that impair neuronal cells.

#### **4.5.3 A $\beta$ (1-40) oligomers mediate toxicity via neuronal cell surface receptors**

In comparison to other studies based on cell culture models or animal injections<sup>[14, 199]</sup>, this thesis substantiated animal-based discoveries regarding A $\beta$ (1-40) toxicity *in vivo* without additional external manipulation. Nevertheless, the exact mechanism of toxicity of A $\beta$  oligomers *in vivo* remained elusive. Studies suggested that neuronal cell death is mediated by A $\beta$  oligomer interaction with neuronal cell surface receptors such as nerve growth factor (NGF), RAGE, NMDA, Insulin or Frizzled receptor (figure 4.3)<sup>[180, 264, 277-280]</sup>. Furthermore, other studies demonstrated that A $\beta$

induced cell death could be inhibited by extracellular insulin or NMDA receptor antagonists<sup>[95, 278, 279, 281]</sup>. Recent observations also implied that the cellular prion protein (PrP<sup>C</sup>) can act as an A $\beta$  oligomer receptor and that this interaction may block the PrP<sup>C</sup> – NMDA receptor interaction leading to synaptic dysfunction<sup>[282]</sup>. Thus, A $\beta$  mediated toxicity may occur via multiple pathways.

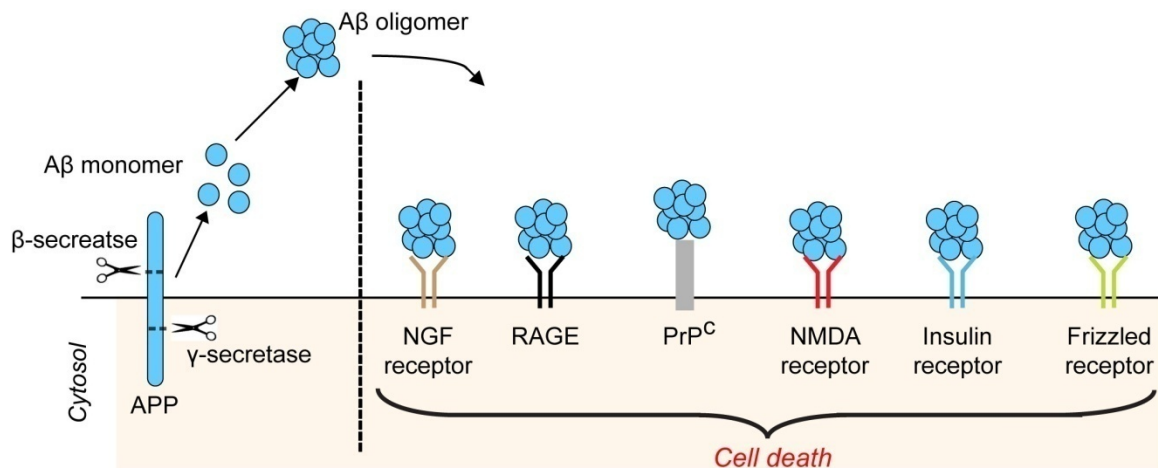


Figure 4.3 Potential mechanisms of A $\beta$  oligomer mediated toxicity on neuronal cells (modified from Sakono *et al.* 2010<sup>[283]</sup>).

A more detailed look into the mechanism of the A $\beta$ (1-40) dependent toxicity was taken by treating KW1;A $\beta$ 40 flies with the NMDA receptor antagonist MK-801 and also using RNAi-mediated down regulation of the NMDA receptor in *Drosophila melanogaster* (figures 3.13.1-2). These two approaches were carried out to test the involvement of the NMDA receptor in the A $\beta$ (1-40) mediated neurotoxicity upon co-expression of KW1. The survival data of both approaches did not display any significant differences in the viability of KW1;A $\beta$ 40 flies upon inhibition of the NMDA receptor. The successful RNAi mediated down regulation of the NMDA receptor was proven by RT-PCR, and resulted in much lower transcription levels of the NMDA receptor subunit 1, which is required to form a functional receptor (figures 3.13.2A). Although a small absolute difference of 3 days occurred between RNAi/KW1;A $\beta$ 40 and KW1;A $\beta$ 40 flies, presenting a slightly lower decline for the RNAi flies, this data was not statistically significant and thus does not prove whether the down-regulation of the NMDA receptor can inhibit the A $\beta$ (1-40) derived viability decrease. Another study that analysed MK-801 on flies showed its beneficial effects with A $\beta$ (1-42) and A $\beta$ (1-42)arc flies<sup>[95]</sup>. Although the results were significant, the lifespan of the flies was prolonged only a couple of days upon MK-801 treatment. Comparing the peptide concentrations of A $\beta$ (1-42) and A $\beta$ (1-40) flies leads to the conclusion that due to the low amount of A $\beta$ (1-40) peptide the MK-801 mediated lifespan extension might be too small to be detectable within this assay.

After consideration of the above data it is neither approved nor disapproved whether A $\beta$ (1-40) mediates its toxicity via the NMDA receptor. Further experiments, e.g. using neuronal cells, which enable specific RNAi mediated down regulation of the cell surface receptors and the usage of greater A $\beta$  amounts, would be required to conclusively demonstrate this point.

#### **4.5.4 KW1 induces the formation of neurotoxic off-pathway aggregates**

A recent publication demonstrated that KW1AP is able to bind A $\beta$ (1-40) oligomers and block their transition into mature fibrils <sup>[135]</sup>. Furthermore, KW1AP completely inhibited the oligomer mediated toxicity towards living brain slices <sup>[135]</sup>. The data presented in this thesis demonstrate that its monovalent counterpart, KW1, indeed prevents the formation of mature amyloid fibrils *in vitro* (figure 3.14). TEM analysis revealed that KW1 does not bind A $\beta$ (1-40) oligomers, but rather stabilises non-fibrillar aggregates which are a heterogeneous mix ranging from spheres to curvilinear structures (figure 3.14 D). Instead of preventing the toxicity of A $\beta$ (1-40) oligomers, these non-fibrillar A $\beta$ (1-40) aggregates comprise neurotoxic species as seen by the reduction of the metabolic activity of cells and the impairment of the LTP (figure 3.15 D). These results enable insights into the possible pathogenic process occurring in *Drosophila melanogaster* when KW1 is present. Similar to the *in vitro* data KW1 binding to A $\beta$ (1-40) inside the fly brain might block the aggregation process and lead to the formation of non-fibrillar aggregates *in vivo*. However, further studies are required to demonstrate the exact mechanism of this process.

*In vitro* studies suggested that KW1 possess a hydrophobic cavity that binds preferentially to hydrophobic molecules <sup>[135]</sup>. Oligomeric aggregates derived from A $\beta$  peptides are known to comprise solvent exposed hydrophobic surfaces <sup>[147]</sup>. Therefore, KW1 might bind to hydrophobic oligomeric aggregates *in vivo* and, instead of blocking the aggregation process, KW1 may redirect the aggregation pathway (figure 4.4). This assumption was supported by ANS spectroscopy data showing that KW1 stabilised A $\beta$ (1-40) aggregates comprise hydrophobic surfaces (figure 3.14). This is also consistent with other data, suggesting that changes of hydrophobic surfaces, which lead to increased ANS fluorescence, are in good correlation with cytotoxicity <sup>[168, 284]</sup>. This correlation has also been shown for the pGlu modification of A $\beta$ , which, due to a higher surface hydrophobicity, potentially enhances the interference of A $\beta$  with neurons <sup>[262]</sup>. Regarding the development of AD, there may exist additional undiscovered hydrophobic molecules within the brain that bind A $\beta$  and induce its toxicity.

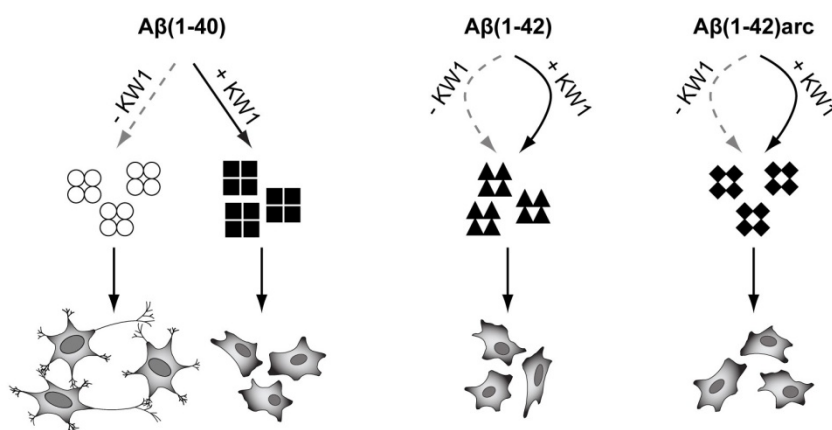


Figure 4.4 KW1AP perturbs the formation of A $\beta$ (1-40) fibrils by inducing the formation of neurotoxic aggregates.

In conclusion, this thesis established that KW1 perturbs the aggregation pathway rather than simply targeting an individual A $\beta$  aggregation species. KW1 induces the formation of, and subsequently maintains, hydrophobic non-fibrillar aggregates which represent a toxic off-pathway species. Potentially, these aggregates could subsequently bind to the lipid membrane or cell surface receptors of neurons and mediate toxicity by interfering with the synaptic processes. Therefore, interaction studies with artificial lipid membranes could confirm the possible binding of these non-fibrillar A $\beta$  to cell membranes *in vivo*. Indeed, *in vitro* studies have already demonstrated that A $\beta$  is able to interact with synthetic lipids and lipid membranes altering the permeability, conductivity and fluidity<sup>[148, 285-289]</sup>. In such cases, the A $\beta$  dependent neurotoxicity could be prevented by blocking its membrane interaction<sup>[290]</sup>.

The inhibition of the cellular redox activity has previously been described as an early indicator of A $\beta$  mediated cell death<sup>[236]</sup>. Hence, it is likely that soluble A $\beta$  aggregates disturb the function of neurons before causing neurodegeneration. This is consistent with the observation that, while neurodegeneration only becomes visible in later phases of AD, there is a good correlation between early disruptions, such as the reduction of synaptic spines and memory deficits<sup>[58]</sup>. This is further underlined by analysis showing that soluble A $\beta$  aggregates such as oligomers and non-fibrillar aggregates commit synaptotoxic effects by inhibition of the LTP (figure 3.15)<sup>[152, 239]</sup>.

#### **4.6 Conformational targeting *in vivo* is essential for understanding AD pathogenesis**

Within this thesis, a unique approach was developed based upon *Drosophila melanogaster* altered to be double transgenic, for both human A $\beta$  and conformation-sensitive antibody domains. For the very first time it was possible to show A $\beta$ (1-40) dependent toxicity, thus demonstrating the

pathogenic potential of this A $\beta$  variant which is known to constitute the bulk of cerebral A $\beta$  <sup>[199, 291]</sup>. Further details into the extent to which A $\beta$ (1-40) contributes to the pathogenesis of human AD remains to be established. The observation of A $\beta$ (1-40) toxicity significantly extends previous research that mainly focussed on C- or N-terminally modified versions of A $\beta$ . These latter variants are clearly more aggregation prone than A $\beta$ (1-40) <sup>[53, 148, 260]</sup>, suggesting a C-terminal influence, and data consistent with this finding are also provided in this thesis. KW1 clearly modified the aggregation of A $\beta$ (1-40), leading to increased hydrophobicity as also seen for posttranslational modifications of A $\beta$  <sup>[260, 262]</sup>. As a result, we theorise that the influence of the length of the C-terminus and the surface hydrophobicity together potentially lead to enhanced neurotoxicity of A $\beta$ .

Additionally, the data presented here imply that blocking the formation of mature fibrils is not necessarily beneficial against AD development. This, consequently, strengthens the theory that early state aggregates provoke neurotoxicity. The obtained results also question the assumption that a single neurotoxic A $\beta$  conformer underlies AD. Instead, the data suggest that multiple pathogenic A $\beta$  conformations, probably also involving different A $\beta$  variants, are required to elicit the full spectrum of neuronal disturbances characteristic for AD *in vivo*. Furthermore conformation-sensitive antibodies have unexpected activities, which may be limitations. One such was the oligomer binder KW1 being able to redirect the aggregation of A $\beta$  to produce off-pathway species. This interconversion created A $\beta$  dependent toxicity and would be damaging, instead of beneficial, for AD patients. From a therapeutic point of view oligomer-targeting, as demonstrated with the highly selective oligomer binder KW1, elucidated that this method of exterminating a single neurotoxic structure will inevitably fail, because several aggregation species are involved in the AD pathology. Thus, despite some evidence supporting the strategy of conformation-sensitive targeting, these results propose that therapeutic approaches generally recognizing A $\beta$  peptide using primarily sequence-sensitive binder seem to be more efficient. Up to now, no *in vivo* experiments or clinical studies exist that state the therapeutic potential of a specific antibody. However, based on the results demonstrated here antibodies, when selected with care, remain still the most powerful tool for passive immunisation studies to abate or cure AD.

The current results are ultimately relevant in the context of AD immunotherapy. Based on IP analysis it was possible to demonstrate that A $\beta$  aggregates formed *in vitro* are also present *in vivo* strengthening the importance of the *in vitro* studies. Using transgenic *Drosophila melanogaster* enabled the characterisation of these aggregates in an intact system without having to extract or inject the proteins, thus removing the need for biochemical procedures that lead to a loss of structural integrity in the aggregates present in AD brains. Combining these studies ultimately lead to fundamental insights into the molecular basis of AD pathogenesis.

---

## 5. Summary

---

Alzheimer's disease (AD) is a neurodegenerative disease that involved the aggregation and deposition of the two polypeptides A $\beta$  and Tau. To date, it remains unclear how the disease is caused and no cure is available. This thesis focused on the A $\beta$  peptide that is found *post mortem* in the extracellular plaques of brains of AD patient. The A $\beta$  aggregation process was elucidated *in vitro* and conformation-sensitive antibodies were raised to study specific aggregation species *in vitro* and *in vivo*.

Two monoclonal camelid heavy-chain antibody domains, termed KW1 and B10 were used in this thesis. B10 and KW1 were generated *in vitro* via phage display using oligomers or fibrils as epitopes for selection. Both antibody domains were characterised in-depth via *in vitro* studies and were shown to be suitable tools to highly selectively target their respective A $\beta$  aggregates. Within this work, these antibody domains were expressed in *Drosophila melanogaster* flies that transgenically expressed A $\beta$ (1-40), A $\beta$ (1-42) or A $\beta$ (1-42)<sub>arc</sub> peptide within the (CNS). Fly models are powerful systems used to investigate aggregating proteins that are involved in neurodegenerative diseases.

The results of the studies described here demonstrated that conformational targeting of A $\beta$  aggregates with appropriately selected antibody fragments is a simple way to determine which types of aggregates are present in the intact CNS of a living animal. The antibody domains enabled further analysis of the functional effects of these aggregates. The transgenic expression of B10 and KW1 *in vivo* together with A $\beta$  showed that oligomer targeting, but not fibril targeting, affects A $\beta$  toxicity and fly viability. In addition, the thesis presented data that reveal specific perturbations of the A $\beta$  aggregation process upon co-expression of KW1 *in vivo* and the subsequent effects. In particular, KW1- targeting of A $\beta$ (1-40) led to the formation of neurotoxic A $\beta$ (1-40) aggregates in *Drosophila melanogaster* while the A $\beta$ (1-42) phenotype was completely unaffected by KW1. This result demonstrated the potential of A $\beta$ (1-40) to contribute to AD pathology *in vivo* and also suggested that multiple toxic A $\beta$  aggregates are required to elicit the full AD pathology rather than one single toxic A $\beta$  aggregation species.

---

## 6. Zusammenfassung

---

Die Alzheimersche Krankheit ist eine neurodegenerative Erkrankung, die mit der Aggregation und Ablagerung der beiden Polypeptide A $\beta$  und Tau einhergeht. bis zum heutigen Tage ist es unklar wie die Krankheit entsteht und es gibt keine Heilung. Diese Arbeit konzentriert sich auf das A $\beta$ -Peptid, welches *post mortem* in den extrazellulären Plaques der Gehirne von Alzheimer Patienten gefunden wird. Der Aggregationsprozess von A $\beta$  wurde bereits *in vitro* aufgeklärt und konformationssensitive Antikörper wurden entwickelt, um einzelne Aggregationsarten zu untersuchen.

Zwei monoklonale kamelide Schwere-Kette-Antikörperdomänen, bezeichnet als B10 und KW1, wurde in dieser Arbeit verwendet. Diese Antikörperdomänen wurden *in vitro* mittels Phagen-Display generiert, wobei A $\beta$  Oligomere oder Fibrillen als Epitope für die Selektion genutzt wurden. Beide Antikörperdomänen wurden eingehend *in vitro* charakterisiert und sind geeignete Werkzeuge um ihre entsprechenden Zielaggregate mit hoher Selektivität zu binden. Innerhalb dieser Arbeit wurden die beiden Antikörperdomänen in *Drosophila melanogaster* eingebracht, die zusätzlich transgen die Peptide A $\beta$ (1-40), A $\beta$ (1-42) oder A $\beta$ (1-42)<sub>arc</sub> innerhalb des zentralen Nervensystems (ZNS) exprimieren. Fliegenmodelle sind ein geeignetes System, um aggregierende Proteine zu untersuchen, die an neurodegenerativen Erkrankungen beteiligt sind.

Die Ergebnisse zeigen, dass gezieltes konformationssensitives Binden von A $\beta$  Aggregaten mit geeigneten Antikörperdomänen eine Möglichkeit ist, zu bestimmen, welche Aggregate im intakten ZNS lebender Organismen vorkommen. Zusätzlich erlauben die Antikörperdomänen weitere Analysen der funktionalen Effekte dieser Aggregate. Die transgene Expression von B10 und KW1 *in vivo* zusammen mit A $\beta$  zeigte, dass Oligomer-Bindung, jedoch nicht Fibrillen-Bindung, die A $\beta$ -Toxizität und Lebenserwartung von Fliegen beeinflusst. Besonders, die A $\beta$ (1-40)-Bindung durch KW1 führte zur Bildung von neurotoxischen A $\beta$ (1-40) Aggregaten in *Drosophila melanogaster*, während A $\beta$ (1-42) von KW1 unbeeinflusst blieb. Das Ergebnis zeigte das Potenzial von A $\beta$ (1-40) an der Alzheimer-Symptomatik *in vivo* mitzuwirken und deutete darauf hin, dass eher mehrere toxische A $\beta$  Aggregates an der Ausprägung der Alzheimer Pathologie beteiligt sind als eine einzige toxische A $\beta$  Aggregationsform.

---

## 7. Literature

---

1. Ross, CA and Poirier, MA, *Protein aggregation and neurodegenerative disease*. Nat Med, 2004. **10 Suppl**: p. S10-7.
2. Chiti, F and Dobson, CM, *Protein misfolding, functional amyloid, and human disease*. Annu Rev Biochem, 2006. **75**: p. 333-66.
3. Forman, MS; Trojanowski, JQ and Lee, VM, *Neurodegenerative diseases: a decade of discoveries paves the way for therapeutic breakthroughs*. Nat Med, 2004. **10**(10): p. 1055-63.
4. Prusiner, SB, *Shattuck lecture--neurodegenerative diseases and prions*. N Engl J Med, 2001. **344**(20): p. 1516-26.
5. Keller, JN; Dimayuga, E; Chen, Q; Thorpe, J; Gee, J *et al.*, *Autophagy, proteasomes, lipofuscin, and oxidative stress in the aging brain*. Int J Biochem Cell Biol, 2004. **36**(12): p. 2376-91.
6. Shintani, T and Klionsky, DJ, *Autophagy in health and disease: a double-edged sword*. Science, 2004. **306**(5698): p. 990-5.
7. Martinez-Vicente, M; Sovak, G and Cuervo, AM, *Protein degradation and aging*. Exp Gerontol, 2005. **40**(8-9): p. 622-33.
8. Dawson, TM and Dawson, VL, *Molecular pathways of neurodegeneration in Parkinson's disease*. Science, 2003. **302**(5646): p. 819-22.
9. Scherzinger, E; Sittler, A; Schweiger, K; Heiser, V; Lurz, R *et al.*, *Self-assembly of polyglutamine-containing huntingtin fragments into amyloid-like fibrils: implications for Huntington's disease pathology*. Proc Natl Acad Sci U S A, 1999. **96**(8): p. 4604-9.
10. Gotz, J and Ittner, LM, *Animal models of Alzheimer's disease and frontotemporal dementia*. Nat Rev Neurosci, 2008. **9**(7): p. 532-44.
11. AFI, <http://www.alzheimer-forschung.de/alzheimer-krankheit/index.htm>.
12. Alzheimer, A, *Über eine eigenartige Erkrankung der Hirnrinde*. Allg. Z. Psychiatr., 1907. **64**(1-2): p. 146-148.
13. Selkoe, DJ, *Alzheimer's disease is a synaptic failure*. Science, 2002. **298**(5594): p. 789-91.
14. Haass, C and Selkoe, DJ, *Soluble protein oligomers in neurodegeneration: lessons from the Alzheimer's amyloid beta-peptide*. Nat Rev Mol Cell Biol, 2007. **8**(2): p. 101-12.
15. Ittner, LM and Gotz, J, *Amyloid-beta and tau - a toxic pas de deux in Alzheimer's disease*. Nat Rev Neurosci, 2011.
16. Rapoport, M; Dawson, HN; Binder, LI; Vitek, MP and Ferreira, A, *Tau is essential to beta - amyloid-induced neurotoxicity*. Proc Natl Acad Sci U S A, 2002. **99**(9): p. 6364-9.
17. Gotz, J; Chen, F; van Dorpe, J and Nitsch, RM, *Formation of neurofibrillary tangles in P301 tau transgenic mice induced by A $\beta$  42 fibrils*. Science, 2001. **293**(5534): p. 1491-5.
18. Roberson, ED; Scarce-Levie, K; Palop, JJ; Yan, F; Cheng, IH *et al.*, *Reducing endogenous tau ameliorates amyloid beta-induced deficits in an Alzheimer's disease mouse model*. Science, 2007. **316**(5825): p. 750-4.
19. Shahani, N and Brandt, R, *Functions and malfunctions of the tau proteins*. Cell Mol Life Sci, 2002. **59**(10): p. 1668-80.
20. Mandelkow, EM; Stamer, K; Vogel, R; Thies, E and Mandelkow, E, *Clogging of axons by tau, inhibition of axonal traffic and starvation of synapses*. Neurobiol Aging, 2003. **24**(8): p. 1079-85.
21. Mudher, A; Shepherd, D; Newman, TA; Mildren, P; Jukes, JP *et al.*, *GSK-3beta inhibition reverses axonal transport defects and behavioural phenotypes in Drosophila*. Mol Psychiatry, 2004. **9**(5): p. 522-30.
22. Morishima-Kawashima, M; Hasegawa, M; Takio, K; Suzuki, M; Yoshida, H *et al.*, *Proline-directed and non-proline-directed phosphorylation of PHF-tau*. J Biol Chem, 1995. **270**(2): p. 823-9.

23. Kopke, E; Tung, YC; Shaikh, S; Alonso, AC; Iqbal, K *et al.*, *Microtubule-associated protein tau. Abnormal phosphorylation of a non-paired helical filament pool in Alzheimer disease.* J Biol Chem, 1993. **268**(32): p. 24374-84.
24. Garver, TD; Harris, KA; Lehman, RA; Lee, VM; Trojanowski, JQ *et al.*, *Tau phosphorylation in human, primate, and rat brain: evidence that a pool of tau is highly phosphorylated in vivo and is rapidly dephosphorylated in vitro.* J Neurochem, 1994. **63**(6): p. 2279-87.
25. Bramblett, GT; Goedert, M; Jakes, R; Merrick, SE; Trojanowski, JQ *et al.*, *Abnormal tau phosphorylation at Ser396 in Alzheimer's disease recapitulates development and contributes to reduced microtubule binding.* Neuron, 1993. **10**(6): p. 1089-99.
26. Bramblett, GT; Trojanowski, JQ and Lee, VM, *Regions with abundant neurofibrillary pathology in human brain exhibit a selective reduction in levels of binding-competent tau and accumulation of abnormal tau-isoforms (A68 proteins).* Lab Invest, 1992. **66**(2): p. 212-22.
27. Lee, VM; Balin, BJ; Otvos, L, Jr. and Trojanowski, JQ, *A68: a major subunit of paired helical filaments and derivatized forms of normal Tau.* Science, 1991. **251**(4994): p. 675-8.
28. Schindowski, K; Bretteville, A; Leroy, K; Begard, S; Brion, JP *et al.*, *Alzheimer's disease-like tau neuropathology leads to memory deficits and loss of functional synapses in a novel mutated tau transgenic mouse without any motor deficits.* Am J Pathol, 2006. **169**(2): p. 599-616.
29. Kimura, T; Yamashita, S; Fukuda, T; Park, JM; Murayama, M *et al.*, *Hyperphosphorylated tau in parahippocampal cortex impairs place learning in aged mice expressing wild-type human tau.* Embo J, 2007. **26**(24): p. 5143-52.
30. Ishihara, T; Zhang, B; Higuchi, M; Yoshiyama, Y; Trojanowski, JQ *et al.*, *Age-dependent induction of congophilic neurofibrillary tau inclusions in tau transgenic mice.* Am J Pathol, 2001. **158**(2): p. 555-62.
31. Khurana, V; Lu, Y; Steinhilb, ML; Oldham, S; Shulman, JM *et al.*, *TOR-mediated cell-cycle activation causes neurodegeneration in a Drosophila tauopathy model.* Curr Biol, 2006. **16**(3): p. 230-41.
32. Brandt, R; Hundelt, M and Shahani, N, *Tau alteration and neuronal degeneration in tauopathies: mechanisms and models.* Biochim Biophys Acta, 2005. **1739**(2-3): p. 331-54.
33. Iqbal, K; Liu, F; Gong, CX; Alonso Adel, C and Grundke-Iqbal, I, *Mechanisms of tau-induced neurodegeneration.* Acta Neuropathol, 2009. **118**(1): p. 53-69.
34. Bancher, C; Brunner, C; Lassmann, H; Budka, H; Jellinger, K *et al.*, *Accumulation of abnormally phosphorylated tau precedes the formation of neurofibrillary tangles in Alzheimer's disease.* Brain Res, 1989. **477**(1-2): p. 90-9.
35. Braak, H and Braak, E, *Staging of Alzheimer's disease-related neurofibrillary changes.* Neurobiol Aging, 1995. **16**(3): p. 271-8; discussion 278-84.
36. Ballatore, C; Lee, VM and Trojanowski, JQ, *Tau-mediated neurodegeneration in Alzheimer's disease and related disorders.* Nat Rev Neurosci, 2007. **8**(9): p. 663-72.
37. Hutton, M; Lendon, CL; Rizzu, P; Baker, M; Froelich, S *et al.*, *Association of missense and 5'-splice-site mutations in tau with the inherited dementia FTDP-17.* Nature, 1998. **393**(6686): p. 702-5.
38. Iijima, K; Gatt, A and Iijima-Ando, K, *Tau Ser262 phosphorylation is critical for Abeta42-induced tau toxicity in a transgenic Drosophila model of Alzheimer's disease.* Hum Mol Genet, 2010. **19**(15): p. 2947-57.
39. Virchow, R, *Zur Cellulose-Frage.* Virchows Arch. Pathol. Anat. Physiol. Klin. Med., 1854. **6**(3): p. 416-426.
40. Virchow, R, *Über eine im Gehirn und Rückenmark des Menschen aufgefundene Substanz mit der chemischen Reaction der Cellulose.* Virchows Arch. Pathol. Anat. Physiol. Klin. Med., 1854. **6**(1): p. 135-138.
41. Virchow, R, *Weitere Mittheilungen über das Vorkommen der pflanzlichen Cellulose beim Menschen.* Virchows Arch. Pathol. Anat. Physiol. Klin. Med., 1854. **6**(2): p. 268-271.
42. Friedreich, N and Kekule, A, *Zur Amyloidfrage.* Virchows Arch. Pathol. Anat. Physiol. Klin. Med., 1859. **16**: p. 50-65.

43. Kazatchkine, MD; Husby, G; Araki, S; Benditt, EP; Benson, MD *et al.*, *Nomenclature of amyloid and amyloidosis - WHO-IUIS Nomenclature Subcommittee*. Bull WHO, 1993. **71**: p. 105-108.
44. Westermarck, P; Benson, MD; Buxbaum, JN; Cohen, AS; Frangione, B *et al.*, *A primer of amyloid nomenclature*. Amyloid, 2007. **14**(3): p. 179-83.
45. Esler, WP and Wolfe, MS, *A portrait of Alzheimer secretases--new features and familiar faces*. Science, 2001. **293**(5534): p. 1449-54.
46. Hardy, J and Selkoe, DJ, *The amyloid hypothesis of Alzheimer's disease: progress and problems on the road to therapeutics*. Science, 2002. **297**(5580): p. 353-6.
47. Hardy, JA and Higgins, GA, *Alzheimer's disease: the amyloid cascade hypothesis*. Science, 1992. **256**(5054): p. 184-5.
48. Kojro, E and Fahrenholz, F, *The non-amyloidogenic pathway: structure and function of alpha-secretases*. Subcell Biochem, 2005. **38**: p. 105-27.
49. Kumar-Singh, S; Theuns, J; Van Broeck, B; Pirici, D; Vennekens, K *et al.*, *Mean age-of-onset of familial Alzheimer disease caused by presenilin mutations correlates with both increased Abeta42 and decreased Abeta40*. Hum Mutat, 2006. **27**(7): p. 686-95.
50. Bentahir, M; Nyabi, O; Verhamme, J; Tolia, A; Horre, K *et al.*, *Presenilin clinical mutations can affect gamma-secretase activity by different mechanisms*. J Neurochem, 2006. **96**(3): p. 732-42.
51. Luheshi, LM; Tartaglia, GG; Brorsson, AC; Pawar, AP; Watson, IE *et al.*, *Systematic in vivo analysis of the intrinsic determinants of amyloid Beta pathogenicity*. PLoS Biol, 2007. **5**(11): p. e290.
52. Kim, W and Hecht, MH, *Mutations enhance the aggregation propensity of the Alzheimer's A beta peptide*. J Mol Biol, 2008. **377**(2): p. 565-74.
53. Nilsberth, C; Westlind-Danielsson, A; Eckman, CB; Condron, MM; Axelman, K *et al.*, *The 'Arctic' APP mutation (E693G) causes Alzheimer's disease by enhanced Abeta protofibril formation*. Nat Neurosci, 2001. **4**(9): p. 887-93.
54. Citron, M; Oltersdorf, T; Haass, C; McConlogue, L; Hung, AY *et al.*, *Mutation of the beta-amyloid precursor protein in familial Alzheimer's disease increases beta-protein production*. Nature, 1992. **360**(6405): p. 672-4.
55. Moncaster, JA; Pineda, R; Moir, RD; Lu, S; Burton, MA *et al.*, *Alzheimer's disease amyloid-beta links lens and brain pathology in Down syndrome*. PLoS One, 2009. **5**(5): p. e10659.
56. Rovelet-Lecrux, A; Hannequin, D; Raux, G; Le Meur, N; Laquerriere, A *et al.*, *APP locus duplication causes autosomal dominant early-onset Alzheimer disease with cerebral amyloid angiopathy*. Nat Genet, 2006. **38**(1): p. 24-6.
57. Zhang, C and Saunders, AJ, *Therapeutic targeting of the alpha-secretase pathway to treat Alzheimer's disease*. Discov Med, 2007. **7**(39): p. 113-7.
58. Terry, RD; Masliah, E; Salmon, DP; Butters, N; DeTeresa, R *et al.*, *Physical basis of cognitive alterations in Alzheimer's disease: synapse loss is the major correlate of cognitive impairment*. Ann Neurol, 1991. **30**(4): p. 572-80.
59. Klein, WL; Krafft, GA and Finch, CE, *Targeting small Abeta oligomers: the solution to an Alzheimer's disease conundrum?* Trends Neurosci, 2001. **24**(4): p. 219-24.
60. Irizarry, MC; Soriano, F; McNamara, M; Page, KJ; Schenk, D *et al.*, *Abeta deposition is associated with neuropil changes, but not with overt neuronal loss in the human amyloid precursor protein V717F (PDAPP) transgenic mouse*. J Neurosci, 1997. **17**(18): p. 7053-9.
61. Wang, J; Dickson, DW; Trojanowski, JQ and Lee, VM, *The levels of soluble versus insoluble brain Abeta distinguish Alzheimer's disease from normal and pathologic aging*. Exp Neurol, 1999. **158**(2): p. 328-37.
62. Goldsbury, C; Frey, P; Olivieri, V; Aebi, U and Muller, SA, *Multiple assembly pathways underlie amyloid-beta fibril polymorphisms*. J Mol Biol, 2005. **352**(2): p. 282-98.
63. Scheidt, HA; Morgado, I; Rothmund, S; Huster, D and Fandrich, M, *Solid-State NMR Spectroscopic Investigation of Abeta Protofibrils: Implication of a beta-Sheet Remodeling upon Maturation into Terminal Amyloid Fibrils*. Angew Chem Int Ed Engl, 2011. **50**(12): p. 2837-40.

64. Deshpande, A; Mina, E; Glabe, C and Busciglio, J, *Different conformations of amyloid beta induce neurotoxicity by distinct mechanisms in human cortical neurons*. J Neurosci, 2006. **26**(22): p. 6011-8.
65. Isaacs, AM; Senn, DB; Yuan, M; Shine, JP and Yankner, BA, *Acceleration of amyloid beta-peptide aggregation by physiological concentrations of calcium*. J Biol Chem, 2006. **281**(38): p. 27916-23.
66. Eckert, A; Hauptmann, S; Scherping, I; Meinhardt, J; Rhein, V *et al.*, *Oligomeric and fibrillar species of beta-amyloid (A beta 42) both impair mitochondrial function in P301L tau transgenic mice*. J Mol Med, 2008. **86**(11): p. 1255-67.
67. Woodruff-Pak, DS, *Animal models of Alzheimer's disease: therapeutic implications*. J Alzheimers Dis, 2008. **15**(4): p. 507-21.
68. Sibley, CG and Ahlquist, JE, *DNA hybridization evidence of hominoid phylogeny: results from an expanded data set*. J Mol Evol, 1987. **26**(1-2): p. 99-121.
69. Herndon, JG; Moss, MB; Rosene, DL and Killiany, RJ, *Patterns of cognitive decline in aged rhesus monkeys*. Behav Brain Res, 1997. **87**(1): p. 25-34.
70. Gearing, M; Tigges, J; Mori, H and Mirra, SS, *beta-Amyloid (A beta) deposition in the brains of aged orangutans*. Neurobiol Aging, 1997. **18**(2): p. 139-46.
71. Voytko, ML and Tinkler, GP, *Cognitive function and its neural mechanisms in nonhuman primate models of aging, Alzheimer disease, and menopause*. Front Biosci, 2004. **9**: p. 1899-914.
72. Jucker, M, *The benefits and limitations of animal models for translational research in neurodegenerative diseases*. Nat Med, 2010. **16**(11): p. 1210-4.
73. Games, D; Adams, D; Alessandrini, R; Barbour, R; Berthelette, P *et al.*, *Alzheimer-type neuropathology in transgenic mice overexpressing V717F beta-amyloid precursor protein*. Nature, 1995. **373**(6514): p. 523-7.
74. Hsiao, K; Chapman, P; Nilsen, S; Eckman, C; Harigaya, Y *et al.*, *Correlative memory deficits, Abeta elevation, and amyloid plaques in transgenic mice*. Science, 1996. **274**(5284): p. 99-102.
75. Sturchler-Pierrat, C; Abramowski, D; Duke, M; Wiederhold, KH; Mistl, C *et al.*, *Two amyloid precursor protein transgenic mouse models with Alzheimer disease-like pathology*. Proc Natl Acad Sci U S A, 1997. **94**(24): p. 13287-92.
76. Chishti, MA; Yang, DS; Janus, C; Phinney, AL; Horne, P *et al.*, *Early-onset amyloid deposition and cognitive deficits in transgenic mice expressing a double mutant form of amyloid precursor protein 695*. J Biol Chem, 2001. **276**(24): p. 21562-70.
77. Ronnback, A; Zhu, S; Dillner, K; Aoki, M; Lilius, L *et al.*, *Progressive neuropathology and cognitive decline in a single Arctic APP transgenic mouse model*. Neurobiol Aging, 2009. **32**(2): p. 280-92.
78. Oakley, H; Cole, SL; Logan, S; Maus, E; Shao, P *et al.*, *Intraneuronal beta-amyloid aggregates, neurodegeneration, and neuron loss in transgenic mice with five familial Alzheimer's disease mutations: potential factors in amyloid plaque formation*. J Neurosci, 2006. **26**(40): p. 10129-40.
79. Oddo, S; Caccamo, A; Shepherd, JD; Murphy, MP; Golde, TE *et al.*, *Triple-transgenic model of Alzheimer's disease with plaques and tangles: intracellular Abeta and synaptic dysfunction*. Neuron, 2003. **39**(3): p. 409-21.
80. Arslanova, D; Yang, T; Xu, X; Wong, ST; Augelli-Szafran, CE *et al.*, *Phenotypic analysis of images of zebrafish treated with Alzheimer's gamma-secretase inhibitors*. BMC Biotechnol, 2010. **10**: p. 24.
81. Link, CD, *Expression of human beta-amyloid peptide in transgenic Caenorhabditis elegans*. Proc Natl Acad Sci U S A, 1995. **92**(20): p. 9368-72.
82. Link, CD, *C. elegans models of age-associated neurodegenerative diseases: lessons from transgenic worm models of Alzheimer's disease*. Exp Gerontol, 2006. **41**(10): p. 1007-13.

83. Drake, J; Link, CD and Butterfield, DA, *Oxidative stress precedes fibrillar deposition of Alzheimer's disease amyloid beta-peptide (1-42) in a transgenic Caenorhabditis elegans model*. Neurobiol Aging, 2003. **24**(3): p. 415-20.
84. Adams, MD and Celniker, SE and Holt, RA and Evans, CA and Gocayne, JD et al., *The genome sequence of Drosophila melanogaster*. Science, 2000. **287**(5461): p. 2185-95.
85. Reiter, LT; Potocki, L; Chien, S; Gribskov, M and Bier, E, *A systematic analysis of human disease-associated gene sequences in Drosophila melanogaster*. Genome Res, 2001. **11**(6): p. 1114-25.
86. Stork, T; Engelen, D; Krudewig, A; Silies, M; Bainton, RJ et al., *Organization and function of the blood-brain barrier in Drosophila*. J Neurosci, 2008. **28**(3): p. 587-97.
87. Rosen, DR; Martin-Morris, L; Luo, LQ and White, K, *A Drosophila gene encoding a protein resembling the human beta-amyloid protein precursor*. Proc Natl Acad Sci U S A, 1989. **86**(7): p. 2478-82.
88. Gunawardena, S and Goldstein, LS, *Disruption of axonal transport and neuronal viability by amyloid precursor protein mutations in Drosophila*. Neuron, 2001. **32**(3): p. 389-401.
89. Luo, L; Tully, T and White, K, *Human amyloid precursor protein ameliorates behavioral deficit of flies deleted for Appl gene*. Neuron, 1992. **9**(4): p. 595-605.
90. Fossgreen, A; Bruckner, B; Czech, C; Masters, CL; Beyreuther, K et al., *Transgenic Drosophila expressing human amyloid precursor protein show gamma-secretase activity and a blistered-wing phenotype*. Proc Natl Acad Sci U S A, 1998. **95**(23): p. 13703-8.
91. Carmine-Simmen, K; Proctor, T; Tschape, J; Poeck, B; Triphan, T et al., *Neurotoxic effects induced by the Drosophila amyloid-beta peptide suggest a conserved toxic function*. Neurobiol Dis, 2009. **33**(2): p. 274-81.
92. Greeve, I; Kretschmar, D; Tschape, JA; Beyn, A; Brellinger, C et al., *Age-dependent neurodegeneration and Alzheimer-amyloid plaque formation in transgenic Drosophila*. J Neurosci, 2004. **24**(16): p. 3899-906.
93. Finelli, A; Kelkar, A; Song, HJ; Yang, H and Konsolaki, M, *A model for studying Alzheimer's Abeta42-induced toxicity in Drosophila melanogaster*. Mol Cell Neurosci, 2004. **26**(3): p. 365-75.
94. Iijima, K; Liu, HP; Chiang, AS; Hearn, SA; Konsolaki, M et al., *Dissecting the pathological effects of human Abeta40 and Abeta42 in Drosophila: a potential model for Alzheimer's disease*. Proc Natl Acad Sci U S A, 2004. **101**(17): p. 6623-8.
95. Crowther, DC; Kinghorn, KJ; Miranda, E; Page, R; Curry, JA et al., *Intraneuronal Abeta, non-amyloid aggregates and neurodegeneration in a Drosophila model of Alzheimer's disease*. Neuroscience, 2005. **132**(1): p. 123-35.
96. Rival, T; Page, RM; Chandraratna, DS; Sendall, TJ; Ryder, E et al., *Fenton chemistry and oxidative stress mediate the toxicity of the beta-amyloid peptide in a Drosophila model of Alzheimer's disease*. Eur J Neurosci, 2009. **29**(7): p. 1335-47.
97. Liu, B; Moloney, A; Meehan, S; Morris, K; Thomas, SE et al., *Iron Promotes the Toxicity of Amyloid {beta} Peptide by Impeding Its Ordered Aggregation*. J Biol Chem, 2011. **286**(6): p. 4248-56.
98. Iijima-Ando, K; Hearn, SA; Granger, L; Shenton, C; Gatt, A et al., *Overexpression of neprilysin reduces alzheimer amyloid-beta42 (Abeta42)-induced neuron loss and intraneuronal Abeta42 deposits but causes a reduction in cAMP-responsive element-binding protein-mediated transcription, age-dependent axon pathology, and premature death in Drosophila*. J Biol Chem, 2008. **283**(27): p. 19066-76.
99. Iijima-Ando, K; Hearn, SA; Shenton, C; Gatt, A; Zhao, L et al., *Mitochondrial mislocalization underlies Abeta42-induced neuronal dysfunction in a Drosophila model of Alzheimer's disease*. PLoS One, 2009. **4**(12): p. e8310.
100. Bohrmann, B; Adrian, M; Dubochet, J; Kuner, P; Muller, F et al., *Self-assembly of beta-amyloid 42 is retarded by small molecular ligands at the stage of structural intermediates*. J Struct Biol, 2000. **130**(2-3): p. 232-46.

101. Wood, SJ; MacKenzie, L; Maleeff, B; Hurle, MR and Wetzel, R, *Selective inhibition of Abeta fibril formation*. J Biol Chem, 1996. **271**(8): p. 4086-92.
102. Reixach, N; Crooks, E; Ostresh, JM; Houghten, RA and Blondelle, SE, *Inhibition of beta-amyloid-induced neurotoxicity by imidazopyridindoles derived from a synthetic combinatorial library*. J Struct Biol, 2000. **130**(2-3): p. 247-58.
103. Sabbagh, MN, *Drug development for Alzheimer's disease: where are we now and where are we headed?* Am J Geriatr Pharmacother, 2009. **7**(3): p. 167-85.
104. Wollen, KA, *Alzheimer's disease: the pros and cons of pharmaceutical, nutritional, botanical, and stimulatory therapies, with a discussion of treatment strategies from the perspective of patients and practitioners*. Altern Med Rev, 2010. **15**(3): p. 223-44.
105. McShane, R; Areosa Sastre, A and Minakaran, N, *Memantine for dementia*. Cochrane Database Syst Rev, 2006(2): p. CD003154.
106. Hansen, RA; Gartlehner, G; Webb, AP; Morgan, LC; Moore, CG *et al.*, *Efficacy and safety of donepezil, galantamine, and rivastigmine for the treatment of Alzheimer's disease: a systematic review and meta-analysis*. Clin Interv Aging, 2008. **3**(2): p. 211-25.
107. Sjogren, M; Gustafsson, K; Syversen, S; Olsson, A; Edman, A *et al.*, *Treatment with simvastatin in patients with Alzheimer's disease lowers both alpha- and beta-cleaved amyloid precursor protein*. Dement Geriatr Cogn Disord, 2003. **16**(1): p. 25-30.
108. Simons, M; Schwarzler, F; Lutjohann, D; von Bergmann, K; Beyreuther, K *et al.*, *Treatment with simvastatin in normocholesterolemic patients with Alzheimer's disease: A 26-week randomized, placebo-controlled, double-blind trial*. Ann Neurol, 2002. **52**(3): p. 346-50.
109. Eriksen, JL; Sagi, SA; Smith, TE; Weggen, S; Das, P *et al.*, *NSAIDs and enantiomers of flurbiprofen target gamma-secretase and lower Abeta 42 in vivo*. J Clin Invest, 2003. **112**(3): p. 440-9.
110. Green, RC; Schneider, LS; Amato, DA; Beelen, AP; Wilcock, G *et al.*, *Effect of tarenfluril on cognitive decline and activities of daily living in patients with mild Alzheimer disease: a randomized controlled trial*. Jama, 2009. **302**(23): p. 2557-64.
111. Weggen, S; Eriksen, JL; Das, P; Sagi, SA; Wang, R *et al.*, *A subset of NSAIDs lower amyloidogenic Abeta42 independently of cyclooxygenase activity*. Nature, 2001. **414**(6860): p. 212-6.
112. McLaurin, J; Kierstead, ME; Brown, ME; Hawkes, CA; Lambermon, MH *et al.*, *Cyclohexanehexol inhibitors of Abeta aggregation prevent and reverse Alzheimer phenotype in a mouse model*. Nat Med, 2006. **12**(7): p. 801-8.
113. Schenk, D, *Amyloid-beta immunotherapy for Alzheimer's disease: the end of the beginning*. Nat Rev Neurosci, 2002. **3**(10): p. 824-8.
114. Lemere, CA and Masliah, E, *Can Alzheimer disease be prevented by amyloid-beta immunotherapy?* Nat Rev Neurol, 2010. **6**(2): p. 108-19.
115. Schenk, D; Barbour, R; Dunn, W; Gordon, G; Grajeda, H *et al.*, *Immunization with amyloid-beta attenuates Alzheimer-disease-like pathology in the PDAPP mouse*. Nature, 1999. **400**(6740): p. 173-7.
116. Chen, G; Chen, KS; Knox, J; Inglis, J; Bernard, A *et al.*, *A learning deficit related to age and beta-amyloid plaques in a mouse model of Alzheimer's disease*. Nature, 2000. **408**(6815): p. 975-9.
117. Janus, C; Pearson, J; McLaurin, J; Mathews, PM; Jiang, Y *et al.*, *A beta peptide immunization reduces behavioural impairment and plaques in a model of Alzheimer's disease*. Nature, 2000. **408**(6815): p. 979-82.
118. Morgan, D; Diamond, DM; Gottschall, PE; Ugen, KE; Dickey, C *et al.*, *A beta peptide vaccination prevents memory loss in an animal model of Alzheimer's disease*. Nature, 2000. **408**(6815): p. 982-5.
119. Orgogozo, JM; Gilman, S; Dartigues, JF; Laurent, B; Puel, M *et al.*, *Subacute meningoencephalitis in a subset of patients with AD after Abeta42 immunization*. Neurology, 2003. **61**(1): p. 46-54.

120. Gilman, S; Koller, M; Black, RS; Jenkins, L; Griffith, SG *et al.*, *Clinical effects of Abeta immunization (AN1792) in patients with AD in an interrupted trial*. *Neurology*, 2005. **64**(9): p. 1553-62.
121. Petrushina, I; Ghochikyan, A; Mktrichyan, M; Mamikonyan, G; Movsesyan, N *et al.*, *Alzheimer's disease peptide epitope vaccine reduces insoluble but not soluble/oligomeric Abeta species in amyloid precursor protein transgenic mice*. *J Neurosci*, 2007. **27**(46): p. 12721-31.
122. Axelsen, TV; Holm, A; Christiansen, G and Birkelund, S, *Identification of the shortest Abeta-peptide generating highly specific antibodies against the C-terminal end of amyloid-beta42*. *Vaccine*, 2011.
123. Solomon, B; Koppel, R; Hanan, E and Katzav, T, *Monoclonal antibodies inhibit in vitro fibrillar aggregation of the Alzheimer beta-amyloid peptide*. *Proc Natl Acad Sci U S A*, 1996. **93**(1): p. 452-5.
124. Solomon, B; Koppel, R; Frankel, D and Hanan-Aharon, E, *Disaggregation of Alzheimer beta-amyloid by site-directed mAb*. *Proc Natl Acad Sci U S A*, 1997. **94**(8): p. 4109-12.
125. DeMattos, RB; Bales, KR; Cummins, DJ; Dodart, JC; Paul, SM *et al.*, *Peripheral anti-A beta antibody alters CNS and plasma A beta clearance and decreases brain A beta burden in a mouse model of Alzheimer's disease*. *Proc Natl Acad Sci U S A*, 2001. **98**(15): p. 8850-5.
126. Bard, F; Cannon, C; Barbour, R; Burke, RL; Games, D *et al.*, *Peripherally administered antibodies against amyloid beta-peptide enter the central nervous system and reduce pathology in a mouse model of Alzheimer disease*. *Nat Med*, 2000. **6**(8): p. 916-9.
127. Wilcock, DM; Rojiani, A; Rosenthal, A; Subbarao, S; Freeman, MJ *et al.*, *Passive immunotherapy against Abeta in aged APP-transgenic mice reverses cognitive deficits and depletes parenchymal amyloid deposits in spite of increased vascular amyloid and microhemorrhage*. *J Neuroinflammation*, 2004. **1**(1): p. 24.
128. Hyman, BT; Smith, C; Buldyrev, I; Whelan, C; Brown, H *et al.*, *Autoantibodies to amyloid-beta and Alzheimer's disease*. *Ann Neurol*, 2001. **49**(6): p. 808-10.
129. Nath, A; Hall, E; Tuzova, M; Dobbs, M; Jons, M *et al.*, *Autoantibodies to amyloid beta-peptide (Abeta) are increased in Alzheimer's disease patients and Abeta antibodies can enhance Abeta neurotoxicity: implications for disease pathogenesis and vaccine development*. *Neuromolecular Med*, 2003. **3**(1): p. 29-39.
130. Weksler, ME; Relkin, N; Turkenich, R; LaRusse, S; Zhou, L *et al.*, *Patients with Alzheimer disease have lower levels of serum anti-amyloid peptide antibodies than healthy elderly individuals*. *Exp Gerontol*, 2002. **37**(7): p. 943-8.
131. Du, Y; Dodel, R; Hampel, H; Buerger, K; Lin, S *et al.*, *Reduced levels of amyloid beta-peptide antibody in Alzheimer disease*. *Neurology*, 2001. **57**(5): p. 801-5.
132. Dodel, R; Balakrishnan, K; Keyvani, K; Deuster, O; Neff, F *et al.*, *Naturally Occurring Autoantibodies against {beta}-Amyloid: Investigating Their Role in Transgenic Animal and In Vitro Models of Alzheimer's Disease*. *J Neurosci*. **31**(15): p. 5847-54.
133. Kaye, R; Head, E; Thompson, JL; McIntire, TM; Milton, SC *et al.*, *Common structure of soluble amyloid oligomers implies common mechanism of pathogenesis*. *Science*, 2003. **300**(5618): p. 486-9.
134. Lafaye, P; Achour, I; England, P; Duyckaerts, C and Rougeon, F, *Single-domain antibodies recognize selectively small oligomeric forms of amyloid beta, prevent Abeta-induced neurotoxicity and inhibit fibril formation*. *Mol Immunol*, 2009. **46**(4): p. 695-704.
135. Morgado, I; Wieligmann, K; Bereza, M; Ronicke, R; Meinhardt, K *et al.*, *Molecular basis of beta-amyloid oligomer recognition with a conformational antibody fragment*. *Proc Natl Acad Sci U S A*, 2012.
136. O'Nuallain, B and Wetzel, R, *Conformational Abs recognizing a generic amyloid fibril epitope*. *Proc Natl Acad Sci U S A*, 2002. **99**(3): p. 1485-90.
137. Kaye, R; Head, E; Sarsoza, F; Saing, T; Cotman, CW *et al.*, *Fibril specific, conformation dependent antibodies recognize a generic epitope common to amyloid fibrils and fibrillar oligomers that is absent in prefibrillar oligomers*. *Mol Neurodegener*, 2007. **2**: p. 18.

138. Habicht, G; Haupt, C; Friedrich, RP; Hortschansky, P; Sachse, C *et al.*, *Directed selection of a conformational antibody domain that prevents mature amyloid fibril formation by stabilizing Abeta protofibrils*. Proc Natl Acad Sci U S A, 2007. **104**(49): p. 19232-7.
139. Lambert, MP; Viola, KL; Chromy, BA; Chang, L; Morgan, TE *et al.*, *Vaccination with soluble Abeta oligomers generates toxicity-neutralizing antibodies*. J Neurochem, 2001. **79**(3): p. 595-605.
140. Hamers-Casterman, C; Atarhouch, T; Muyldermans, S; Robinson, G; Hamers, C *et al.*, *Naturally occurring antibodies devoid of light chains*. Nature, 1993. **363**(6428): p. 446-8.
141. Muyldermans, S; Atarhouch, T; Saldanha, J; Barbosa, JA and Hamers, R, *Sequence and structure of VH domain from naturally occurring camel heavy chain immunoglobulins lacking light chains*. Protein Eng, 1994. **7**(9): p. 1129-35.
142. Muyldermans, S; Cambillau, C and Wyns, L, *Recognition of antigens by single-domain antibody fragments: the superfluous luxury of paired domains*. Trends Biochem Sci, 2001. **26**(4): p. 230-5.
143. Muyldermans, S, *Single domain camel antibodies: current status*. J Biotechnol, 2001. **74**(4): p. 277-302.
144. Upadhaya, AR; Lungrin, I; Yamaguchi, H; Fandrich, M and Thal, DR, *High-molecular weight Abeta-oligomers and protofibrils are the predominant Abeta-species in the native soluble protein fraction of the AD brain*. J Cell Mol Med.
145. Haupt, C; Bereza, M; Kumar, ST; Kieninger, B; Morgado, I *et al.*, *Pattern recognition with a fibril-specific antibody fragment reveals the surface variability of natural amyloid fibrils*. J Mol Biol. **408**(3): p. 529-40.
146. Haupt, C; Morgado, I; Kumar, ST; Parthier, C; Bereza, M *et al.*, *Amyloid fibril recognition with the conformational B10 antibody fragment depends on electrostatic interactions*. J Mol Biol. **405**(2): p. 341-8.
147. Chen, YR and Glabe, CG, *Distinct early folding and aggregation properties of Alzheimer amyloid-beta peptides Abeta40 and Abeta42: stable trimer or tetramer formation by Abeta42*. J Biol Chem, 2006. **281**(34): p. 24414-22.
148. Lashuel, HA and Lansbury, PT, Jr., *Are amyloid diseases caused by protein aggregates that mimic bacterial pore-forming toxins?* Q Rev Biophys, 2006. **39**(2): p. 167-201.
149. Brorsson, AC; Bolognesi, B; Tartaglia, GG; Shammass, SL; Favrin, G *et al.*, *Intrinsic determinants of neurotoxic aggregate formation by the amyloid beta peptide*. Biophys J, 2010. **98**(8): p. 1677-84.
150. Balducci, C; Beeg, M; Stravalaci, M; Bastone, A; Scip, A *et al.*, *Synthetic amyloid-beta oligomers impair long-term memory independently of cellular prion protein*. Proc Natl Acad Sci U S A, 2010. **107**(5): p. 2295-300.
151. Ronicke, R; Mikhaylova, M; Ronicke, S; Meinhardt, J; Schroder, UH *et al.*, *Early neuronal dysfunction by amyloid beta oligomers depends on activation of NR2B-containing NMDA receptors*. Neurobiol Aging, 2011. **32**(12): p. 2219-28.
152. Haupt, C; Leppert, J; Ronicke, R; Meinhardt, J; Yadav, JK *et al.*, *Structural Basis of beta-Amyloid-Dependent Synaptic Dysfunctions*. Angew Chem Int Ed Engl, 2012.
153. Maurer, R; Meyer, B and Ptashne, M, *Gene regulation at the right operator (OR) bacteriophage lambda. I. OR3 and autogenous negative control by repressor*. J Mol Biol, 1980. **139**(2): p. 147-61.
154. Lindsley, DL and Zimm, GG, *The genome of Drosophila melanogaster*. Academic Press 1992, San Diego, Calif. [u.a.].
155. Bischof, J; Maeda, RK; Hediger, M; Karch, F and Basler, K, *An optimized transgenesis system for Drosophila using germ-line-specific phiC31 integrases*. Proc Natl Acad Sci U S A, 2007. **104**(9): p. 3312-7.
156. Green, C; Levashina, E; McKimmie, C; Dafforn, T; Reichhart, JM *et al.*, *The necrotic gene in Drosophila corresponds to one of a cluster of three serpin transcripts mapping at 43A1.2*. Genetics, 2000. **156**(3): p. 1117-27.

157. Brand, AH and Perrimon, N, *Targeted gene expression as a means of altering cell fates and generating dominant phenotypes*. Development, 1993. **118**(2): p. 401-15.
158. Seiki, M, *Amplification of genomic DNA*. PCR-Protocols-A guide to methods and applications. 1990: Academic Press. 13-20.
159. Christopeit, T; Hortschansky, P; Schroeckh, V; Guhrs, K; Zandomeneghi, G *et al.*, *Mutagenic analysis of the nucleation propensity of oxidized Alzheimer's beta-amyloid peptide*. Protein Sci, 2005. **14**(8): p. 2125-31.
160. Gill, SC and von Hippel, PH, *Calculation of protein extinction coefficients from amino acid sequence data*. Anal Biochem, 1989. **182**(2): p. 319-26.
161. Shankar, GM; Li, S; Mehta, TH; Garcia-Munoz, A; Shepardson, NE *et al.*, *Amyloid-beta protein dimers isolated directly from Alzheimer's brains impair synaptic plasticity and memory*. Nat Med, 2008. **14**(8): p. 837-42.
162. Kieninger, B; Gioeva, Z; Kruger, S; Westermark, GT; Friedrich, RP *et al.*, *PTAA and B10: new approaches to amyloid detection in tissue-evaluation of amyloid detection in tissue with a conjugated polyelectrolyte and a fibril-specific antibody fragment*. Amyloid, 2011. **18**(2): p. 47-52.
163. Schneider, I, *Cell lines derived from late embryonic stages of Drosophila melanogaster*. J Embryol Exp Morphol, 1972. **27**(2): p. 353-65.
164. Johansen, H; van der Straten, A; Sweet, R; Otto, E; Maroni, G *et al.*, *Regulated expression at high copy number allows production of a growth-inhibitory oncogene product in Drosophila Schneider cells*. Genes Dev, 1989. **3**(6): p. 882-9.
165. Biedler, JL; Roffler-Tarlov, S; Schachner, M and Freedman, LS, *Multiple neurotransmitter synthesis by human neuroblastoma cell lines and clones*. Cancer Res, 1978. **38**(11 Pt 1): p. 3751-7.
166. Semisotnov, GV; Rodionova, NA; Razgulyaev, OI; Uversky, VN; Gripas, AF *et al.*, *Study of the "molten globule" intermediate state in protein folding by a hydrophobic fluorescent probe*. Biopolymers, 1991. **31**(1): p. 119-28.
167. Frare, E; Mossuto, MF; de Laureto, PP; Tolin, S; Menzer, L *et al.*, *Characterization of oligomeric species on the aggregation pathway of human lysozyme*. J Mol Biol, 2009. **387**(1): p. 17-27.
168. Bolognesi, B; Kumita, JR; Barros, TP; Esbjorner, EK; Luheshi, LM *et al.*, *ANS binding reveals common features of cytotoxic amyloid species*. ACS Chem Biol, 2010. **5**(8): p. 735-40.
169. LeVine, H, 3rd, *Thioflavine T interaction with synthetic Alzheimer's disease beta-amyloid peptides: detection of amyloid aggregation in solution*. Protein Sci, 1993. **2**(3): p. 404-10.
170. Klunk, WE; Jacob, RF and Mason, RP, *Quantifying amyloid beta-peptide (A $\beta$ ) aggregation using the Congo red-A $\beta$  (CR-A $\beta$ ) spectrophotometric assay*. Anal Biochem, 1999. **266**(1): p. 66-76.
171. Haupt, C; Bereza, M; Kumar, ST; Kieninger, B; Morgado, I *et al.*, *Pattern recognition with a fibril-specific antibody fragment reveals the surface variability of natural amyloid fibrils*. J Mol Biol, 2011. **408**(3): p. 529-40.
172. Haupt, C; Morgado, I; Kumar, ST; Parthier, C; Bereza, M *et al.*, *Amyloid fibril recognition with the conformational B10 antibody fragment depends on electrostatic interactions*. J Mol Biol, 2011. **405**(2): p. 341-8.
173. Berg, I; Thor, S and Hammarstrom, P, *Modeling familial amyloidotic polyneuropathy (Transthyretin V30M) in Drosophila melanogaster*. Neurodegener Dis, 2009. **6**(3): p. 127-38.
174. Iijima, K; Chiang, HC; Hearn, SA; Hakker, I; Gatt, A *et al.*, *A $\beta$ 42 mutants with different aggregation profiles induce distinct pathologies in Drosophila*. PLoS One, 2008. **3**(2): p. e1703.
175. Zhang, Y; Kurup, P; Xu, J; Carty, N; Fernandez, SM *et al.*, *Genetic reduction of striatal-enriched tyrosine phosphatase (STEP) reverses cognitive and cellular deficits in an Alzheimer's disease mouse model*. Proc Natl Acad Sci U S A, 2010. **107**(44): p. 19014-9.
176. Wolff, T and Ready, DF, *Cell death in normal and rough eye mutants of Drosophila*. Development, 1991. **113**(3): p. 825-39.

177. Bilen, J and Bonini, NM, *Drosophila as a model for human neurodegenerative disease*. Annu Rev Genet, 2005. **39**: p. 153-71.
178. Verdier, Y; Zarandi, M and Penke, B, *Amyloid beta-peptide interactions with neuronal and glial cell plasma membrane: binding sites and implications for Alzheimer's disease*. J Pept Sci, 2004. **10**(5): p. 229-48.
179. Snyder, EM; Nong, Y; Almeida, CG; Paul, S; Moran, T et al., *Regulation of NMDA receptor trafficking by amyloid-beta*. Nat Neurosci, 2005. **8**(8): p. 1051-8.
180. Yan, SD; Bierhaus, A; Nawroth, PP and Stern, DM, *RAGE and Alzheimer's disease: a progression factor for amyloid-beta-induced cellular perturbation?* J Alzheimers Dis, 2009. **16**(4): p. 833-43.
181. Wong, PT; Schauerte, JA; Wisser, KC; Ding, H; Lee, EL et al., *Amyloid-beta membrane binding and permeabilization are distinct processes influenced separately by membrane charge and fluidity*. J Mol Biol, 2009. **386**(1): p. 81-96.
182. Mayer, ML and Westbrook, GL, *The physiology of excitatory amino acids in the vertebrate central nervous system*. Prog Neurobiol, 1987. **28**(3): p. 197-276.
183. Morris, RG, *Synaptic plasticity and learning: selective impairment of learning rats and blockade of long-term potentiation in vivo by the N-methyl-D-aspartate receptor antagonist AP5*. J Neurosci, 1989. **9**(9): p. 3040-57.
184. Tsien, JZ; Huerta, PT and Tonegawa, S, *The essential role of hippocampal CA1 NMDA receptor-dependent synaptic plasticity in spatial memory*. Cell, 1996. **87**(7): p. 1327-38.
185. Barnes, CA; Danysz, W and Parsons, CG, *Effects of the uncompetitive NMDA receptor antagonist memantine on hippocampal long-term potentiation, short-term exploratory modulation and spatial memory in awake, freely moving rats*. Eur J Neurosci, 1996. **8**(3): p. 565-71.
186. Reisberg, B; Doody, R; Stoffler, A; Schmitt, F; Ferris, S et al., *Memantine in moderate-to-severe Alzheimer's disease*. N Engl J Med, 2003. **348**(14): p. 1333-41.
187. Tariot, PN; Farlow, MR; Grossberg, GT; Graham, SM; McDonald, S et al., *Memantine treatment in patients with moderate to severe Alzheimer disease already receiving donepezil: a randomized controlled trial*. Jama, 2004. **291**(3): p. 317-24.
188. Minkeviciene, R; Banerjee, P and Tanila, H, *Memantine improves spatial learning in a transgenic mouse model of Alzheimer's disease*. J Pharmacol Exp Ther, 2004. **311**(2): p. 677-82.
189. Melnikova, I, *Therapies for Alzheimer's disease*. Nat Rev Drug Discov, 2007. **6**(5): p. 341-2.
190. Xia, S; Miyashita, T; Fu, TF; Lin, WY; Wu, CL et al., *NMDA receptors mediate olfactory learning and memory in Drosophila*. Curr Biol, 2005. **15**(7): p. 603-15.
191. Kumar, S and Walter, J, *Phosphorylation of amyloid beta (A $\beta$ ) peptides - a trigger for formation of toxic aggregates in Alzheimer's disease*. Aging (Albany NY), 2011. **3**(8): p. 803-12.
192. Schieb, H; Kratzin, H; Jahn, O; Mobius, W; Rabe, S et al., *Beta-amyloid peptide variants in brains and cerebrospinal fluid from amyloid precursor protein (APP) transgenic mice: comparison with human Alzheimer amyloid*. J Biol Chem, 2011. **286**(39): p. 33747-58.
193. Naslund, J; Schierhorn, A; Hellman, U; Lannfelt, L; Roses, AD et al., *Relative abundance of Alzheimer A $\beta$  amyloid peptide variants in Alzheimer disease and normal aging*. Proc Natl Acad Sci U S A, 1994. **91**(18): p. 8378-82.
194. Jakob-Roetne, R and Jacobsen, H, *Alzheimer's disease: from pathology to therapeutic approaches*. Angew Chem Int Ed Engl, 2009. **48**(17): p. 3030-59.
195. McGowan, E; Pickford, F; Kim, J; Onstead, L; Eriksen, J et al., *A $\beta$ 42 is essential for parenchymal and vascular amyloid deposition in mice*. Neuron, 2005. **47**(2): p. 191-9.
196. Jarrett, JT; Berger, EP and Lansbury, PT, Jr., *The carboxy terminus of the beta amyloid protein is critical for the seeding of amyloid formation: implications for the pathogenesis of Alzheimer's disease*. Biochemistry, 1993. **32**(18): p. 4693-7.

197. Harper, JD and Lansbury, PT, Jr., *Models of amyloid seeding in Alzheimer's disease and scrapie: mechanistic truths and physiological consequences of the time-dependent solubility of amyloid proteins*. *Annu Rev Biochem*, 1997. **66**: p. 385-407.
198. Bitan, G; Vollers, SS and Teplow, DB, *Elucidation of primary structure elements controlling early amyloid beta-protein oligomerization*. *J Biol Chem*, 2003. **278**(37): p. 34882-9.
199. Walsh, DM and Selkoe, DJ, *A beta oligomers - a decade of discovery*. *J Neurochem*, 2007. **101**(5): p. 1172-84.
200. Fandrich, M, *Oligomeric Intermediates in Amyloid Formation: Structure Determination and Mechanisms of Toxicity*. *J Mol Biol*, 2012.
201. Gotz, J and Gotz, NN, *Animal models for Alzheimer's disease and frontotemporal dementia: a perspective*. *ASN Neuro*, 2009. **1**(4).
202. Van Dam, D and De Deyn, PP, *Animal models in the drug discovery pipeline for Alzheimer's disease*. *Br J Pharmacol*, 2011. **164**(4): p. 1285-300.
203. Bonini, NM and Fortini, ME, *Human neurodegenerative disease modeling using Drosophila*. *Annu Rev Neurosci*, 2003. **26**: p. 627-56.
204. Driscoll, M and Gerstbrein, B, *Dying for a cause: invertebrate genetics takes on human neurodegeneration*. *Nat Rev Genet*, 2003. **4**(3): p. 181-94.
205. Marsh, JL and Thompson, LM, *Can flies help humans treat neurodegenerative diseases?* *Bioessays*, 2004. **26**(5): p. 485-96.
206. Jeibmann, A and Paulus, W, *Drosophila melanogaster as a model organism of brain diseases*. *Int J Mol Sci*, 2009. **10**(2): p. 407-40.
207. Wolfgang, WJ; Miller, TW; Webster, JM; Huston, JS; Thompson, LM *et al.*, *Suppression of Huntington's disease pathology in Drosophila by human single-chain Fv antibodies*. *Proc Natl Acad Sci U S A*, 2005. **102**(32): p. 11563-8.
208. Luheshi, LM; Hoyer, W; de Barros, TP; van Dijk Hard, I; Brorsson, AC *et al.*, *Sequestration of the A beta peptide prevents toxicity and promotes degradation in vivo*. *PLoS Biol*, 2010. **8**(3): p. e1000334.
209. Weiner, HL and Frenkel, D, *Immunology and immunotherapy of Alzheimer's disease*. *Nat Rev Immunol*, 2006. **6**(5): p. 404-16.
210. Frenkel, D; Solomon, B and Benhar, I, *Modulation of Alzheimer's beta-amyloid neurotoxicity by site-directed single-chain antibody*. *J Neuroimmunol*, 2000. **106**(1-2): p. 23-31.
211. Schenk, D; Hagen, M and Seubert, P, *Current progress in beta-amyloid immunotherapy*. *Curr Opin Immunol*, 2004. **16**(5): p. 599-606.
212. Zago, W; Buttini, M; Comery, TA; Nishioka, C; Gardai, SJ *et al.*, *Neutralization of soluble, synaptotoxic amyloid beta species by antibodies is epitope specific*. *J Neurosci*, 2012. **32**(8): p. 2696-702.
213. Dodart, JC; Bales, KR; Gannon, KS; Greene, SJ; DeMattos, RB *et al.*, *Immunization reverses memory deficits without reducing brain A beta burden in Alzheimer's disease model*. *Nat Neurosci*, 2002. **5**(5): p. 452-7.
214. Lord, A; Gumucio, A; Englund, H; Sehlin, D; Sundquist, VS *et al.*, *An amyloid-beta protofibril-selective antibody prevents amyloid formation in a mouse model of Alzheimer's disease*. *Neurobiol Dis*, 2009. **36**(3): p. 425-34.
215. Mamikonyan, G; Necula, M; Mkrtychyan, M; Ghochikyan, A; Petrushina, I *et al.*, *Anti-A beta 1-11 antibody binds to different beta-amyloid species, inhibits fibril formation, and disaggregates preformed fibrils but not the most toxic oligomers*. *J Biol Chem*, 2007. **282**(31): p. 22376-86.
216. Frenkel, D; Balass, M; Katchalski-Katzir, E and Solomon, B, *High affinity binding of monoclonal antibodies to the sequential epitope EFRH of beta-amyloid peptide is essential for modulation of fibrillar aggregation*. *J Neuroimmunol*, 1999. **95**(1-2): p. 136-42.
217. Kheterpal, I; Williams, A; Murphy, C; Bledsoe, B and Wetzel, R, *Structural features of the A beta amyloid fibril elucidated by limited proteolysis*. *Biochemistry*, 2001. **40**(39): p. 11757-67.

218. Luhrs, T; Ritter, C; Adrian, M; Riek-Loher, D; Bohrmann, B *et al.*, *3D structure of Alzheimer's amyloid-beta(1-42) fibrils*. Proc Natl Acad Sci U S A, 2005. **102**(48): p. 17342-7.
219. Hoyer, W; Gronwall, C; Jonsson, A; Stahl, S and Hard, T, *Stabilization of a beta-hairpin in monomeric Alzheimer's amyloid-beta peptide inhibits amyloid formation*. Proc Natl Acad Sci U S A, 2008. **105**(13): p. 5099-104.
220. Pride, M; Seubert, P; Grundman, M; Hagen, M; Eldridge, J *et al.*, *Progress in the active immunotherapeutic approach to Alzheimer's disease: clinical investigations into AN1792-associated meningoencephalitis*. Neurodegener Dis, 2008. **5**(3-4): p. 194-6.
221. Ferrer, I; Boada Rovira, M; Sanchez Guerra, ML; Rey, MJ and Costa-Jussa, F, *Neuropathology and pathogenesis of encephalitis following amyloid-beta immunization in Alzheimer's disease*. Brain Pathol, 2004. **14**(1): p. 11-20.
222. Nicoll, JA; Wilkinson, D; Holmes, C; Steart, P; Markham, H *et al.*, *Neuropathology of human Alzheimer disease after immunization with amyloid-beta peptide: a case report*. Nat Med, 2003. **9**(4): p. 448-52.
223. Nemirovsky, A; Shapiro, J; Baron, R; Kompaniets, A and Monsonego, A, *Active Abeta vaccination fails to enhance amyloid clearance in a mouse model of Alzheimer's disease with Abeta42-driven pathology*. J Neuroimmunol, 2012. **247**(1-2): p. 95-9.
224. Monsonego, A; Zota, V; Karni, A; Krieger, JI; Bar-Or, A *et al.*, *Increased T cell reactivity to amyloid beta protein in older humans and patients with Alzheimer disease*. J Clin Invest, 2003. **112**(3): p. 415-22.
225. Agadjanyan, MG; Ghochikyan, A; Petrushina, I; Vasilevko, V; Movsesyan, N *et al.*, *Prototype Alzheimer's disease vaccine using the immunodominant B cell epitope from beta-amyloid and promiscuous T cell epitope pan HLA DR-binding peptide*. J Immunol, 2005. **174**(3): p. 1580-6.
226. Fukuchi, K; Accavitti-Loper, MA; Kim, HD; Tahara, K; Cao, Y *et al.*, *Amelioration of amyloid load by anti-Abeta single-chain antibody in Alzheimer mouse model*. Biochem Biophys Res Commun, 2006. **344**(1): p. 79-86.
227. Liu, R; Yuan, B; Emadi, S; Zameer, A; Schulz, P *et al.*, *Single chain variable fragments against beta-amyloid (Abeta) can inhibit Abeta aggregation and prevent abeta-induced neurotoxicity*. Biochemistry, 2004. **43**(22): p. 6959-67.
228. Robert, R; Dolezal, O; Waddington, L; Hattarki, MK; Cappai, R *et al.*, *Engineered antibody intervention strategies for Alzheimer's disease and related dementias by targeting amyloid and toxic oligomers*. Protein Eng Des Sel, 2009. **22**(3): p. 199-208.
229. Perchiacca, JM; Ladiwala, AR; Bhattacharya, M and Tessier, PM, *Structure-based design of conformation- and sequence-specific antibodies against amyloid beta*. Proc Natl Acad Sci U S A, 2012. **109**(1): p. 84-9.
230. Chartier, A; Raz, V; Sterrenburg, E; Verrips, CT; van der Maarel, SM *et al.*, *Prevention of oculopharyngeal muscular dystrophy by muscular expression of Llama single-chain intrabodies in vivo*. Hum Mol Genet, 2009. **18**(10): p. 1849-59.
231. Jin, M; Shepardson, N; Yang, T; Chen, G; Walsh, D *et al.*, *Soluble amyloid beta-protein dimers isolated from Alzheimer cortex directly induce Tau hyperphosphorylation and neuritic degeneration*. Proc Natl Acad Sci U S A, 2011. **108**(14): p. 5819-24.
232. Esiri, MM; Hyman, BT; Beyreuther, K and Masters, CL, *Aging and dementia.*, in *Greenfield's neuropathology*. 1997. p. 153-233.
233. Pike, CJ; Walencewicz, AJ; Glabe, CG and Cotman, CW, *In vitro aging of beta-amyloid protein causes peptide aggregation and neurotoxicity*. Brain Res, 1991. **563**(1-2): p. 311-4.
234. Mattson, MP; Tomaselli, KJ and Rydel, RE, *Calcium-destabilizing and neurodegenerative effects of aggregated beta-amyloid peptide are attenuated by basic FGF*. Brain Res, 1993. **621**(1): p. 35-49.
235. Hartley, DM; Walsh, DM; Ye, CP; Diehl, T; Vasquez, S *et al.*, *Protofibrillar intermediates of amyloid beta-protein induce acute electrophysiological changes and progressive neurotoxicity in cortical neurons*. J Neurosci, 1999. **19**(20): p. 8876-84.

236. Shearman, MS; Ragan, CI and Iversen, LL, *Inhibition of PC12 cell redox activity is a specific, early indicator of the mechanism of beta-amyloid-mediated cell death*. Proc Natl Acad Sci U S A, 1994. **91**(4): p. 1470-4.
237. Meinhardt, J; Sachse, C; Hortschansky, P; Grigorieff, N and Fandrich, M, *Abeta(1-40) fibril polymorphism implies diverse interaction patterns in amyloid fibrils*. J Mol Biol, 2009. **386**(3): p. 869-77.
238. Upadhaya, AR; Lungrin, I; Yamaguchi, H; Fandrich, M and Thal, DR, *High-molecular weight Abeta-oligomers and protofibrils are the predominant Abeta-species in the native soluble protein fraction of the AD brain*. J Cell Mol Med, 2011.
239. Ronicke, R; Klemm, A; Meinhardt, J; Schroder, UH; Fandrich, M *et al.*, *Abeta mediated diminution of MTT reduction--an artefact of single cell culture?* PLoS One, 2008. **3**(9): p. e3236.
240. Caughey, B and Lansbury, PT, *Protofibrils, pores, fibrils, and neurodegeneration: separating the responsible protein aggregates from the innocent bystanders*. Annu Rev Neurosci, 2003. **26**: p. 267-98.
241. Uptain, SM and Lindquist, S, *Prions as protein-based genetic elements*. Annu Rev Microbiol, 2002. **56**: p. 703-41.
242. Barnhart, MM and Chapman, MR, *Curli biogenesis and function*. Annu Rev Microbiol, 2006. **60**: p. 131-47.
243. Fowler, DM; Koulov, AV; Alory-Jost, C; Marks, MS; Balch, WE *et al.*, *Functional amyloid formation within mammalian tissue*. PLoS Biol, 2006. **4**(1): p. e6.
244. Fandrich, M and Dobson, CM, *The behaviour of polyamino acids reveals an inverse side chain effect in amyloid structure formation*. EMBO J, 2002. **21**(21): p. 5682-90.
245. Narayan, P; Orte, A; Clarke, RW; Bolognesi, B; Hook, S *et al.*, *The extracellular chaperone clusterin sequesters oligomeric forms of the amyloid-beta(1-40) peptide*. Nat Struct Mol Biol, 2011. **19**(1): p. 79-83.
246. Martins, IC; Kuperstein, I; Wilkinson, H; Maes, E; Vanbrabant, M *et al.*, *Lipids revert inert Abeta amyloid fibrils to neurotoxic protofibrils that affect learning in mice*. Embo J, 2008. **27**(1): p. 224-33.
247. McLean, CA; Cherny, RA; Fraser, FW; Fuller, SJ; Smith, MJ *et al.*, *Soluble pool of Abeta amyloid as a determinant of severity of neurodegeneration in Alzheimer's disease*. Ann Neurol, 1999. **46**(6): p. 860-6.
248. Roher, AE; Chaney, MO; Kuo, YM; Webster, SD; Stine, WB *et al.*, *Morphology and toxicity of Abeta-(1-42) dimer derived from neuritic and vascular amyloid deposits of Alzheimer's disease*. J Biol Chem, 1996. **271**(34): p. 20631-5.
249. Lue, LF; Kuo, YM; Roher, AE; Brachova, L; Shen, Y *et al.*, *Soluble amyloid beta peptide concentration as a predictor of synaptic change in Alzheimer's disease*. Am J Pathol, 1999. **155**(3): p. 853-62.
250. Bitan, G; Kirkitadze, MD; Lomakin, A; Vollers, SS; Benedek, GB *et al.*, *Amyloid beta -protein (Abeta) assembly: Abeta 40 and Abeta 42 oligomerize through distinct pathways*. Proc Natl Acad Sci U S A, 2003. **100**(1): p. 330-5.
251. Eisenhauer, PB; Johnson, RJ; Wells, JM; Davies, TA and Fine, RE, *Toxicity of various amyloid beta peptide species in cultured human blood-brain barrier endothelial cells: increased toxicity of dutch-type mutant*. J Neurosci Res, 2000. **60**(6): p. 804-10.
252. Zou, K; Kim, D; Kakio, A; Byun, K; Gong, JS *et al.*, *Amyloid beta-protein (Abeta)1-40 protects neurons from damage induced by Abeta1-42 in culture and in rat brain*. J Neurochem, 2003. **87**(3): p. 609-19.
253. Kim, J; Onstead, L; Randle, S; Price, R; Smithson, L *et al.*, *Abeta40 inhibits amyloid deposition in vivo*. J Neurosci, 2007. **27**(3): p. 627-33.
254. Sandberg, A; Luheshi, LM; Sollvander, S; Pereira de Barros, T; Macao, B *et al.*, *Stabilization of neurotoxic Alzheimer amyloid-beta oligomers by protein engineering*. Proc Natl Acad Sci U S A, 2010. **107**(35): p. 15595-600.

255. Moloney, A; Sattelle, DB; Lomas, DA and Crowther, DC, *Alzheimer's disease: insights from Drosophila melanogaster models*. Trends Biochem Sci, 2010. **35**(4): p. 228-35.
256. Kumar, S; Rezaei-Ghaleh, N; Terwel, D; Thal, DR; Richard, M *et al.*, *Extracellular phosphorylation of the amyloid beta-peptide promotes formation of toxic aggregates during the pathogenesis of Alzheimer's disease*. EMBO J, 2011. **30**(11): p. 2255-65.
257. Saido, TC; Yamao-Harigaya, W; Iwatsubo, T and Kawashima, S, *Amino- and carboxyl-terminal heterogeneity of beta-amyloid peptides deposited in human brain*. Neurosci Lett, 1996. **215**(3): p. 173-6.
258. Murakami, K; Uno, M; Masuda, Y; Shimizu, T; Shirasawa, T *et al.*, *Isomerization and/or racemization at Asp23 of Abeta42 do not increase its aggregative ability, neurotoxicity, and radical productivity in vitro*. Biochem Biophys Res Commun, 2008. **366**(3): p. 745-51.
259. Hartig, W; Goldhammer, S; Bauer, U; Wegner, F; Wirths, O *et al.*, *Concomitant detection of beta-amyloid peptides with N-terminal truncation and different C-terminal endings in cortical plaques from cases with Alzheimer's disease, senile monkeys and triple transgenic mice*. J Chem Neuroanat, 2010. **40**(1): p. 82-92.
260. Schilling, S; Zeitschel, U; Hoffmann, T; Heiser, U; Francke, M *et al.*, *Glutaminyl cyclase inhibition attenuates pyroglutamate Abeta and Alzheimer's disease-like pathology*. Nat Med, 2008. **14**(10): p. 1106-11.
261. Harigaya, Y; Saido, TC; Eckman, CB; Prada, CM; Shoji, M *et al.*, *Amyloid beta protein starting pyroglutamate at position 3 is a major component of the amyloid deposits in the Alzheimer's disease brain*. Biochem Biophys Res Commun, 2000. **276**(2): p. 422-7.
262. Schlenzig, D; Ronicke, R; Cynis, H; Ludwig, HH; Scheel, E *et al.*, *N-Terminal pyroglutamate formation of Abeta38 and Abeta40 enforces oligomer formation and potency to disrupt hippocampal long-term potentiation*. J Neurochem, 2012. **121**(5): p. 774-84.
263. Barghorn, S; Nimmrich, V; Striebinger, A; Krantz, C; Keller, P *et al.*, *Globular amyloid beta-peptide oligomer - a homogenous and stable neuropathological protein in Alzheimer's disease*. J Neurochem, 2005. **95**(3): p. 834-47.
264. Shankar, GM; Bloodgood, BL; Townsend, M; Walsh, DM; Selkoe, DJ *et al.*, *Natural oligomers of the Alzheimer amyloid-beta protein induce reversible synapse loss by modulating an NMDA-type glutamate receptor-dependent signaling pathway*. J Neurosci, 2007. **27**(11): p. 2866-75.
265. Walsh, DM; Klyubin, I; Fadeeva, JV; Cullen, WK; Anwyl, R *et al.*, *Naturally secreted oligomers of amyloid beta protein potently inhibit hippocampal long-term potentiation in vivo*. Nature, 2002. **416**(6880): p. 535-9.
266. Wang, HW; Pasternak, JF; Kuo, H; Ristic, H; Lambert, MP *et al.*, *Soluble oligomers of beta amyloid (1-42) inhibit long-term potentiation but not long-term depression in rat dentate gyrus*. Brain Res, 2002. **924**(2): p. 133-40.
267. Tomiyama, T; Matsuyama, S; Iso, H; Umeda, T; Takuma, H *et al.*, *A mouse model of amyloid beta oligomers: their contribution to synaptic alteration, abnormal tau phosphorylation, glial activation, and neuronal loss in vivo*. J Neurosci, 2010. **30**(14): p. 4845-56.
268. Lesne, S; Koh, MT; Kotilinek, L; Kaye, R; Glabe, CG *et al.*, *A specific amyloid-beta protein assembly in the brain impairs memory*. Nature, 2006. **440**(7082): p. 352-7.
269. Selkoe, DJ, *Soluble oligomers of the amyloid beta-protein impair synaptic plasticity and behavior*. Behav Brain Res, 2008. **192**(1): p. 106-13.
270. Medecigo, M; Manoutcharian, K; Vasilevko, V; Govezensky, T; Munguia, ME *et al.*, *Novel amyloid-beta specific scFv and VH antibody fragments from human and mouse phage display antibody libraries*. J Neuroimmunol, 2010. **223**(1-2): p. 104-14.
271. Aloisi, F, *Immune function of microglia*. Glia, 2001. **36**(2): p. 165-79.
272. Rezaie, P and Lantos, PL, *Microglia and the pathogenesis of spongiform encephalopathies*. Brain Res Brain Res Rev, 2001. **35**(1): p. 55-72.
273. Rogers, J and Lue, LF, *Microglial chemotaxis, activation, and phagocytosis of amyloid beta-peptide as linked phenomena in Alzheimer's disease*. Neurochem Int, 2001. **39**(5-6): p. 333-40.

274. Bolmont, T; Haiss, F; Eicke, D; Radde, R; Mathis, CA *et al.*, *Dynamics of the microglial/amyloid interaction indicate a role in plaque maintenance*. J Neurosci, 2008. **28**(16): p. 4283-92.
275. Govind, S, *Innate immunity in Drosophila: Pathogens and pathways*. Insect Sci, 2008. **15**(1): p. 29-43.
276. Sonnenfeld, MJ and Jacobs, JR, *Macrophages and glia participate in the removal of apoptotic neurons from the Drosophila embryonic nervous system*. J Comp Neurol, 1995. **359**(4): p. 644-52.
277. Yamamoto, N; Matsubara, E; Maeda, S; Minagawa, H; Takashima, A *et al.*, *A ganglioside-induced toxic soluble Abeta assembly. Its enhanced formation from Abeta bearing the Arctic mutation*. J Biol Chem, 2007. **282**(4): p. 2646-55.
278. De Felice, FG; Velasco, PT; Lambert, MP; Viola, K; Fernandez, SJ *et al.*, *Abeta oligomers induce neuronal oxidative stress through an N-methyl-D-aspartate receptor-dependent mechanism that is blocked by the Alzheimer drug memantine*. J Biol Chem, 2007. **282**(15): p. 11590-601.
279. Zhao, WQ; De Felice, FG; Fernandez, S; Chen, H; Lambert, MP *et al.*, *Amyloid beta oligomers induce impairment of neuronal insulin receptors*. FASEB J, 2008. **22**(1): p. 246-60.
280. Magdesian, MH; Carvalho, MM; Mendes, FA; Saraiva, LM; Juliano, MA *et al.*, *Amyloid-beta binds to the extracellular cysteine-rich domain of Frizzled and inhibits Wnt/beta-catenin signaling*. J Biol Chem, 2008. **283**(14): p. 9359-68.
281. Rensink, AA; Otte-Holler, I; de Boer, R; Bosch, RR; ten Donkelaar, HJ *et al.*, *Insulin inhibits amyloid beta-induced cell death in cultured human brain pericytes*. Neurobiol Aging, 2004. **25**(1): p. 93-103.
282. Lauren, J; Gimbel, DA; Nygaard, HB; Gilbert, JW and Strittmatter, SM, *Cellular prion protein mediates impairment of synaptic plasticity by amyloid-beta oligomers*. Nature, 2009. **457**(7233): p. 1128-32.
283. Sakono, M and Zako, T, *Amyloid oligomers: formation and toxicity of Abeta oligomers*. FEBS J, 2010. **277**(6): p. 1348-58.
284. Krishnan, R; Goodman, JL; Mukhopadhyay, S; Pacheco, CD; Lemke, EA *et al.*, *Conserved features of intermediates in amyloid assembly determine their benign or toxic states*. Proc Natl Acad Sci U S A, 2012. **109**(28): p. 11172-7.
285. Terzi, E; Holzemann, G and Seelig, J, *Interaction of Alzheimer beta-amyloid peptide(1-40) with lipid membranes*. Biochemistry, 1997. **36**(48): p. 14845-52.
286. Kaye, R; Sokolov, Y; Edmonds, B; McIntire, TM; Milton, SC *et al.*, *Permeabilization of lipid bilayers is a common conformation-dependent activity of soluble amyloid oligomers in protein misfolding diseases*. J Biol Chem, 2004. **279**(45): p. 46363-6.
287. Demuro, A; Mina, E; Kaye, R; Milton, SC; Parker, I *et al.*, *Calcium dysregulation and membrane disruption as a ubiquitous neurotoxic mechanism of soluble amyloid oligomers*. J Biol Chem, 2005. **280**(17): p. 17294-300.
288. Quist, A; Doudevski, I; Lin, H; Azimova, R; Ng, D *et al.*, *Amyloid ion channels: a common structural link for protein-misfolding disease*. Proc Natl Acad Sci U S A, 2005. **102**(30): p. 10427-32.
289. Kremer, JJ; Pallitto, MM; Sklansky, DJ and Murphy, RM, *Correlation of beta-amyloid aggregate size and hydrophobicity with decreased bilayer fluidity of model membranes*. Biochemistry, 2000. **39**(33): p. 10309-18.
290. Hertel, C; Terzi, E; Hauser, N; Jakob-Rotne, R; Seelig, J *et al.*, *Inhibition of the electrostatic interaction between beta-amyloid peptide and membranes prevents beta-amyloid-induced toxicity*. Proc Natl Acad Sci U S A, 1997. **94**(17): p. 9412-6.
291. Masters, CL; Simms, G; Weinman, NA; Multhaup, G; McDonald, BL *et al.*, *Amyloid plaque core protein in Alzheimer disease and Down syndrome*. Proc Natl Acad Sci U S A, 1985. **82**(12): p. 4245-9.
292. Halford, SE; Schlesinger, MJ and Gutfreund, H, *Escherichia coli alkaline phosphatase. Kinetic studies with the tetrameric enzyme*. Biochem J, 1972. **126**(5): p. 1081-90.

293. Tibbitts, TT; Murphy, JE and Kantrowitz, ER, *Kinetic and structural consequences of replacing the aspartate bridge by asparagine in the catalytic metal triad of Escherichia coli alkaline phosphatase*. J Mol Biol, 1996. **257**(3): p. 700-15.
294. Stec, B; Hehir, MJ; Brennan, C; Nolte, M and Kantrowitz, ER, *Kinetic and X-ray structural studies of three mutant E. coli alkaline phosphatases: insights into the catalytic mechanism without the nucleophile Ser102*. J Mol Biol, 1998. **277**(3): p. 647-62.

## 8. Appendix

### Appendix A Amino acid sequences

**A**

```

10      20      30      40      50      60
Aβ40    MASKVSILLLLTVHLLAAOTFAAQDAEFRHDSGYEVHHQKLVFFAEDVGSNKGAIIGLMVGGV--
Aβ42    MASKVSILLLLTVHLLAAOTFAAQDAEFRHDSGYEVHHQKLVFFAEDVGSNKGAIIGLMVGGVIA
Aβ42arc MASKVSILLLLTVHLLAAOTFAAQDAEFHDSGYEVHHQKLVFFAGDVGSNKGAIIGLMVGGVIA

10      20      30      40      50      60      70      80      90      100
B10     MASKVSILLLLTVHLLAAOTFAAQDYKDEVQLVESGGGLVQPGGSLRLSCTASGYTFSHRYHRWFRQAPGKEREIVAVISQSGMRTYYADSVKGRFTISRD
KW1     MASKVSILLLLTVHLLAAOTFAAQDYKDEVQLVESGGGSVQPGGSLRLSCTASGYTFSGEFVIWFRQAPGKEREIVSGISLRKGWTTYADSVKGRFTISQD

110     120     130     140     150     160
B10     NAKNTVYLQMNSLKPEDTAMYCAAGTRRKNVWTRRQHPFDYWGQTQVTVSSASGADEEQKLISEEDL
KW1     NAKNTVYLQMNSLKPEDTAMYCAAAP---TATHALYFDYWGQTQVTVSSASGA-EQKLISEEDL

```

**B**

```

10      20      30      40      50      60      70      80      90      100
B10AP-S2 DYKDEVQLVESGGGLVQPGGSLRLSCTASGYTFSHRYHRWFRQAPGKEREIVAVISQSGMRTYYADSVKGRFTISRDNAKNTVYLQMNSLKPEDTAMYYC
KW1AP-S2 DYKDEVQLVESGGGSVQPGGSLRLSCTASGYTFSGEFVIWFRQAPGKEREIVSGISLRKGWTTYADSVKGRFTISQDNAKNTVYLQMNSLKPEDTAMYYC

110     120     130     140     150     160     170     180     190     200
B10AP-S2 AAGTRRKNVWTRRQHPFDYWGQTQVTVSSASGADEEQKLISEEDLLEFTPEMPVLENRAAQGDITAPGGARRLTGDQTAALRDSLSDKPAKNIILLIGDMGD
KW1AP-S2 AAAP---TATHALYFDYWGQTQVTVSSASGA-EQKLISEEDLLEFTPEMPVLENRAAQGDITAPGGARRLTGDQTAALRDSLSDKPAKNIILLIGDMGD

210     220     230     240     250     260     270     280     290     300
B10AP-S2 SEITAARNYAEAGAGFFKIDALPLTGQYTHYALNKTKGPDYVTDSAASATAWSTGVKTYNGALGVDIHEKDHPTILEMAKAGIATGNVSTAELQDAT
KW1AP-S2 SEITAARNYAEAGAGFFKIDALPLTGQYTHYALNKTKGPDYVTDSAASATAWSTGVKTYNGALGVDIHEKDHPTILEMAKAGIATGNVSTAELQDAT

310     320     330     340     350     360     370     380     390     400
B10AP-S2 PAALVAHVTSRKCYGPSATSEKCPGNALEKGKGSITEQLLNARADVTLGGAKTFAETATAGEWQGKTLREQARGYQLVSDAASLNSVTEANQQKPL
KW1AP-S2 PAALVAHVTSRKCYGPSATSEKCPGNALEKGKGSITEQLLNARADVTLGGAKTFAETATAGEWQGKTLREQARGYQLVSDAASLNSVTEANQQKPL

410     420     430     440     450     460     470     480     490     500
B10AP-S2 LGLFADGNMPVRWIGPKATYHGNIDKPAVTCTPNPQRNDSVPTLAQMTDKAIELLSKNEKGFFLQVEGASIDKQDHAANPCGIGETVDLDEAVQRALEF
KW1AP-S2 LGLFADGNMPVRWIGPKATYHGNIDKPAVTCTPNPQRNDSVPTLAQMTDKAIELLSKNEKGFFLQVEGASIDKQDHAANPCGIGETVDLDEAVQRALEF

510     520     530     540     550     560     570     580     590     600
B10AP-S2 AKKEGNTLVIVTADHAHASQIVAPDTKAPGLTQALNTKDGAVMSYGNSEEDSQEHTGSQIRIAAYGPHAANVVGLTDQTDLFYTMKALGLKGAPGLE
KW1AP-S2 AKKEGNTLVIVTADHAHASQIVAPDTKAPGLTQALNTKDGAVMSYGNSEEDSQEHTGSQIRIAAYGPHAANVVGLTDQTDLFYTMKALGLKGAPGLE

610     620
B10AP-S2 SRGPFEGKPIPNPLLGLDSTRTGHHHHHH
KW1AP-S2 SRGPFEGKPIPNPLLGLDSTRTGHHHHHH

```

**C**

```

10      20      30      40      50      60      70      80      90      100
B10-myc DYKDEVQLVESGGGLVQPGGSLRLSCTASGYTFSHRYHRWFRQAPGKEREIVAVISQSGMRTYYADSVKGRFTISRDNAKNTVYLQMNSLKPEDTAMYYC
110     120     130     140
B10-myc AAGTRRKNVWTRRQHPFDYWGQTQVTVSSASGADEEQKLISEEDL

```

Polypeptide chains expressed in *Drosophila melanogaster* (A), in *Drosophila* S2 cells (B) and *E. coli* (C). Underlined is the secretion signal peptide used in *Drosophila*. Flag-tags (DYKD), Myc-tags (EQKLISEEDL) and His-tags (HHHHHH) are marked in bold and italic. The coding sequence for B10 is highlighted in red and the coding sequence for KW1 is highlighted in blue.

---

## Appendix B                      Establishment of *Drosophila melanogaster* transgenic for bivalent antibody domains

---

### B.1.1 Generation of an inactive alkaline phosphatase

*In vitro* studies found that B10 and KW1 have higher affinities when expressed as dimeric version. This was achieved by N-terminal fusion of each antibody domain to alkaline phosphatase (AP), which naturally forms dimers<sup>[292]</sup>, thus leading to bivalent B10 and KW1 moieties. Since alkaline phosphatase is a widely distributed enzyme that also exists in *Drosophila melanogaster* (Aph-1 - Aph-4) its expression may have an effect in the fruit fly. Therefore we decided to clone a mutated version of the AP where two amino acids were exchanged to obtain an enzyme whose activity is close to the level of non-enzymatic reactions. Site-specific mutagenesis of the Zn<sup>2+</sup> and Mg<sup>2+</sup> binding amino acid 51 (D51A) revealed that this mutant was not able to catalyse phosphate ester hydrolysis and a mutation in the active site (S102G) had a 6 x 10<sup>5</sup>-fold lower efficiency compared to the non-mutated enzyme<sup>[293, 294]</sup>. Consequently, the double-mutant D51A/S102G should lead to complete abolishing of the enzymatic activity of the alkaline phosphatase (B10AP<sub>i</sub>). To prove this assumption the resultant alkaline phosphatase was fused to B10 and expressed in *E. coli*. After purification using a Ni-NTA and a Q-Sepharose column we obtained a pure fraction (≥ 95 %) containing B10AP<sub>i</sub> as seen in a SDS-PAGE (figure B.1.1 A). Afterwards the protein was tested in a dot blot assay in comparison with non-mutated B10AP. Therefore Aβ1-40 fibrils were bound to a nitrocellulose membrane (figure B.1.1 B). The protein load was examined using Ponceau S staining (left lane). Three more Aβ1-40 fibril membranes were stained with either B10AP, B10AP<sub>i</sub> alone or in combination with an anti-AP antibody and detection with anti-rabbit-AP conjugated secondary antibody. An active alkaline phosphatase can easily be detected using a one step alkaline phosphatase substrate (NBP/BCIP, Pierce).

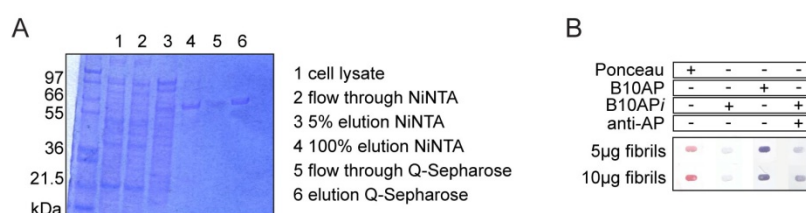


**Figure B.1.1** Establishment of an inactive alkaline phosphatase. (A) Purification of B10AP\_D51A/S102G from *E. coli* leads to ≥ 95 % pure protein as demonstrated by SDS-PAGE and a respective band around 66 kDa. (B) The binding of B10AP<sub>i</sub> was tested in a dot blot assay. B10AP<sub>i</sub> was tested alone (2<sup>nd</sup> lane) or detected using an anti-AP antibody (4<sup>th</sup> lane). The staining was done in comparison to a B10AP staining (3<sup>rd</sup> lane). Ponceau S was used to confirm equal protein loading.

A $\beta$ 1-40 fibrils incubated with B10AP develop distinct dark purple signals, which are absent in case of the B10AP*i* incubation. To examine the binding ability of B10AP*i* a third membrane was incubated first with the B10AP*i* variant, followed by detection using an anti-AP antibody and subsequently developed using a secondary antibody and the same alkaline phosphatase substrate. This led to resultant purple signals which were also concentration dependent but weaker, compared to the non-mutated B10AP. Nevertheless the blot demonstrates the abolished enzymatic activity of the mutated B10AP*i* without losing its binding ability to A $\beta$ (1-40) fibrils.

### B.1.2 Characterisation of B10AP*i*, B10mAP*i* and KW1AP*i*

Subsequently to the generation of an inactive AP variant, the gene for the AP double-mutant was cloned into the existing *Drosophila melanogaster* expression plasmids pUASTattB-B10 and pUASTattB-KW1 to obtain the bivalent antibody domains B10AP*i* and KW1AP*i* *in vivo*. Additionally the gene sequence B10 was mutated to generate a negative control. With respect to the fact that an amino acid exchange at position 39 and 61 results in a nearly complete loss of its binding ability<sup>[172]</sup> the same mutations R39A and R61A were introduced into the original B10 vector pGA4\_B10 leading to pGA4\_B10R39AR61A (B10m). This vector was then used to generate the mutated variant pUASTattB-B10mAP*i*.

The constructs (figure B.1.2A) were used to generate transgenic *Drosophila melanogaster* and the resulting fly lines were crossed with the neuronal driver line Gal4-elav<sup>c155</sup>. The transcription was analysed by RT-PCR. A control PCR was carried out using rp49 primers to confirm equal cDNA quantities in all PCR samples (figure B.1.2B). B10 and KW1 specific primers were used to determine the transcription of the antibody domain displaying strong transcription in the fly heads and also some expression in the remaining fly bodies (figure B.1.2C). No KW1-mRNA was detected in WT flies or in the absence of the elav driver. However, small amounts of B10-mRNA and B10m-mRNA were detected in the samples without the elav driver demonstrating that the construct is not fully inactive. A PCR using AP specific primers confirmed the existence of the AP in all three fly lines (figure B.1.2D) being transcribed in the same samples as the antibody domains.

Western blot analysis was carried out to investigate the translation of the antibody domains (figure B.1.2E). Detection with the anti-myc antibody shows strong bands at around 17 kDa only in the fly heads similar to the distribution of the mRNAs. No bands are visible in flies lacking the elav driver. A control staining using the anti-actin antibody displays indistinguishable bands around 35 kDa confirming equal protein loading. These data revealed that all three dimeric antibody domains are translated correctly in the fly neurons.

A western blot using the monoclonal antibody 6E10 (figure B.1.2F) demonstrated that none of the dimeric antibody domains has an influence on the overall expression level of A $\beta$ . Again equal protein loading was confirmed using the anti actin-antibody.

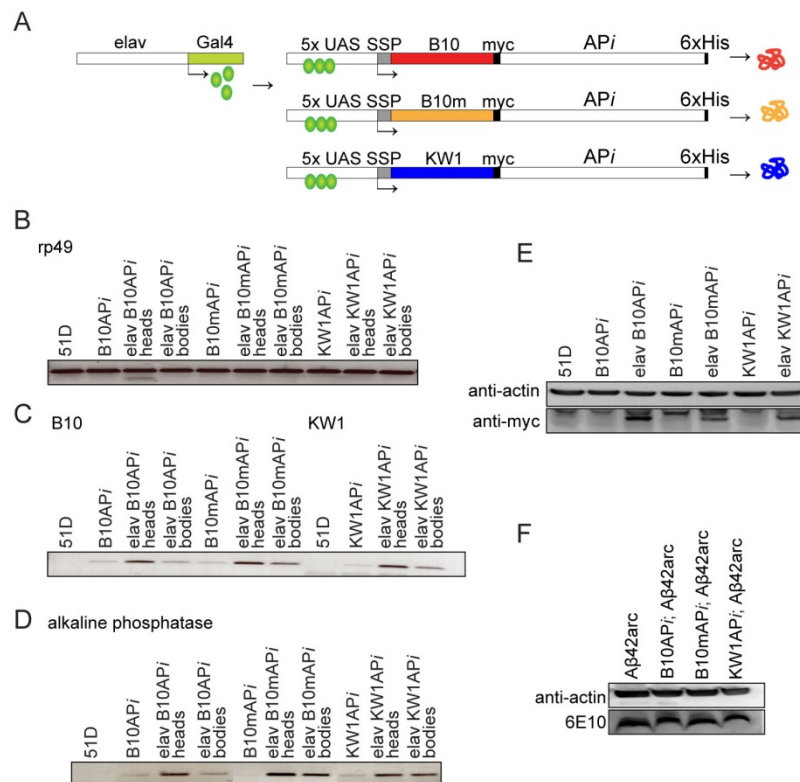


**Figure B.1.2** Expression of dimeric antibody domains in *Drosophila melanogaster*. (A) Schematic representation of the expression constructs. (B-D) RT-PCR analysis of B10-, B10m- and KW1-mRNA transcription in the head or remaining body; i.e. thorax and abdomen, of different fly lines as indicated in the panels. Constitutively transcribed rp49 mRNA presented equal cDNA loading (B). Antibody-domain specific primers were used in (C) and AP specific primers in (D). (E) Western blot with an anti-myc primary antibody showed strong band at around 17 kDa in the fly heads upon expression and no band in absence of the elav driver. Anti-actin western blot served as loading control. (F) Western blot with 6E10 primary antibody to detect A $\beta$  displayed a strong band at around 4 kDa in A $\beta$  expressing *Drosophila melanogaster*. Anti-actin western blot served as loading control.

A survival assay was carried out to determine the lifespan of the flies expressing the dimeric antibody domains B10APi, B10mAPi and KW1APi. 100 flies per genotype were analysed to determine the medium survival. The obtained survival plots (figure B.1.3A) demonstrated a medium survival of  $44 \pm 0.46$  days for the WT flies. Flies expressing B10APi lived slightly longer ( $48 \pm 0.11$  days). Similar values were obtained for B10mAPi ( $48 \pm 0.42$  days) and KW1APi flies ( $49 \pm 0$  days).

A negative-geotaxis assay was carried out to estimate the climbing ability of the flies (figure B.1.3B). All young flies were highly agile and the mobility decreases during ageing. All WT flies were immobile by day 30. Expression of B10APi, B10mAPi or KW1APi did not lead to any obvious difference compared to the WT flies.

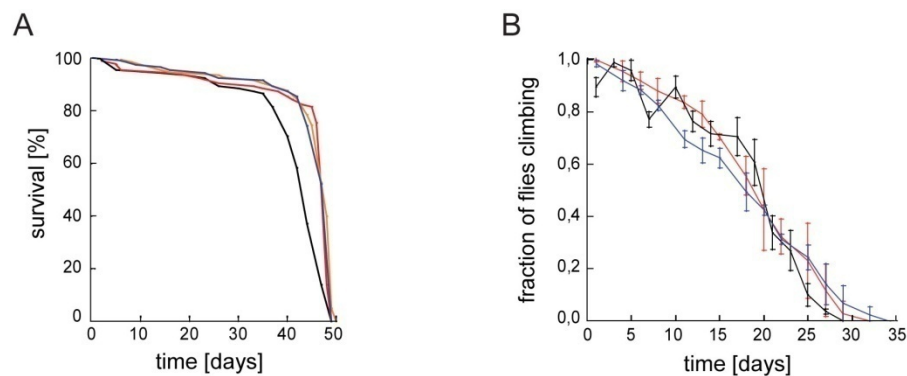


**Figure B.1.3** Phenotypic characterisation of bivalent antibody domains in *Drosophila melanogaster*. (A) Percentage of survival from an initial stock of 100 flies per genotype. The lifespan of B10APi (red), B10mAPi (orange) and KW1APi (blue) expressing flies is compared to WT flies (black). (B) Fraction of flies, reaching the vial top within 45 sec relative to total number of flies and depending on fly age. Error bars show standard deviation from three independent experiments using 15 flies each. The climbing ability of B10AP (red) and KW1AP (blue) flies is shown in comparison to WT flies (black).

All three dimeric antibody domain fly stocks were used subsequent to establish double transgenic *Drosophila melanogaster* stocks for further analysis. The flies were crossed with *Drosophila melanogaster* transgenic for A $\beta$ (1-40), A $\beta$ (1-42) and A $\beta$ (1-42)E22G (see method 2.2.1.2). This led to the following fly lines:

**Table B.1** *Drosophila melanogaster* double transgenic for A $\beta$  and B10APi, B10mAPi or KW1APi.

+/+; B10APi/CyO; A $\beta$ 40/TM6B	+/+; B10APi/CyO; A $\beta$ 42/TM6B	+/+; B10APi/CyO; A $\beta$ 42arc/TM6B
+/+; B10mAPi/CyO; A $\beta$ 40/TM6B	+/+; B10mAPi/CyO; A $\beta$ 42/TM6B	+/+; B10mAPi/CyO; A $\beta$ 42arc/TM6B
+/+; KW1APi/CyO; A $\beta$ 40/TM6B	+/+; KW1APi/CyO; A $\beta$ 42/TM6B	+/+; KW1APi/CyO; A $\beta$ 42arc/TM6B

## B.2. Dimeric antibody domains do not lead to different phenotypes

*In vitro* studies enclosed that B10 and KW1 have higher affinities for their respective species when expressed as dimeric variants (3.4). *Drosophila melanogaster* transgenic for the dimeric antibody domains B10APi and KW1APi and A $\beta$  were crossed with the neuronal driver line Gal4-elav<sup>c155</sup>. The offspring was analysed regarding their lifespan and climbing ability (figure B.2.1). For both assays the flies were raised and kept at 29°C during the whole experiment with fresh food every two days. Additionally, the double mutant B10mAPi was included into the examination because it has been shown to lack its binding ability to A $\beta$  fibrils<sup>[172]</sup>.

The measurement of the lifespan and the climbing ability of A $\beta$ 42arc flies is shown in figure B.2.1A,D. The A $\beta$ 42arc flies have a medium survival of  $7 \pm 0.1$  days and lose their climbing ability

within 5 days. Upon expression of B10APi, KW1APi and B10mAPi these values do not change significantly presenting medium survivals of  $7 \pm 0.03$  days,  $7 \pm 0.05$  days and  $7 \pm 0.07$  days, respectively. Thus, none of the dimeric antibody domains has an effect on the phenotype of A $\beta$ 42arc flies. Analysing A $\beta$ 42 flies leads to similar results. The medium survival of A $\beta$ 42 flies is  $33 \pm 0.31$  days and by day 20 all flies are immobile. None of the three dimeric antibody domains alter the medium survival values significantly. B10APi;A $\beta$ 42 flies have a medium survival of  $32 \pm 0.29$  days while KW1APi;A $\beta$ 42 flies present a medium survival value of  $32 \pm 0.26$  days and the medium survival of B10mAPi;A $\beta$ 42 flies is  $30 \pm 0.55$  days. Neither B10APi nor KW1APi change the progression of the climbing ability curve (B10mAPi was not tested). Finally the phenotype of A $\beta$ 40 flies was assessed upon expression of the dimeric antibody domains. As seen before the A $\beta$ 40 flies behave like WT flies showing a medium survival of  $43 \pm 0.6$  days. These flies have the slowest decline of the lifespan and are immobile by day 26. Compared to A $\beta$ 40 flies alone all three antibody domains B10APi, KW1APi and B10mAPi lead to a reduced lifespan (medium survival of  $33 \pm 0.31$  days;  $35 \pm 0.68$  days and  $33 \pm 0.49$  days, respectively). No effect is seen on the climbing ability when B10APi or KW1APi is co-expressed (B10mAPi was not tested).

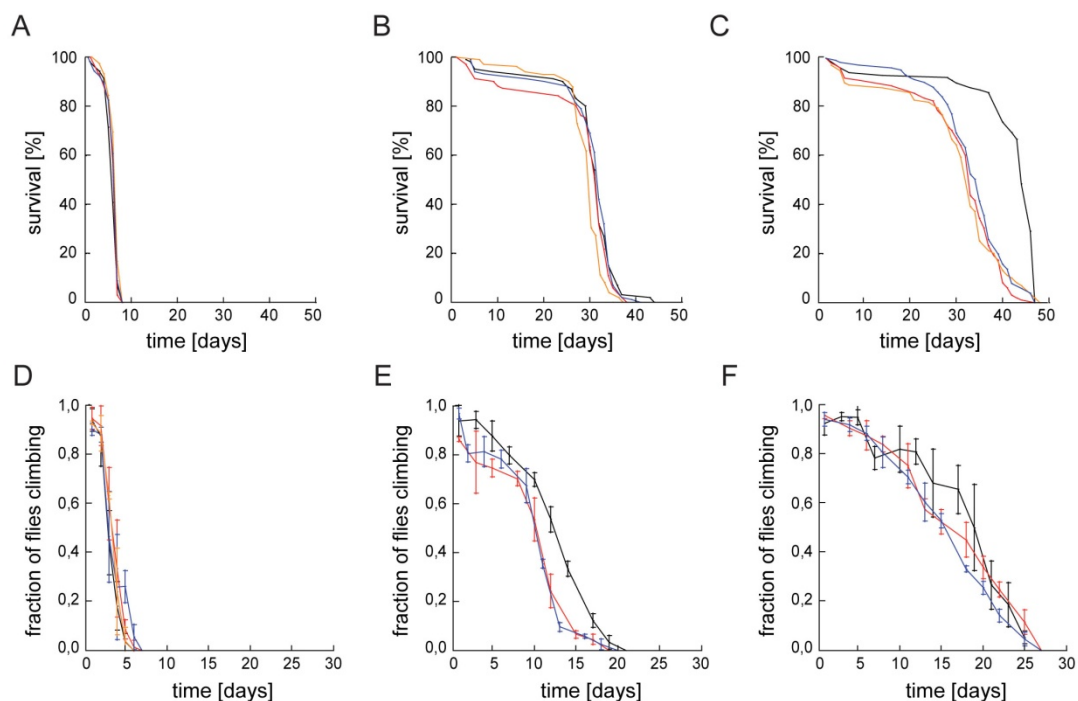


**Figure B.2.1** Phenotypic characterisation of the dimeric antibody domains in *Drosophila melanogaster*. (A-C) Lifespan measurement and (D-E) determination of climbing ability of A $\beta$ 42arc (A,D), A $\beta$ 42 (B,E) and A $\beta$ 40 (C,F) flies in presence or absence of the dimeric antibody variants B10APi (red curve), KW1APi (blue) and B10mAPi (orange). All A $\beta$  variants without antibody domain are displayed in the black curves. Error bars in D-F stand for standard deviation of three independent measurements using 15 flies each.

To investigate this result further the A $\beta$ (1-40) concentration in all four A $\beta$  fly lines used in the survival assay in figure B.2.1E was characterised. Western blot analysis was carried out using the

antibodies 6E10 (A $\beta$ ) and anti-actin. The anti-actin staining in figure B.2.2 confirms equal protein loading in all samples while the 6E10 staining reveals no difference in the band intensity and thus no difference in the A $\beta$  concentration. Because B10mAPi does not bind to A $\beta$  fibrils this result is more likely due to the flies itself and cannot be trusted.

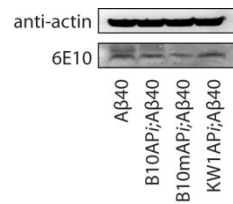


*Figure B.2.2 The A $\beta$ 40 level is not affected by the co-expression of the dimeric antibody domains. Western blot analysis was carried out to determine the expression level of A $\beta$ (1-40) upon co-expression of B10APi, KW1APi and B10mAPi. The monoclonal antibody 6E10 was used for detection of A $\beta$  while anti-actin staining displayed equal protein loading.*

---

**Curriculum Vitae**

---

**Date of birth** 10.01.1983  
**Place of birth** Schkeuditz  
**Marital status** single  
**Nationality** German

**Address** 06122 Halle (Saale), Weidaweg 11

**Education**

10/2012 – current **Research assistant**  
MVZ Labor GmbH Dessau

05/2008 – 09/2012 **Ph.D. student**  
Max-Planck research unit for enzymology of protein folding, Halle  
Advisor: PD Marcus Fändrich

10/2002 - 04/2008 **Studies of Biology**  
Martin-Luther-Universität Halle-Wittenberg  
Topic: „Analyse der keimbahnspezifischen Chromatinregulation in  
ausgewählten Regionen von *Drosophila melanogaster*“  
Degree: Diplom-Biologin; Grade: 1.5

08/1993 - 07/2001 **Secondary School**  
A-levels, Grade: 1.8  
Leibnizschule Gymnasium Leipzig

Jessica Wacker

---

**Publication**

---

**Molecular basis of  $\beta$ -amyloid oligomer recognition with a conformational antibody fragment.**

Morgado I, Wieligmann K, Bereza M, Rönicke R, Meinhardt K, Annamalai K, Baumann M, Wacker J, Hortschansky P, Malešević M, Parthier C, Mawrin C, Schiene-Fischer C, Reymann KG, Stubbs MT, Balbach J, Görlach M, Horn U, Fändrich M.

Proc Natl Acad Sci U S A. **2012 109(31)**:12503-8.

**Toxic Relevance of Polymorphic A $\beta$  States Revealed by Conformational Targeting *In Vivo*.**

Wacker J, Rönicke R, Wulff M, Westermann M, Reymann KG, Dobson CM, Horn U, Crowther DC, Luheshi LM, Fändrich M

*in preparation*

---

## Acknowledgements

---

To PD Marcus Fändrich: Thanks for offering me the possibility to work in your group and on the promising project. Thank you for believing in me, supporting my work with critical discussions and suggestions. I'm glad to have received excellent training in your lab that I can use in my future jobs.

To Prof. Demuth and PD Crowther: Thank you very much for evaluating my thesis as well as for fruitful discussions about AD.

To Leila Luheshi: You supported my project very much and I'm grateful for your help in developing *Drosophila* experiments and discussing the results. Thanks you for excellent supervision during my times in Cambridge and also for private support to settle and overcome language problems.

To Megan Garvey: Thank you for being patient with me and my thesis as well as for your willingness to do the native proof-reading. You gave me so much encouragement especially during the last months

To AG Fändrich: I had a great time during my PhD with many humor, support, scientific discussions and private gossip within and outside the lab. Especially to Karo, Mela, Katrin: I hope we keep our tradition alive!

To all people from the Cambridge lab: Thank you for the warm welcome every time I spend in your lab. I'm glad to have met so many different characters in a very short period of time. I also thank you for all experimental ideas that helped me solve many unanswered questions.

To all my friends: You made me laugh every time I was down. Thanks for your support during hard times and all the times we spent together.

To my family: You know how challenging it was for me to do the PhD. I thank my parents, who supported all my decisions and encouraged me to make my own way. I'm proud we've come that far. I would also like to thank Olaf for being with me all the time and help to see my problems so much smaller.

To all people I've met during my PhD: The sun not always shines in live – but you made every day a bit brighter. I'm grateful to have started and finally finished my PhD.

---

**Eidesstaatliche Erklärung**

---

Hiermit erkläre ich an Eides statt, dass die vorliegende Arbeit gemäß der Promotionsordnung der Naturwissenschaftlichen Fakultät der Martin-Luther-Universität Halle-Wittenberg vom 13.06.2012 selbstständig und nur unter Benutzung der angegebenen Quellen und Hilfsmittel erstellt wurde.

Ich versichere, dass ich mich mit dieser Arbeit weder an der Martin-Luther-Universität Halle-Wittenberg, noch an einer anderen Einrichtung um die Erlangung eines akademischen Grades beworben habe.

Halle (Saale), d.20.11.2012

Jessica Wacker